

**SYNTHESIS AND STRUCTURAL STUDY OF MATERIALS
COMBINING METFORMIN WITH OTHER COMPOUNDS
USED FOR DIABETES THERAPY**

Aungkana Chatkon

**A Thesis Submitted in Partial Fulfillment of the Requirements for the
Degree of Doctor of Philosophy in Chemistry
Suranaree University of Technology
Academic Year 2012**

การสังเคราะห์และศึกษาโครงสร้างของสารที่ประกอบด้วยเมทฟอร์มินกับสารอื่น
เพื่อใช้ในการรักษาโรคเบาหวาน

นางสาวอังคณา ชาติก้อน

วิทยานิพนธ์นี้เป็นส่วนหนึ่งของการศึกษาตามหลักสูตรปริญญาวิทยาศาสตรดุษฎีบัณฑิต
สาขาวิชาเคมี
มหาวิทยาลัยเทคโนโลยีสุรนารี
ปีการศึกษา 2555

**SYNTHESIS AND STRUCTURAL STUDY OF MATERIALS
COMBINING METFORMIN WITH OTHER COMPOUNDS
USED FOR DIABETES THERAPY**

Suranaree University of Technology has approved this thesis submitted in partial fulfillment of the requirements for the Degree of Doctor of Philosophy.

Thesis Examining Committee

(Assoc. Prof. Dr. Jatuporn Wittayakun)

Chairperson

(Assoc. Prof. Dr. Kenneth J. Haller)

Member (Thesis Advisor)

(Prof. Dr. Debbie C. Crans)

Member

(Asst. Prof. Dr. Kunwadee Rangriwatananon)

Member

(Prof. Dr. Adrian E. Flood)

Member

(Prof. Dr. Sukit Limpijumnong)

Vice Rector for Academic Affairs

(Assoc. Prof. Dr. Prapun Manyum)

Dean of Institute of Science

อังคณา ชาดิก้อน : การสังเคราะห์และศึกษาโครงสร้างของสารที่ประกอบด้วยเมทฟอร์มินกับสารอื่นเพื่อใช้ในการรักษาโรคเบาหวาน (SYNTHESIS AND STRUCTURAL STUDY OF MATERIALS COMBINING METFORMIN WITH OTHER COMPOUNDS USED FOR DIABETES THERAPY) อาจารย์ที่ปรึกษา : รองศาสตราจารย์ ดร.เก็นเนท เจ. แสลดอร์, 120 หน้า.

การสังเคราะห์ผลึกสารตัวใหม่ที่เกิดจากการรวมเมทฟอร์มินกับเคอะเวเนเดตเพื่อใช้ในการรักษาโรคเบาหวาน โดยคาดว่าสารที่สังเคราะห์ขึ้นมานี้จะช่วยเพิ่มประสิทธิภาพในการรักษา โดยลดปริมาณการใช้เมทฟอร์มินหรือโลหะ ส่งผลให้ความเป็นพิษของสารลดลง ทั้งนี้ยังได้มีการศึกษาวิเคราะห์ว่าสารนั้นเกิดอันตรกิริยากับผิวสัมผัสของไมเซลล์ฝักกลับอย่างไร ซึ่งอาจนำไปสู่ความเข้าใจเกี่ยวกับอันตรกิริยาของสารกับเยื่อหุ้มเซลล์

เมทฟอร์มินไฮโดรคลอไรด์เป็นสารที่มีฤทธิ์ทางยาที่แยกได้จากยาเบาหวาน และพิสูจน์เอกลักษณ์ได้โดยใช้เทคนิคอินฟราเรดสเปกโทรสโคปี การหาจุดหลอมเหลว และการเลี้ยวเบนของรังสีเอกซ์ ผลด้านผลึกศาสตร์แสดงให้เห็นว่ามีการเคลื่อนที่ของ π อิเล็กตรอนในกลุ่มของไบแก้วไนด์แต่ถูกขัดขวางที่อะตอมกลางของไนโตรเจนที่เป็นตัวเชื่อมระหว่างสองกลุ่มแก้วไนด์ เนื่องจากค่ามุมไดฮีดรัล (φ) ที่กว้างมากระหว่างกลุ่มแก้วไนด์ นอกจากนี้ยังมีแรงดึงดูดระหว่างโมเลกุลของกลุ่มประจุบวก เป็นพันธะไฮโดรเจนชนิด $N-H \cdots N$ รวมทั้งแรงดึงดูดระหว่างประจุบวกและประจุลบในโครงข่ายสามมิติแบบ $N-H \cdots Cl$ และ $C-H \cdots Cl$

ทั้งนี้ยังมีการศึกษาสารละลายของเมทฟอร์มินไฮโดรคลอไรด์ที่พีเอชต่างๆ พบว่าค่าการเลื่อนทางเคมีของโปรตอนในหมู่เมทิลพบที่ 3.05 พีพีเอ็ม ที่พีเอช 1 และ 2.77 พีพีเอ็ม ที่พีเอช 14 แสดงให้เห็นว่ามีการรับโปรตอนของเมทฟอร์มินในสภาวะที่สารละลายเป็นเบส และผลจากการศึกษาระบบไมเซลล์ฝักกลับของเมทฟอร์มินไฮโดรคลอไรด์ในโซเดียมบิส(2-เอทิลเฮกซิล)ซัลโฟซัลโฟเนต (AOT) พบว่าโปรตอนของหมู่เมทิลมีค่าเคมีคัลชิฟท์ที่สนามแม่เหล็กต่ำลง จึงได้เสนอแนะว่าไอออนของเมทฟอร์มินจับอยู่กับผิวสัมผัส

ได้มีการสังเคราะห์และพิสูจน์เอกลักษณ์ของสารที่เกิดจากการรวมตัวกันของไอออนบวกของเมทฟอร์มินและไอออนลบของเคอะเวเนเดต พบว่าสารประกอบนี้ไม่ละลายในน้ำแต่ละลายได้เล็กน้อยในไดเมทิลซัลโฟลค์และละลายได้ดีในสารละลายที่ไม่เป็นเนื้อเดียวกันของ AOT ไมเซลล์ฝักกลับซึ่งแตกต่างอย่างมีนัยสำคัญเมื่อเปรียบเทียบกับสมบัติการละลายของโซเดียมเคอะเวเนเดต เมื่อพิจารณาจากข้อมูลอ้างอิงพบว่า V_{10} มีคุณสมบัติที่ช่วยเพิ่มประสิทธิภาพการทำหน้าที่ของอินซูลินในหนูที่ถูกกระตุ้นให้เป็นโรคเบาหวาน ดังนั้นจึงได้ทำการตรวจวัดสมบัติพื้นฐานของออกโซเมทอลเลตว่าสามารถเกิดอันตรกิริยากับผิวสัมผัสร่วมอย่างไร ตามรายงานอ้างอิงถึงเมทฟอร์มินส่งผลต่อพันธะไฮโดรเจนของน้ำ ดังนั้นจึงได้ทำการวิเคราะห์ว่าเมทฟอร์มินมีผลต่อน้ำภายในไมเซลล์ฝักกลับและการ

จัดตัวของน้ำบริเวณผิวสัมผัสร่วมอย่างไร ในงานวิจัยนี้รายงานผลของไอออนบวกของเคอะเวเนเดต ส่งผลอย่างมีนัยสำคัญต่อการละลายของเกลือ แม้เพียง 1% ของการแทนที่ไอออนบวกโซเดียมในสถานะของสารละลายที่ไม่เป็นเนื้อเดียวกัน การแทนที่ของไอออนบวกในระบบของโซเดียม AOT ไมเซลล์ผันกลับด้วยไอออนของเมทฟอร์เมียมส่งผลต่อการจัดโครงสร้างในระดับนาโนนั้นช่วยเพิ่มประสิทธิภาพในการละลายและคาดว่าจะส่งผลต่อความสามารถในการผ่านเข้าออกเยื่อเลือกผ่านของไอออนลบ

ดังนั้นการศึกษานี้อาจนำมาประยุกต์สำหรับออกแบบและติดตามการเกิดอันตรกิริยาของไอออนเมทฟอร์เมียมและเคอะเวเนเดตกับผิวสัมผัสร่วมของไมเซลล์ผันกลับ และการผ่านเข้าสู่เยื่อหุ้มเซลล์ของไอออนเคอะเวเนเดตที่ถูกกระตุ้น โดยผลของไอออนบวกของเมทฟอร์มีน



AUNGKANA CHATKON : SYNTHESIS AND STRUCTURAL STUDY OF MATERIALS COMBINING METFORMIN WITH OTHER COMPOUNDS USED FOR DIABETES THERAPY. THESIS ADVISOR : ASSOC. PROF. KENNETH J. HALLER, Ph.D. 120 PP.

METFORMIN/DECAVANADATE/AOT REVERSE MICELLES/DIABETES

Syntheses of new crystalline materials containing metformin in combination with the therapeutic agent decavanadate, used in treating diabetes, are of interest as potential candidates for new synergistic materials to decrease required dosage of metformin or metal resulting in a decrease in their toxicity as treatments. Investigation into how these combined materials interact with the interface of reverse micelles may give insight into their interactions with cell membranes.

The active pharmaceutical agent, metformin hydrochloride (MetHCl), was isolated from the drug and characterized by FTIR, melting point, and X-ray diffraction techniques. The crystallographic results show a pronounced π -electron delocalization on the biguanide group that is interrupted at the center bridging N atom, with a large dihedral angle (φ) between the two guanidine groups. The presence of intermolecular N–H...N' hydrogen bonding interactions between cation groups and N–H...Cl and C–H...Cl hydrogen bonding between cation and anion form a 3D supramolecular network.

Solutions of MetHCl at various pH were studied; ^1H NMR chemical shifts at 3.05 ppm at pH = 1 and 2.77 ppm at pH = 14 of the $-\text{CH}_3$ group are consistent with deprotonation of metformin at alkaline pH. In sodium bis(2-ethylhexyl)sulfosuccinate (AOT) reverse micelle systems the methyl protons show downfield chemical shifts that can suggest that metformium ion is associated with the interface.

A compound containing metformium cation (HMet^+) and decavanadate anion (V_{10}) was synthesized and characterized. The material is not soluble in water but slightly soluble in dimethylsulfoxide and very soluble in the inhomogeneous environment of AOT reverse micelles, deviating significantly from the properties of sodium decavanadate. Considering the fact that V_{10} is reported to have insulin enhancing activity in STZ induced diabetic rats, the fundamental properties of how this oxometalate interacts with interfaces was investigated. Since metformin is reported to affect the H-bonding in water, how it affects the water pool and water organization near the interface of the reverse micelles was investigated. These studies demonstrate that the counterion to the decavanadate anion significantly affects the solubility of the salt, and thus illustrates the importance of even 1% substitution of the sodium cations in inhomogeneous environments. The presence of HMet^+ ions that replace the counter ion to AOT in a sodium AOT reverse micellar system affects the organization of the nanostructure and significantly improves the solubility and presumed permeability of the anion.

This may have important implications in the design and monitoring of metformium and decavanadate ion interactions with the interface of reverse micelles and implies the potency of coadministration of metformin cation to activate transfer of decavanadate across the cell membrane.

ACKNOWLEDGEMENTS

I would like to express my sincerest gratitude to my advisor, Assoc. Prof. Dr. Kenneth J. Haller, for his advice, enthusiasm, valuable suggestions, and patience throughout the years of my studies. Indeed I have become stronger because of his philosophy and psychology. It is very fortunate to have worked under his supervision. I would also like to extend my sincerest gratitude to Prof. Dr. Debbie C. Crans, Colorado State University (CSU), USA for her help and assistance as coadvisor. Thank you for chemicals, equipment, support, and inspiring advice during my overseas research in the USA.

I would also like to express my gratitude to all of the teachers at the School of Chemistry who have taught and helped me during my study at SUT.

I wish to express my special thanks to the chairman of the School of Chemistry, Assoc. Prof. Dr. Jatuporn Wittayakun, and thesis examining committee members, Asst. Prof. Dr. Kunwadee Rangriwatananon, and Prof. Dr. Adrian E. Flood for their warm hearted support, encouragement, help, and suggestions.

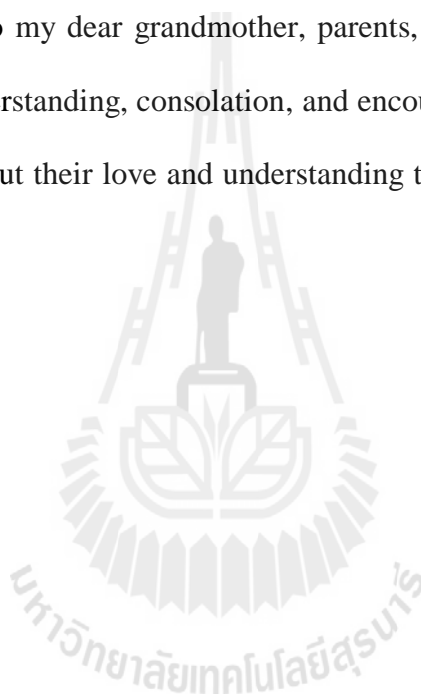
Thank you to the Commission on Higher Education, Thailand for financial support (CHE-PHD-SW-2549) of my Ph.D. program and an overseas travel grant allowing me to spend one year at CSU as part of my Ph.D. research program, and for opportunities to present parts of my work at conferences of the Asian Crystallographic Association (Korea, 2010), the American Crystallographic Association (USA, 2011), the International Union of Crystallography (Spain, 2011), the 242nd meeting of the American Chemical Society USA, 2011, and the 27th European Crystallographic

Meeting (Norway, 2012). Thanks to the Asian Crystallographic Association for a Bursary student award to support my attendance at Taiwan, 2007, and Korea, 2010.

I would also like to thank all of my colleagues in Dr. Crans's research group at CSU, Dr. Haller's research group at SUT, and my other friends at CSU and SUT for all their support, help, and encouragement throughout the time of my studies.

Finally, I would like to take this opportunity to express my deepest appreciation and sincerest gratitude to my dear grandmother, parents, sister, and my best friend for their love, devotion, understanding, consolation, and encouragement throughout the long years of my study. Without their love and understanding this work would not have been successful.

Aungkana Chatkon



CONTENTS

	Page
ABSTRACT IN THAI	I
ABSTRACT IN ENGLISH	III
ACKNOWLEDGEMENTS	V
CONTENTS	VII
LIST OF TABLES	X
LIST OF FIGURES	XI
LIST OF ABBREVIATIONS	XIII
CHAPTER	
I INTRODUCTION	1
1.1 Diabetes and Diabetes Treatment	1
1.2 Chemistry and Biochemistry	9
Metformin	9
Chromium	11
Decavanadate	15
1.3 Cocrystals and Complexes	20
1.4 References	21
II REVERSE MICELLES	30
2.1 Introduction	30
2.2 Molecular Aggregation of Surfactant	31
Thermodynamics of Self-Assembly	31
Geometrical Surfactant Parameter	33

CONTENTS (Continued)

	Page
2.3 Reverse Micelles	37
AOT/isooctane/water reverse micelles	38
Polydispersity	41
2.4 References	42
III EXPERIMENTAL	46
3.1 Materials, Methods, and Synthesis	46
3.2 Instrumentations	50
3.3 Research Procedure	52
3.4 References	52
IV METFORMIN HYDROCHLORIDE	54
4.1 Introduction	54
4.2 Experimental	55
4.2.1 Materials	55
4.2.2 Sample Preparation	56
4.2.3 Characterization	56
4.2.4 Instrumentations	57
4.3 Results and Discussion	57
4.4 Conclusions	66
4.5 References	66

CONTENTS (Continued)

	Page
V DECAVANADATE COUNTERION AFFECTS INTERACTION WITH INTERFACES: COMPLEXATION WITH THE ANTIDIABETIC DRUG METFORMIN	72
5.1 Introduction	72
5.2 Experimental	77
5.2.1 Materials	77
5.2.2 Sample Preparation	77
5.2.3 Characterization	79
5.2.4 Instrumentation	80
5.3 Results and Discussion	81
5.4 Conclusions	95
5.5 References	96
VI CONCLUSIONS	107
Conclusions	107
Suggestions for Future Work	109
APPENDICES	110
APPENDIX A GLOSSARY	111
APPENDIX B OCCUPATION NUMBER	115
APPENDIX C SUPPORTING INFORMATION CHAPTER V	117
CURRICULUM VITAE	120

LIST OF TABLES

Table	Page
1.1 Therapeutic agents used in diabetes mellitus treatment	3
1.2 Combinations of metformin with other compounds in diabetes treatment	8
1.3 Adequate intakes for trivalent chromium	14
2.1 Surfactant packing parameter range for various surfactant aggregates	36
3.1 Component volume in 1 mL sample of 0.2 M and 0.75 M AOT RMs at various w_0	49
4.1 IR band assignments for metformin hydrochloride	58
4.2 Bond lengths of metformin hydrochloride	60
4.3 Hydrogen bonding in metformin hydrochloride	62
4.4 ^1H NMR chemical shifts of metformin hydrochloride as a function of pH	63
4.5 ^1H NMR chemical shifts of MetHCl in 0.2 M AOT/isooctane RMs	64
5.1 Chemical shifts and line widths for the three ^{51}V NMR signals of V_{10} in NaV_{10} and MetV_{10} in 0.75 M AOT RMs with various w_0	86
5.2 The sizes of 0.2 M AOT/isooctane reverse micelles containing water with Met:HCl , NaV_{10} , and MetV_{10} as determined by dynamic light scattering	87
5.3 FT-IR data for the OD stretch of 5% HOD in H_2O in 0.2 M AOT RMs prepared with and without MetV_{10}	90

LIST OF FIGURES

Figure	Page
1.1 Schematic diagrams of the structure of neutral biguanide	9
1.2 Formal diagrams illustrating speciation of metformin	10
1.3 Proposed mechanism for the activation of insulin receptor activity by chromodulin in response to insulin	13
1.4 Structure of $V_{10}O_{28}^{6-}$ anion	16
1.5 Reaction of peroxovanadate formation by SSAO metabolization	17
1.6 Proposed mechanism for action of hexa(benzylammonium) decavanadate in the cell	17
1.7 Proposed mechanism of decavanadate to cellular targets	19
2.1 Geometrical model of surfactant molecules with different characteristics	34
2.2 Structure of an AOT molecule	38
2.3 Phase diagram for AOT/isooctane/water ternary mixtures at ambient pressure and room temperature	40
2.4 Schematic diagram of an AOT reverse micelle	41
3.1 1H NMR of NaAOT in d_6 -DMSO	48
4.1 The IR spectrum of metformin hydrochloride	58
4.2 XRD spectra of metformin hydrochloride	59
4.3 Diagram of metformin hydrochloride	60
4.4 Aggregation of $HMet^+$ cations in one chain	61
4.5 Packing diagram of metformin hydrochloride	61
4.6 1H NMR spectrum of $HMet^+$ cation in d_6 -DMSO	63

LIST OF FIGURES (Continued)

Figure	Page
4.7	^1H NMR spectra of HMet^+ in D_2O , MeOH, and 0.2 M AOT RMs at $w_0 = 6$ and 10 64
5.1	Structures of decavanadate; $[\text{V}_{10}\text{O}_{28}]^{6-}$, neutral metformin, the protonated form of metformin, and AOT 75
5.2	^1H NMR spectra of Met:HCl in DMSO and MetV_{10} in DMSO and in Met:HCl, NaV_{10} , and MetV_{10} measured using IR spectroscopy 83
5.3	^{51}V NMR spectra of 2.0 mM of NaV_{10} and MetV_{10} in 0.75 M AOT RMs with $w_0 = 5, 6, 8, 10,$ and 16 85
5.4	Absorbances for the O–D stretch in AOT RMs containing aqueous solutions of MetHCl, NaV_{10} , and MetV_{10} measured using IR spectroscopy 90
5.5	Schematic representation of MetV_{10} in RMs consistent with the spectroscopic observations by NMR and IR as well as DLS experiments 92

LIST OF ABBREVIATIONS

มะระขี้เมีน	Momordica charantia or bitter melon
Å	Ångstrom, non-SI unit of distance commonly used in crystallography
δ	chemical shift
$\Delta\mu^0$	difference in standard chemical potential
$\Delta\nu_2$	line width
ΔG^0	difference in standard gibbs free energy
μ_i^0	standard chemical potential for molecule in an aggregate of size i
μ_l^0	standard chemical potential in monomer state
μ_n^0	standard chemical potential of molecules in aggregate state
φ	dihedral angle
2L	unstable phase in ternary phase diagram
a	effective area of the head group
AC	anion channel
AOT	sodium bis(2-ethylhexyl)sulfosuccinate
BMOV	bis(maltolato)oxovanadium(IV)
B_n	formation of aggregates of n molecule
C	surfactant concentration
cal	calorie, non-SI unit of energy
CMC	critical micelle concentration
CTAB	hexadecyl-trimethyl ammonium bromide
D	lamellar
D ₂ O	deuterium oxide

LIST OF ABBREVIATIONS (Continued)

DLS	dynamic light scattering
DMSO	dimethyl sulfoxide
F	hexagonal
FBG	fasting blood glucose
FPG	fasting plasma glucose
FT-IR	Fourier transform infrared spectroscopy
GLUT	glucose transporter
GSK3	glycogen syntase kinase 3
GTF	glucose tolerance factor
HbA _{1c}	hemoglobin A _{1c}
HDL	high density lipoprotein
HMet ⁺	metformium cation
IDDM	insulin dependent diabetes mellitus
IFG	impaired fasting glycaemia
IGT	impaired glucose tolerance
IRS	insulin receptor
k_B	Boltzmann constant
k_{eq}	equilibrium constant
k_n	molar concentration of reactant
l	length of surfactant hydrocarbon chain
L	liquid crystalline structure
L ₁	aqueous micellar phase
L ₂	isotropic reversed micellar phase

LIST OF ABBREVIATIONS (Continued)

LC	lyotropic liquid crystal phases
LDL	low-density lipoprotein
LMWCr	low-molecular-weight chromium-binding substance
Met	neutral molecule form of metformin
Met:HCl	metformin hydrochloride
MetV ₁₀	metformium decavanadate
N_A	Avogadro constant
n_{avg}	surfactant aggregation number
n_c	number of carbon atoms in the surfactant tail
NIDDM	Noninsulin dependent diabetes mellitus
nM	nanomolar
NMR	Nuclear magnetic resonance
N_s	surfactant packing parameter
O_{cc}	occupation number
PD	polydispersity
PPG	postprandial plasma glucose
r	average micelle radius
R	gas constant
r_h	radius of micelle
RM _s	reverse micelles
r_w	radius of water pool
SANS	Small angle neutron scattering
SAXS	Small angle X-ray scattering

LIST OF ABBREVIATIONS (Continued)

SEM	Scanning electron microscopy
<i>S. cerevisiae</i>	<i>saccharomyces cerevisiae</i>
SSAO	semicarbazide-sensitive amine oxidase
<i>T</i>	temperature (K)
TEM	transmission electron microscopy
TMS	tetramethylsilane
<i>V</i>	volume of surfactant
v_0	effective volume of a water molecule
V_{10}	decavanadate
$[\text{VO}_2\text{dipic}]^-$	vanadium dipicolinate anion
v_s	surfactant head group volume
w_0	molar ratio of concentration of water and surfactant
WHO	World Health Organization
X_l	mole fraction of isolated surfactant molecules
X_n	mole fraction of surfactant molecules in aggregates
XRD	X-ray diffraction

CHAPTER I

INTRODUCTION

1.1 Diabetes and Diabetes Treatment

Diabetes mellitus has been defined as a chronic metabolism disorder characterized by high blood glucose concentration caused by insulin deficiency, often combined with insulin resistance (Gardner and Shoback, 2011). Insulin is a hormone that regulates blood sugar. The body of a diabetic patient does not produce or use insulin properly to stimulate the uptake of glucose, fatty acids, and amino acids from blood circulation for storage or utilization. Undersupply of glucose leads to apoptosis (cell death) and oversupply leads to damage of various organs. It is necessary to maintain regulation of the blood glucose concentration before meal in the optimal range, 72-106.2 mg/dL (International Diabetes Federation, 2007). Most patients can be classified clinically as having either type 1 diabetes mellitus (insulin dependent diabetes mellitus or IDDM) or type 2 diabetes mellitus (noninsulin dependent diabetes mellitus or NIDDM). Type 1 diabetes includes cases resulting from pancreatic β -cell (cells that produce insulin) destruction or gestational diabetes characterized by hyperglycemia during pregnancy. About 5% to 10% of all diagnosed cases of diabetes were found in children and young adults. Risk factors for type 1 diabetes may be autoimmune, genetic, or environmental. Type 2 diabetes is mainly due to insulin resistance or reduced insulin sensitivity, combined with reduced insulin secretion and is largely as a result of excess body weight and physical inactivity. Diabetes mellitus is now becoming one of the major health problems worldwide. Over 285 million adults (6.4%) are affected, and this number is

expected to double by 2030. The greatest increase in prevalence is occurring in Asia and Africa. Similar trends are occurring in Thailand; the prevalence of diabetes in Thai adults has increased to 3.54 million (7.7%) in 2010 and is expected to reach 4.96 million in 2030 (Shaw, Sicree, and Zimmet, 2010). Diabetes can lead to serious microvascular and macrovascular complications including retinopathy^{*}, nephropathy, coronary heart disease, cerebrovascular disease, and peripheral vascular disease. It causes individual and societal problems in the costs of treatment, lower work efficiency, and premature death.

The basic treatment for type 2 diabetes mellitus in the initial phase is dietary modification and exercise to induce weight loss and lower plasma glucose levels (normalize blood glucose levels) with or without pharmacologic agents, generally prescribed as monotherapy. When this management regime fails to control blood glucose levels, a combination of hypoglycemic drugs may be used to control blood glucose levels (Joslin Diabetes Center, 2007). Therapeutic agents used in diabetes mellitus and their effects are summarized in Table 1.1.

Monotherapy. Metformin is widely available and used in many countries as an oral drug for treatment of type 2 diabetes mellitus patients. In the drug market, metformin is a valuable pharmaceutical product at 192nd on Wikipedia's best selling drugs list with sales of 459 million US dollars from Merck KGaA, and Bristol-Myers Squibb in 2006 (Wikipedia, 2011). Metformin has many benefits but adverse effects can occur in patients on high drug dosage for long periods of time.

* This and other medical terms, as well as abbreviations are defined in Appendix A.

Table 1.1 Therapeutic agents used in diabetes mellitus treatment.

Class of therapeutic agent	How it works
Examples	
Drugs^a	
Oral hypoglycemic drugs	
1. Sulfonylurea Glyburide, Gliclazide, Glimepiride	-Stimulate pancreatic β -cell insulin secretion
2. Biguanide ^b Metformin, Phenformin, Buformin	-Decrease hepatic glucose production, and increase glucose uptake by skeletal muscle and fat
3. Thiazolidinedione Pioglitazone, Rosiglitazone	-Improve cell response to insulin, and increase glucose uptake by skeletal muscle and fat
4. Meglitinide (nonsulfonylurea) Repaglinide, Nateglinide	-Stimulate pancreatic β -cell insulin secretion
5. α -glucosidase inhibitor Acarbose, Miglitol, Voglibose	-Slow the digestion and absorption of carbohydrates
6. Dipeptidyl peptidase-IV inhibitor Sitagliptin, Vildagliptin	-Help intestinal hormones stimulate insulin release
Subcutaneous injection drugs	
7. Insulin and analogs	-Replace or supplement endogenous insulin hormone to correct deficiency
8. Incretin mimetics Exenatide, Liraglutide	-Regulate glucose metabolism and insulin secretion
9. Pramlintide ^c	-Suppress glucagon secretion, and regulates food intake
Nutritional supplements^d	
1. Chromium Chromium picolinate, Brewer's yeast	-Increase activation of the insulin receptor in the presence of insulin, and increase binding of insulin to the insulin receptor
2. Vanadium Decavanadate	-Acts primarily as an insulin mimetic agent
3. Magnesium	-Improve insulin resistance and normal metabolism of macronutrients
4. Vitamin E	-Acts primarily as an antioxidant, preventing and treating common complications of diabetes
5. L-Arginine ^e	-Improve peripheral insulin sensitivity and hepatic insulin sensitivity
Herbal supplements^f	
1. <i>Gymnema Sylvestre</i> (Gurmar)	-Stimulate the production of insulin
2. <i>Momordica Charantia</i> (Bitter melon)	-Help cells use glucose and promote insulin release

a. Nielsen, 2005. b. Biguanide class: phenformin and buformin were withdrawn from the market because of an association with lactic acidosis. c. Goldstein and Müller-Wieland, 2008. d. Okochi and Okpuzor, 2005. e. Piatti, *et al.*, 2001. f. Mentreddy, 2007.

Metformin combination therapy with drugs. Researchers are studying reduced metformin dosage (to reduce harmful side effects) in combination with other therapeutic agents used for diabetes treatment. In a population of patients whose disease was insufficiently treated with glyburide, glyclazide, or glimepiride (sulfonylurea class) addition of metformin reduced fasting plasma glucose (FPG) and hemoglobin A_{1c} (HbA_{1c}) levels and increased high density lipoprotein (HDL) cholesterol (Hanefeld, Brunetti, Schernthaner, Matthews, and Charbonnel, 2004).

Therapy of rosiglitazone plus metformin can improve plasma glucose levels, insulin sensitivity, and β -cell function more effectively than treatment with metformin alone. The group that received metformin plus 8 mg/day rosiglitazone also achieved significant improvement in HbA_{1c} relative to the metformin plus 4 mg/day rosiglitazone group (Fonseca, Rosenstock, Patwardhan, and Salzman, 2000). After 1 year of therapy with pioglitazone plus metformin, insulin sensitivity was improved in diabetes patients (Ceriello, Johns, Widel, Eckland, Gilmore, and Tan, 2005).

In patients whose disease was inadequately controlled with diet and maximal metformin therapy, the addition of 25-50 mg/day acarbose to metformin therapy for 24 weeks significantly lowered HbA_{1c}, plasma glucose levels, and insulin level (Rosenstock, Brown, Fischer, Jain, Littlejohn, Nadeau, Sussman, Taylor, Krol, and Magner, 1998).

Metformin combination therapy with nutrition supplements. Administration of trivalent chromium to improve glucose tolerance has been reported since the 1960s (Glinsmann and Mertz, 1966) and its ability to act as an agent to improve insulin sensitivity has been confirmed by different researchers (Anderson, Polansky, Bryden, and Canary, 1991; Cefalu, Bell-Farrou, Stigner, Wang, King, Morgan, and Terry, 1999). Chromium supplements have been used in diabetic patients to improve glycemic control by monotherapy or combination therapy. In a chromium supplement study, Brewer's yeast (23.3 μ g Cr/day) or CrCl₃ (200 μ g Cr/day), plus metformin, no patient needed a

higher dosage of metformin, and both blood glucose and triglyceride levels decreased. Moreover, some patients no longer required insulin while taking chromium supplements (Bahijiri, Mira, Mufti, and Ajabnoor, 2000). Type 2 diabetic patients had improved blood glucose, insulin, and glucagon levels with dietary chromium chloride intake (200 µg/day for 14 weeks) (Anderson, Polansky, Bryden, and Canary, 1991). Chromium can be used to maintain normal blood glucose levels, to enhance insulin signaling, and to regulate proper carbohydrate, lipid, and protein metabolism (Anderson, 2000; Krejpcio, 2001).

Another mineral supplement, sodium metavanadate, could normalize blood glucose levels by stimulating glucose uptake in rats (Meyerovitch, Farfel, Sack, and Shechter, 1987). Bis(maltolato)oxovanadium(IV), or BMOV, used in a single dose can improve hyperglycemia with no adverse effects in diabetic rats (Caravan, Gelmini, Glover, Herring, Li, McNeill, Rettig, Setyawati, Shuter, Sun, Tracey, Yuen, and Orvig, 1995). Oral vanadyl sulfate (100 mg/day for 3 weeks) could improve hepatic and peripheral insulin sensitivity in type 2 diabetic patients (Cohen, Halberstam, Shlimovich, Chang, Shamoon, and Rossetti, 1995). Vanadyl sulfate (150 mg/day or 300 mg/day for six weeks) in diabetic patients decreased the fasting blood glucose and HbA_{1c} levels. At the higher dose, total cholesterol also decreased but there was gastrointestinal discomfort as well (Goldfine, Patti, Zuberi, Goldstein, LeBlanc, Landaker, Jiang, Willsky, and Kahn, 2000). The decavanadate compound was useful for diabetic patients, decreasing blood glucose levels and body weight (Nomiya, Torii, Hasegawa, Nemoto, Nomura, Hashino, Uchida, Kato, Shimizu, and Oda, 2001).

Metformin combination therapy with herbal Supplements. Oral treatment with a natural extract of *Momordica charantia* (มะระขี้นก) (500 mg/kg 3.5 hours after eating) has been reported to depress the level of plasma glucose by increasing glucose utilization in rat liver. *Momordica charantia* reduced plasma glucose by 26% while metformin caused 40-50% reduction (Shubhashish, Maddali, and Marita, 1996). *Momordica charantia* 6

$\mu\text{g/mL}$ could enhance glucose uptake through glucose transporter, GLUT4 (Kumar, Balaji, Uma, and Sehgal, 2009). Moreover, *Momordica charantia* 400 mg/day with 250 mg/day metformin for 7 days could potentiate their plasma glucose levels in type 2 diabetes patients (Tongia, Tongia, and Dave, 2004).

The harmful effect of hyperglycemia, induced oxidative stress, was reduced in diabetic rats treated with the combination regimen of 500 mg/day metformin and 120 mg/day of baicalin (flavonoid compound) for 30 days (Waisundara, Hsu, Tan, and Huang, 2009).

Diabetes therapies noted above as well as other combinations of metformin with hypoglycemic drugs and amino acids for restoring glycemic control are summarized in Table 1.2.

Single material combination therapies. Combination tablets containing metformin/glyburide (250/1.25 mg, 500/2.5 mg, and 500/5 mg) improved glycemic control and lowered levels of glycosylated hemoglobin, HbA_{1c}, in the blood in type 2 diabetes patients more than either metformin or glyburide treatment alone. Metformin/glyburide 500/2.5 mg is more effective than 500/5 mg and 250/1.25 mg (Garber, Larsen, Schneider, Piper, and Henry, 2002; Marre, Howlett, Lehertt, and Allavoine, 2002).

The bis(*N,N*-dimethylbiguanidato)oxovanadium(IV) complex given to diabetic rats (0.12 mmol/kg/day) was reported to improve plasma glucose levels to normal, but neither synergistic nor additive effects were observed when compared with vanadyl in BMOV form (Woo, Yuen, Thompson, McNeill, and Orvig, 1999).

A recently synthesized, covalently-bound cysteine and metformin material, cysteinyl metformin, has a much greater hypoglycemic effect than metformin alone. It also improves pancreatic β -cell function, increases insulin levels, and reduces triglycerides in diabetic rats (Liu, Li, Zeng, Liu, and Wang, 2008). The combination of

metformin and arginine in arginine hemisuccinimide metformin hemisuccinate 70 mg/kg/day for 3 weeks was more active to improve glucose levels than metformin alone (Rapin and Halbitte, 2007).

A new crystalline form of metformin and lipoic acid salt (induces glucose uptake through GLUT1 and GLUT4) has been demonstrated to decrease plasma glucose levels and reduce diabetic complications (Mylari and Vaman, 2007). A crystalline combination of metformin with ethyl-*N*-(4-methylphenyl)sulfonyl carbamate in metformin ethyl-*N*-(3-tosulfonyl)carbamate has been suggested to enhance the therapeutic effect of metformin and exhibit additional pancreas protecting effects in diabetic patients (Huang, Xi, Xu, Lui, and Zeng, 2008).

Moreover, it has reported that metformin dosage less than 100 mg/day when combined with bioavailable forms of chromium, vanadium, or magnesium could effect in diabetes treatment (Fine and Kinsella, 2002).

It has been clearly indicated that metformin alone, or chromium(III) and vanadium alone and in combination with metformin, can help to improve blood glucose levels and reduce complications in diabetic patients.

Table 1.2 Combinations of metformin with other compounds in diabetes treatment.

Authors	No. of Patients	Form (mg/day)	Duration	Significant effects
Separate agents				
Rosenstock <i>et al.</i> , 1998	168	Met + Acarbose 25-50	24 weeks	Decrease HbA _{1c} , plasma glucose levels
Bahijiri <i>et al.</i> , 2000	78	Met + Brewer's yeast (Cr 23.3 µg) Met + CrCl ₃ (Cr 200 µg/d)	32 weeks	Decrease drug dosage
Fonseca <i>et al.</i> , 2000	348	Met 2500 + Rosiglitazone 4 Met 2500 + Rosiglitazone 8	26 weeks	Decrease HbA _{1c} , Increase insulin sensitivity and weight gain
Furlong <i>et al.</i> , 2002	80	Met 850 or 1000 + Insulin	13 weeks	Decrease HbA _{1c} , FPG Increase body weight
Tongia <i>et al.</i> , 2004	5	Met 250 + <i>Momordica charantia</i> 400	7 days	Decrease plasma glucose levels
Hanefeld <i>et al.</i> , 2004	320	Met 850 to maximal dose 2550 + glyburide or glyclazide or glimepiride (sulfonylurea class)	52 weeks	Decrease HbA _{1c} , FPG Increase HDL cholesterol
Ceriello <i>et al.</i> , 2005	95	Met + Sulfonylurea	52 weeks	Increase insulin
	54	Met + Pioglitazone		sensitivity, Decrease
	62	Met + Glicazide		plasma glucose levels
Goldstein <i>et al.</i> , 2007	147	Met 500 + Sitagliptin 50	24 weeks	Decrease plasma glucose
	152	Met 1000 + Sitagliptin 50		levels
Waisundara <i>et al.</i> , 2009	Rat	Met 500 mg/kg + Baicalin 120 mg/kg	30 days	Decrease hepatic lipid peroxide concentration, Increase hepatic activity
Combination tablets				
Woo <i>et al.</i> , 1999	Rat	Bis(<i>N,N</i> -dimethylbiguanidato)oxovanadium(IV) 0.12 mmol/kg	72 hours	Decrease plasma glucose levels
Garber <i>et al.</i> , 2002	806	Met 250 / Glyburide 1.25 Met 500/ Glyburide 2.5	20 weeks	Decrease HbA _{1c} and plasma glucose levels
Marre <i>et al.</i> , 2002	411	Met 500 / Glyburide 2.5 Met 500 / Glyburide 5	16 weeks	Decrease HbA _{1c} and plasma glucose levels
Rapin and Halbitte, 2007	Rat	Arginine hemisuccinimide metformin succinate 70 mg/kg	3 weeks	Decrease plasma glucose levels
Mylari and Vaman, 2007	Rat	Metformin R-(+)-lipoate 1mg/kg to 60 mg/kg	12 days	Improve diabetic complication
Liu <i>et al.</i> , 2008	Rat	Cysteinyl metformin 100 mg/kg (to 300 mg/kg)	14 days	Increase insulin levels, Decrease plasma glucose and triglyceride levels

1.2 Chemistry and Biochemistry

Metformin: The biguanide derivatives, metformin, phenformin, and buformin, were introduced in the 1950's for type 2 diabetes treatment. Only metformin is available for use today because of the adverse lactic acidosis effects found with the others.

Biguanides are important compounds with pharmaceutical applications, including treatment of hyperglycemia, malaria, and microbial and viral infections. Biguanide is a strong organic base with $pK_{a'} = 12.8$ and $pK_{a''} = 3.1$ at 25°C. The crystal structure of the biguanide molecule shows it to be almost planar with a dihedral angle between the two planar halves of about 12.5°, and the mean C–N distance of 1.347(2) Å, indicating strong π -electron delocalization is present throughout the structure (Pinkerton and Schwarzenbach, 1978). A strong intramolecular hydrogen bond connects the N atoms of NH and NH₂ groups as shown in Figure 1.1(a). However, in the medicinal chemistry literature, biguanide and its derivatives are generally represented as Figure 1.1(b), which is less stable in energy than (a) by about 9.0 kcal/mol (Bharatam, Patel, and Iqbal, 2005). Biguanides are strong σ -donating ligands which can coordinate as monodentate or bidentate ligands with many metal ions, contributing electron density from the N lone pairs by overlap with vacant metal d orbitals to form σ bonds. The π -electron density of the metal-ligand chelate ring is generally delocalized reinforcing the planarity of the chelate ring (see Figure 1.1(c)).

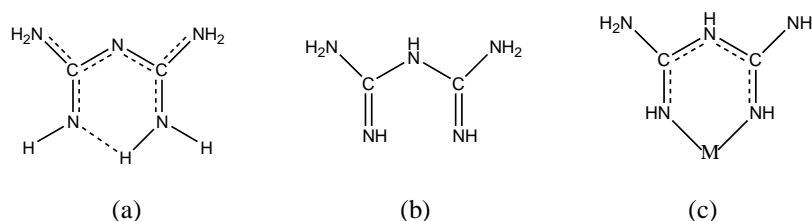


Figure 1.1 Schematic diagrams of the structure of neutral biguanide.

Metformin^{*}, is a biguanide derivative with two methyl groups substituted for the H atoms of one terminal –NH₂ group. Schematic diagrams of the speciation of neutral metformin and cationic metformin are shown in Figure 1.2. The most stable tautomer structure exhibits C=N bonds for the terminal and bridging nitrogen atoms as shown. Metformin has the strong basic character of a biguanide moiety; p*K*₁ 2.8 and p*K*₂ = 11.5 at 32°C in Equation 1.1, 1.2 (Ray, 1960). It forms the HCl salt quite readily giving the form most used in preparation of oral drug formulations of metformin. It also forms dibasic salts (H₂Met²⁺), including metformin oxalate and metformin sulfate (Lu, Zhang, Feng, and Zhu, 2004). The neutral (Met) metformin can form complexes with transition metals, as in [Cu(Met)₂]²⁺, [Ni(Met)₂]²⁻.

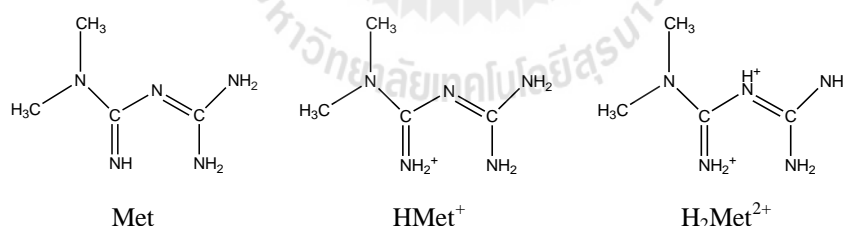


Figure 1.2 Formal diagrams illustrating speciation of metformin.

The oral drug Glucophage, metformin hydrochloride, C₄H₁₁N₅·HCl, has benefits in decreasing hepatic glucose production by reducing gluconeogenesis, and in enhancing

* Metformin is the neutral species, IUPAC name *N,N*-Dimethylimidodicarbonimidic diamide. In the drug and popular literature metformin is often used to refer to the hydrochloride salt, metformin hydrochloride or metformium chloride. The current thesis will use the following abbreviations: Met = neutral metformin; MetHCl = metformium chloride; HMet⁺ = monoprotonated metformin, metformium; H₂Met⁺ = diprotonated metformin; V₁₀ = any of the various protonated or nonprotonated V₁₀O₂₈⁶⁻ oxometalate species; NaV₁₀ = sodium salt of V₁₀O₂₈⁶⁻, MetV₁₀ = the product V₂O₅ and MetHCl at pH ~5, normally (HMet)₃(H₃O)₃V₁₀O₂₈·3H₂O (see page 47).

insulin sensitivity in muscle and fat without affecting the secretion of insulin. It also reduces low-density lipoprotein (LDL) cholesterol and does not induce weight gain (Goodman, Hardman, Limbird, and Gilman, 2001; Rang, Dale, Ritter, and Flower, 2007). The gastrointestinal absorption is about 50% (oral dose) and the maximum recommended daily dose is 2.5 g. The main side effect of metformin is gastrointestinal symptoms (*e.g.* abdominal discomfort, bloating, and nausea). Long term use may interfere with B₁₂ and folate absorption, and this drug cannot be used in patients with renal impairment, liver failure, or heart failure.

Chromium: Chromium occurs in various oxidation states from -2 to $+6$. Chromium oxidation state $+3$ is proposed to be biologically important. Cr³⁺ has a d³ electron configuration, thus half-occupied t_{2g} orbitals in octahedral coordination geometry. Chromium levels in tissues and biological fluids are extremely low, comparable with the magnitude of the detection limit of analytical techniques.

The first demonstrated benefits of chromium in diabetes treatment were reported by Mertz and Schwarz (1959). They reported that Cr³⁺ was an active ingredient of glucose tolerance factor, GTF, and could restore intravenous glucose tolerance more than other inorganic chromium compounds in rats injected with glucose. Brewer's yeast was identified as a natural source of GTF.

Benefits of Brewer's yeast and chromium to improve glucose tolerance were reported for both normal women and hyperglycemic women (Liu and Morris, 1978); Brewer's yeast (5 g, containing 4 µg of Cr, given for 3 months) reduced serum glucose and insulin levels. Isolated fractions from Brewer's yeast with the GTF property contain Cr³⁺, nicotinic acid, glycine, glutamate, and cysteine. Many researchers tried to extract the active component of GTF from yeast and identify its structure. The efforts were not successful and the active component of GTF has never been identified with certainty. Efforts to isolate the active component of GTF stopped in 1985 (Vincent, 2001).

Dietary chromium supplements can help in maintenance of normal glucose tolerance in rats and dietary chromium deficiency can be a cause of impaired glucose tolerance (Striffler, Law, Polansky, Bhathena, and Anderson, 1995). The possible benefit of chromium to improve glucose tolerance in humans has been intensively studied with the main focus on association between Cr^{3+} and type 2 diabetes. Research reviews report that chromium supplements can improve glycemia in type 2 diabetic patients (Balk, Tatsioni, Lichtenstein, Lau, and Pittas, 2007), and lower blood lipid levels (Press, Geller, Diego, and Evans, 1990).

The mechanism of chromium action in the cell is not certain, but Kandror (1999) suggested that Cr binding with transferrin in plasma with increasing insulin in blood stimulated Cr transport to the plasmatic membrane followed by its release to apochromodulin or apo-low-molecular-weight chromium-binding substance (apo-LMWCr) in insulin sensitive cells. The proposed mechanism for activation of insulin receptor kinase activity by chromodulin in response to insulin (Vincent, 2000; 2007) is shown in Figure 1.3.

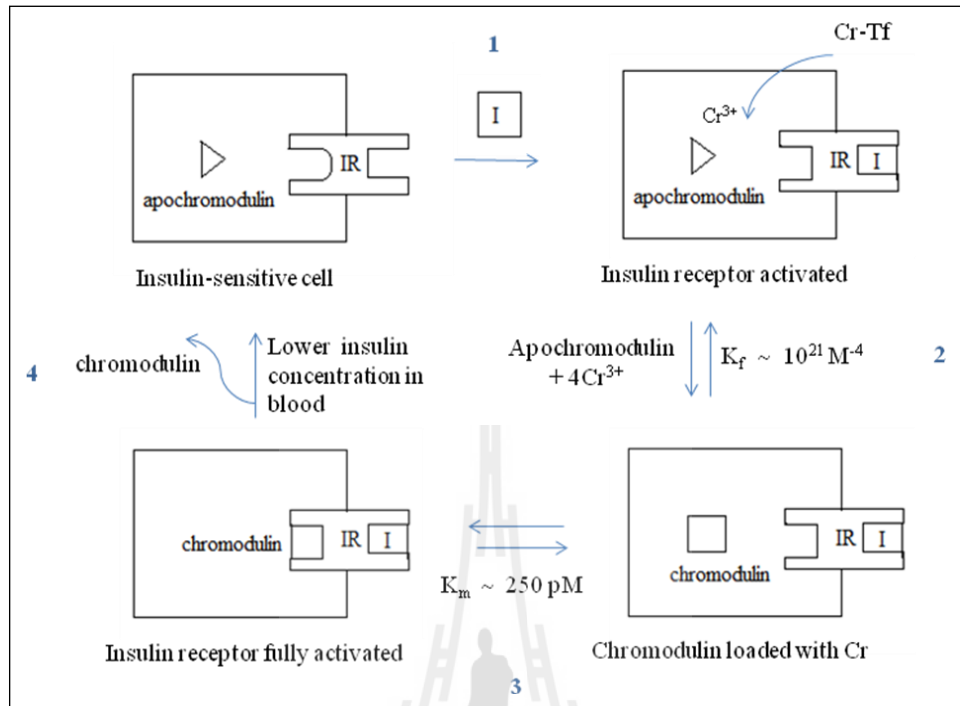


Figure 1.3 Proposed mechanism for the activation of insulin receptor activity by chromodulin in response to insulin. (redrawn after Vincent, 2000)

LMWCr is stored in insulin sensitive cells in an apochromodulin form (inactive form). In response to an increase in blood sugar, insulin is released into the blood stream and binds to an external α subunit of the transmembrane insulin receptor protein inducing the receptor to change conformation. The receptor auto-phosphorylates tyrosine residues on the internal β subunit turning the receptor into an active kinase. At the same time, chromium binding transferrin moves into the insulin dependent cell and releases chromium to the cytosol which results in binding of four chromium atoms to chromodulin (active form of apochromodulin) which binds to the insulin receptor, helping to maintain its active conformation and amplifying the insulin signal to stimulate the translocation of glucose transporters into the plasmic membrane for uptake of glucose from the blood. When the insulin concentration drops, chromodulin is released from the cell into the blood to relieve its effects. Ultimately, chromodulin is excreted in urine.

The human body can absorb only 0.4-2.0% of ingested inorganic chromium, but up to 10% of ingested organic chromium (chromium in food, chromium and amino acid, and Brewer's yeast). Chromium tends to be stored in the liver, spleen, kidneys, lungs, bones, and hair (Morris, Kemp, and Hardisty, 1985). Chromium deficiency in humans induces glucose intolerance, inhibited glucose utilization, neuropathy, abnormalities of nitrogen metabolism, and high free fatty acid levels. Improved chromium nutrition could improve glucose tolerance, insulin sensitivity and diabetes (Jeejeebhoy, Chu, Marliss, Greenberg, and Bruce-Robertson, 1977; Pechova and Pavlata, 2007).

Adequate intake recommendations for normal healthy individuals established for different age/gender groups are shown in Table 1.3. Anderson (1998) and Lamson and Plaza (2002) suggested that diabetic patients need chromium supplement ≥ 200 $\mu\text{g}/\text{day}$ for potent treatment. Trivalent chromium has a low order of toxicity but the effect can occur if intake ≥ 250 $\mu\text{g}/\text{day}$. Cr^{3+} occurs naturally in a wide variety of foods such as egg yolk, Brewer's yeast, beef, cheese, liver, wine, bread, wheat, black pepper, chili, apple, and potatoes.

Table 1.3 Adequate intakes for trivalent chromium.

Age	Infants and children ($\mu\text{g}/\text{day}$)	Males ($\mu\text{g}/\text{day}$)	Females ($\mu\text{g}/\text{day}$)	Pregnancy ($\mu\text{g}/\text{day}$)	Lactation ($\mu\text{g}/\text{day}$)
0-6 months	0.2				
7-12 months	5.5				
1-3 years	11				
4-8 years	15				
9-13 years		25	21		
14-18 years		35	24	29	44
19-50 years		35	25	30	45
>50 years		30	20		

(Institute of Medicine, Food and Nutrition Board, 2001.)

Decavanadate: Vanadium is a trace element which is essential for some living organisms. In biological systems vanadium is found predominantly as vanadyl (+4) and vanadate (+5) forms. In blood plasma vanadium exists in both oxidation states. Vanadates are known inhibitors and also stimulators of many enzymes. For example, they inhibit protein phosphatases, but at the same time induce protein kinase activation, the key factor in the insulin mimetic properties of vanadate species (Verma, Cam, and McNeill, 1998; Rehder, 2003; Crans, Smee, Gaidamauskas, and Yang, 2004; Jelikić-Stankov, Uskoković-Marković, Holclajtner-Antunović, Todorovic, and Djurdjević, 2007). Among the vanadate oligomers, decavanadate ($V_{10}O_{28}^{6-}$) is a strong inhibitor of several enzymes and acts as an insulin mimetic agent (Messmore and Raines, 2000; Aureliano and Gândara, 2005; Ramos, Manuel, Tiago, Duarte, Martins, Gutiérrez-Merino, Moura, and Aureliano, 2006; Aureliano and Crans, 2009) with lower toxicity when compared to the other oligomers (Domingo, 1996; 2002).

During the last two decades, more than three hundred research articles about crystal structures and biological effects of decavanadate species, including fourteen *in vivo* studies on diabetes were reported. In aqueous solution a variety of vanadate species occur in equilibrium including monomeric (V_1), dimeric (V_2), tetrameric (V_4), pentameric (V_5), and decameric (V_{10}) species, depending on pH and concentration (Livage, 1991). Decavanadate species ($V_{10}O_{28}^{6-}$) are prevalent at pH about 3.5-6.3, with the color changing from orange to yellow as the various protonation states dominate in solution, $V_{10}O_{28}^{6-}$, $HV_{10}O_{28}^{5-}$, $H_2V_{10}O_{28}^{4-}$, and $H_3V_{10}O_{28}^{3-}$ as the pH decreases. The structure of decavanadate anion has been established by several X-ray studies. It exhibits approximate D_{2h} symmetry, and consists of ten distorted octahedral VO_6 units, with three types of vanadium atoms: four atoms capping, two atoms in the center, and four atoms on the extremity of the structure (Figure 1.4). The unique structure is compact with dimensions of $8.3 \times 7.7 \times 5.4 \text{ \AA}$ (Aureliana and Crans, 2009).

New decavanadate materials containing amines were reported in 2007. Amine ligands are semicarbazide-sensitive amine oxidase (SSAO) substrates. SSAO is part of the mechanism that transports glucose into the cell. Hexabenzyl ammonium decavanadate dihydrate, $[(C_7H_{10}N)_6V_{10}O_{28} \cdot 2H_2O]$, 2.5 $\mu\text{mol/kg}$ body wt/day, lowered glycemia and normalized plasma lipids in diabetic rats, even in the absence of circulating insulin (Garcia-Vincente, Yraola, Marti, González-Muñoz, Garcia-Barrado, Cantó, Abella, Bour, Artuch, Sierra, Brandi, Carpéné, Moratinos, Camps, Palacin, Testar, Gumà, Albericio, Royo, Mian, and Zorzano, 2007). The authors reported that the compound acts as insulin mimetic and suggested it could be useful for diabetic patients with severe insulin resistance. Benzylamine combined with decavanadate in $[(C_7H_{10}N)_6V_{10}O_{28} \cdot 2H_2O]$ can stimulate glucose uptake in isolated rat adipocytes by generated peroxovanadate insulin mimetic agent. A proposed mechanism for the action of $[(C_7H_{10}N)_6V_{10}O_{28}]$ in the cell is shown in Figure 1.4 (Yraola, Garcia-Vincente, Marti, Albericio, Zorzano, and Royo, 2007; Zorzano, Palacin, Marti, and Garcia-Vincente, 2009)

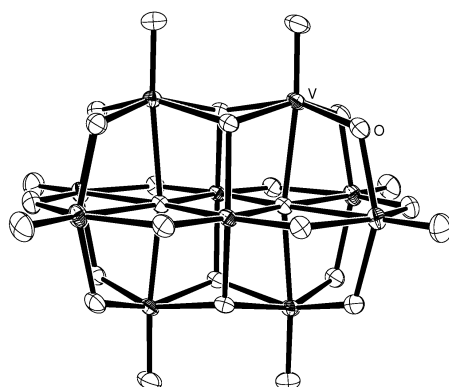


Figure 1.4 Structure of $V_{10}O_{28}^{6-}$ anion.

$(C_7H_{10}N)_6V_{10}O_{28}$ rapidly dissociates and generates various anionic species of vanadium (VO_4^{3-} , $V_2O_7^{4-}$, $V_4O_{14}^{4-}$), monovanadium and tetravanadium species as potentially active vanadates in the blood stream (pH 7.4, at 37°C). In a separate process

benzyl ammonium is metabolized by SSAO to generate six equivalents of hydrogen peroxide (H_2O_2). H_2O_2 reacts with vanadate species to generate peroxovanadate species and orthovanadate in the extracellular space (in Figure 1.5). These species enter the cell through anionic channels to activate insulin receptor (IRS) and glycogen syntase kinase 3 (GSK3) which promotes translocation of glucose transporter 4 (GLUT4) to the cell membrane for stimulated glucose uptake in adipocyte cells (in Figure 1.6).

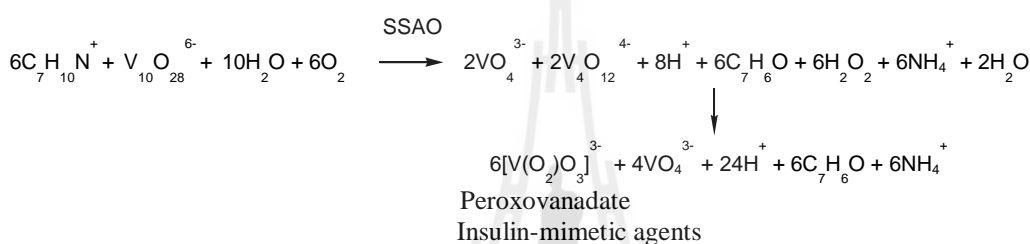


Figure 1.5 Reaction of peroxovanadate formation by SSAO metabolization.

(redrawn from Yraola *et al.*, 2007)

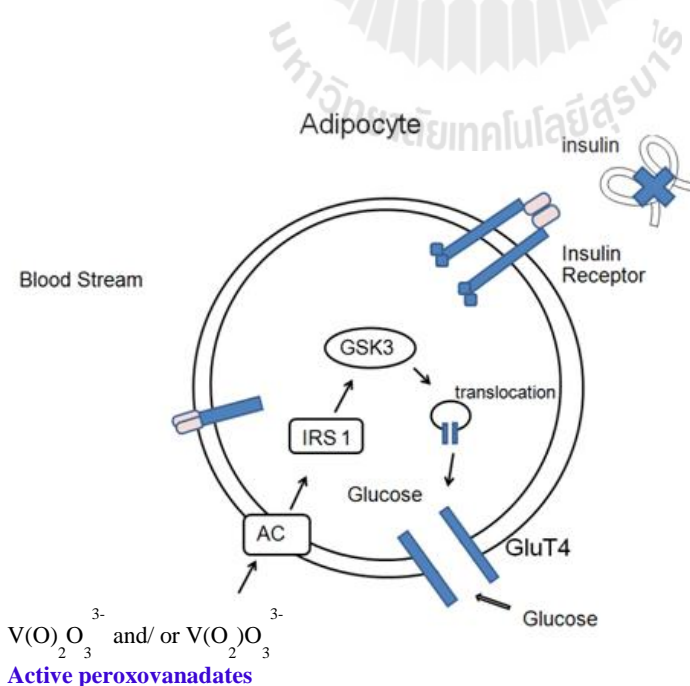


Figure 1.6 Proposed mechanism for action of hexa(benzylammonium) decavanadate in the cell. (redrawn from Yraola *et al.*, 2007).

Decavanadate with amine more effectively stimulated glucose uptake in rat adipocyte cell when insulin was present than other vanadium compounds, including metavanadate, amavadine or bis(*N*-hydroxylamidoiminodiacetate)vanadium(IV), bis(maltolato)oxovanadium(IV), and 2,6-pyridinedicarboxylatodioxovanadium(V) (Pereira, Carvalho, Eriksson, Crans, and Aureliano, 2009).

In 1984 the Willsky group found decavanadate in yeast *S. cerevisiae* that confirmed not only monomeric vanadate but also decavanadate can exist in the cell. Aureliano and Crans proposed a mechanism of decavanadate to cell target as in Figure 1.7. V_{10} uptake occurs through anionic channels (AC) or interaction with membrane protein. V_{10} formation upon intracellular vanadium acidification in cytosol, but most probably in acidic organelles. Reduction of monomeric vanadate by antioxidant agents. Binding of V_{10} to target proteins such as mitochondria, contractile system, and in calcium homeostasis. Moreover, they reported that decavanadate accumulates in the mitochondria, with nM concentration of decavanadate inducing membrane depolarization and inhibition of oxygen consumption (Aureliano and Crans, 2009; Aureliano, 2011).

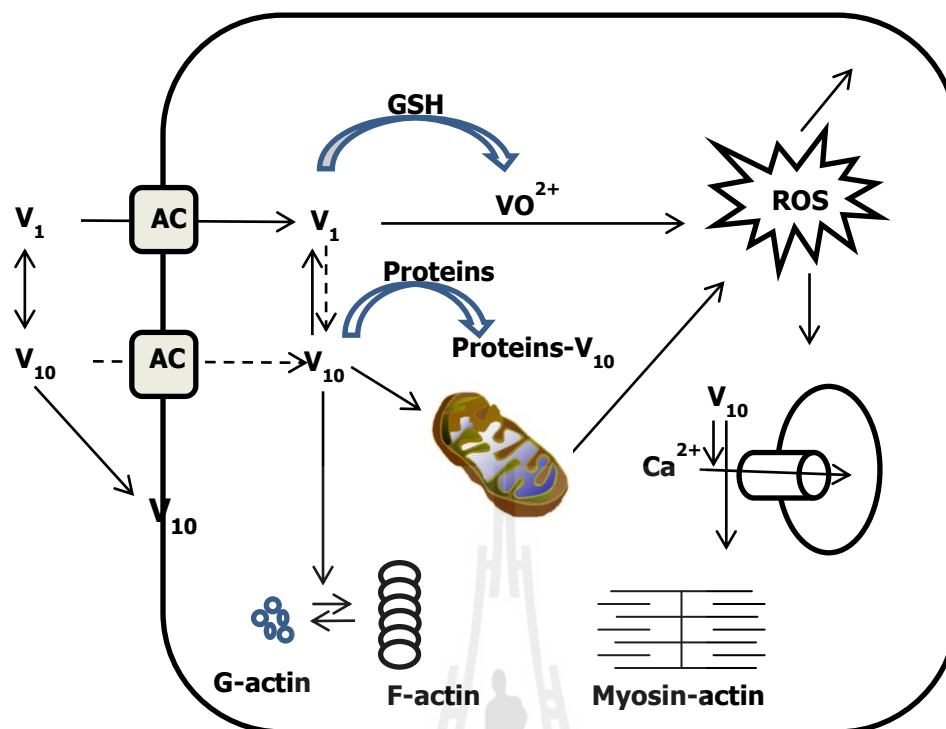


Figure 1.7 Proposed mechanism of decavanadate to cellular targets.

(redrawn from Aureliano and Crans, 2009)

The total amount of vanadium in the human body is about 100-200 μg , with daily intake suggested in the range of 10-20 $\mu\text{g}/\text{day}$. The US Food and Nutrition Board suggested a tolerable upper intake level for dietary intake of 1.8 mg/day for adults (Domingo, 1996). Vanadium deficiency has not been reported in humans but lack of vanadium induces growth impairment and impaired reproductive activity in chicks and rats (Okochi and Okpuzor, 2005). Organic vanadium is usually better absorbed in the gastrointestinal tract than inorganic vanadium and the highest distribution of vanadium is in nail, skin, plasma, and liver, mainly stored in fat and serum lipids. Larger doses are toxic and noxious, irritating the eyes and mucous membranes of the upper respiratory tract, and causing coughing, fatigue, and depression (Goc, 2006). Vanadium occurs naturally in a wide variety of foods such as vegetable oils, fats, olives, black pepper, and sea food.

1.3 Cocrystals and Complexes

Combinations of therapeutic agents can increase effectiveness for diabetic treatment. This has been demonstrated in the case of complexes of chromium or vanadium, cocrystalline metformin materials, salts of vanadates, and salts of metformin itself, as discussed above. Crystals that combine therapeutic agents in the same lattice (salts, and cocrystals) offer immense opportunities, not only in treatment regimes, but also to improve physicochemical properties such as solubility and stability, and to enhance pharmaceutical properties, including bioavailability and therapeutic effect. A common feature of these materials is that multiple components are stabilized into one lattice by supramolecular interactions, bringing the full force and potential of crystal engineering to bear in the quest for improved treatments of not only diabetes mellitus, but also cardiovascular disease, and perhaps several other diseases noted earlier.

In this study the author are interested in separation of metformin hydrochloride and synthesis of new crystalline materials containing metformin in combination with the therapeutic agent, decavanadate. These compounds were characterized by Fourier transform infrared spectroscopy, elemental analysis, thermogravimetric analysis, and single crystal X-ray crystallography. Including, investigate how these compounds interact with the interface of AOT reverse micelles by the nuclear magnetic resonance technique (NMR). NMR is a powerful method allowing us to measure properties of ions in the inhomogeneous environment of reverse micelles (RMs), while differential FT-IR studies probe the effect of H-bonding in the water pool of RMs, and dynamic light scattering (DLS) studies report on accompanying changes in RM size.

1.4 References

- Anderson, R. A. (1998). Chromium, glucose intolerance and diabetes. **Journal of the American College Nutrition**. 17: 548-555.
- Anderson, R. A. (2000). Chromium in the prevention and control of diabetes. **Diabetes & Metabolism (Paris)**. 26: 22-27.
- Anderson, R. A., Polansky, M. M., Bryden, N. A., and Canary, J. J. (1991). Supplemental chromium effects on glucose, insulin, glucagon, and urinary chromium losses in subjects consuming controlled low-chromium diets. **The American Journal of Clinical Nutrition**. 54: 909-916.
- Aureliano, M. (2011). Recent perspectives into biochemistry of decavanadate. **World Journal of Biological Chemistry**. 2: 215-225.
- Aureliano, M. and Crans, D. C. (2009). Decavanadate ($V_{10}O_{28}^{6-}$) and oxovanadates: Oxometalates with many biological activities. **Journal of Inorganic Biochemistry**. 103: 536-546.
- Aureliano, M. and Gândara, R. M. C. (2005). Decavanadate effects in biological systems. **Journal of Inorganic Biochemistry**. 99: 979-985.
- Bahijiri, S. M., Mira, S. A., Mufti, As'aad M., and Ajabnoor, M. A. (2000). The effect of inorganic chromium and brewer's yeast supplementation on glucose tolerance, serum lipid and drug dosage in individuals with type 2 diabetes. **Saudi Medical Journal**. 21: 831-837.
- Balk, E. M., Tatsioni, A., Lichtenstein, A. H., Lau, J., and Pittas, A. G. (2007). Effect of chromium supplementation on glucose metabolism and lipids. **Diabetes Care**. 30: 2154-2163.
- Bharatam, P. V., Patel, D. S., and Iqbal, P. (2005). Pharmacophoric features of biguanide derivatives: An electronic and structure analysis. **Journal of Medicinal Chemistry**. 48: 7615-7622.

- Caravan, P., Gelmini, L., Glover, N., Herring, F. G., Li, H., McNeill, J. H., Rettig, S. J., Setyawati, I. A., Shuter, E., Sun, Y., Tracey, A. S., Yuen, V. G., and Orvig, C. (1995). Reaction chemistry of BMOV, bis(maltolato)oxovanadium(IV): A potent insulin mimetic agent. **Journal of the American Chemical Society**. 117: 12759-12770.
- Cefalu, W. T., Bell-Farrou, A. D., Stigner, J., Wang, Z. Q., King, T., Morgan, T., and Terry, J. G. (1999). Effect of chromium picolinate on insulin sensitivity *in vivo*. **Journal of Trace Elements in Experimental Medicine**. 12: 71-84.
- Ceriello, A., Johns, D., Widel, M., Eckland, D. J., Gilmore, K. J., and Tan, M. H. (2005). Comparison of effect of pioglitazone with metformin or sulfonylurea (monotherapy and combination therapy) on postload glycemia and composite insulin sensitivity index during an oral glucose tolerance test in patients with type 2 diabetes. **Diabetes Care**. 28: 266-272.
- Cohen, N., Halberstam, M., Shlimovich, P., Chang, C. J., Shamoon, H., and Rossetti, L. (1995). Oral vanadyl sulfate improves hepatic and peripheral insulin sensitivity in patients with non-insulin-dependent diabetes mellitus. **The Journal of Clinical Investigation**. 95: 2501-2509.
- Crans, D. C., Smee, J. J., Gaidamauskas, E., and Yang, L. (2004). The chemistry and biochemistry of vanadium and the biological activities exerted by vanadium compounds. **Chemical Reviews**. 104: 849-902.
- Domingo, J. L. (1996). Vanadium: A review of the reproductive and developmental toxicity. **Reproductive Toxicology Review**. 10: 175-182.
- Domingo, J. L. (2002). Vanadium and tungsten derivatives as antidiabetic agents: A review of their toxic effects. **Biological Trace Element Research**. 88: 97-112.
- Fine, S. A. and Kinsella, K. J. (2002). Metformin-containing compositions for the treatment of diabetes. **U.S. Patent**. 6,376,549 B1.

- Fonseca, V., Rosenstock, J., Patwardhan, R., and Salzman, A. (2000). Effect of metformin and rosiglitazone combination therapy in patients with type 2 diabetes mellitus: A randomized controlled trial. **The Journal of the American Medical Association**. 283: 1695-1702.
- Furlong, N. J., Hulme, S. A., O'Brien, S. V., and Hardy, K. J. (2002). Repaglinide versus metformin in combination with bedtime NPH insulin in patients with type 2 diabetes established on insulin/metformin combination therapy. **Diabetes Care**. 25: 1685-1690.
- Garber, A. J., Larsen, J., Schneider, S. H., Piper, B. A., and Henry, D. (2002). Simultaneous glyburide/metformin therapy is superior to component monotherapy as an initial pharmacological treatment for type 2 diabetes. **Diabetes, Obesity and Metabolism**. 4: 201-208.
- Garcia-Vincente, S., Yraola, F., Marti, L., González-Muñoz, E., Garcia-Barrado, M. J., Cantó, C., Abella, A., Bour, S., Artuch, R., Sierra, C., Brandi, N., Carpené, C., Moratinos, J., Camps, M., Palacin, M., Testar, X., Gumà, A., Albericio, F., Royo, M., Mian, A., and Zorzano, A. (2007). Oral insulin-mimetic compounds that act independently of insulin. **Diabetes**. 56: 486-493.
- Gardner, D. G. and Shoback, D. (2011). **Greenspan's Basic & Clinical Endocrinology**. 9th ed. McGraw-Hill Medica: New York. pp. 574-644.
- Glinsmann, W. and Mertz, W. (1966). Effect of trivalent chromium on glucose tolerance. **Metabolism**. 15: 510-520.
- Goc, A. (2006). Biological activity of vanadium compounds. **Central European Journal of Biology**. 1: 314-332.
- Goldfine, A. B., Patti, M.-E., Zuberi, L., Goldstein, B. J., LeBlanc, R., Landaker, E. J., Jiang, Z. Y., Willsky, G. R., and Kahn, C. R. (2000). Metabolic effects of

vanadyl sulfate in humans with non-insulin-dependent diabetes mellitus: *in vivo* and *in vitro* studies. **Metabolism**. 49: 400-410.

Goldstein, B. J. and Müller-Wieland, D. (2008). **Type 2 Diabetes: Principles and Practice**. 2nd ed. Informa: New York. pp. 171-179.

Goldstein, B. J., Feinglos, M. N., Luceford, J. K., Johnson, J., Williams-Herman, D. E., and Sitagliptin 036 Study Group. (2007). Effect of combination therapy with sitagliptin, a dipeptidyl peptidase-4 inhibitor, and metformin on glycemic control patients with type 2 diabetes. **Diabetes Care**. 30: 1979-1987.

Goodman, L. S., Hardman, J. G., Limbird, L. E., and Gilman, A. G. (2001). **Goodman & Gilman's the Pharmacological Basis of Therapeutics**. 10th ed. McGraw-Hill: New York. pp. 1679-1710.

Hanefeld, M., Brunetti, P., Schernthaner, G. H., Matthews, D. R., and Charbonnel, B. H. (2004). One-year glycemic control with a sulfonylurea plus pioglitazone versus a sulfonylurea plus metformin in patients with type 2 diabetes. **Diabetes Care**. 27: 141-147.

Huang, L., Xi, P.-X., Xu, M., Lui, T.-H., and Zeng, Z.-Z. (2008). Crystal structure of metformin ethyl *N*-(3-tosylsulfonyl)carbamate. **Analytical Sciences**. 24: x289-x290.

Institute of Medicine, Food and Nutrition Board. (2001). **Dietary Reference Intakes for Vitamin A, Vitamin K, Arsenic, Boron, Chromium, Copper, Iodine, Iron, Manganese, Molybdenum, Nickel, Silicon, Vanadium, and Zinc**. National Academy Press: Washington, D.C. pp. 197-223.

International Diabetes Federation. (2007). **Guideline for Management of Postmeal Glucose**. Belgium. pp. 1-32.

Jeejeebhoy, K. N., Chu, R. C., Marliss, E. B., Greenberg, G. R., and Bruce-Robertson, A. (1977). Chromium deficiency, glucose intolerance, and neuropathy reversed by

- chromium supplementation, in a patient receiving long-term total parenteral nutrition. **The American Journal of Clinical Nutrition**. 30: 531-538.
- Jelikić-Stankov, M., Uskoković-Marković, S., Holclajtner-Antunović, I., Todorovic, M., and Djurdjević, P. (2007). Compounds of Mo, V and W in biochemistry and their biomedical activity. **Journal of Trace Elements in Medicine and Biology**. 21: 8-16.
- Joslin Diabetes Center. (2007). **Clinical Guideline for Pharmacological Management of Type 2 Diabetes**. Joslin Clinic: Massachusetts. pp. 1-9.
- Kandror, K. V. (1999). Insulin regulation of protein traffic in rat adipose cell. **The Journal of Biological Chemistry**. 274: 25210-25217.
- Krejpcio, Z. (2001). Essentiality of chromium for human nutrition and health. **Polish Journal of Environmental Studies**. 10: 399-404.
- Kumar, R., Balaji, S., Uma, T. S., and Sehgal, P. K. (2009). Fruit extracts of momordica charantia potentiate glucose uptake and up-regulate Glut-4, PPAR γ and PI3K. **Journal of Ethnopharmacology**. 126: 533-537.
- Lamson, D. W. and Plaza, S. M. (2002). The safety and efficacy of high dose chromium. **Alternative Medicine Review**. 7: 218-235.
- Liu, V. J. K. and Morris, S. J. (1978). Relative chromium response as an indicator of chromium status. **The American Journal of Clinical Nutrition**. 31: 972-976.
- Liu, Zh., Li, J., Zeng, Z., Liu, M., and Wang, M. (2008). The antidiabetic effects of cysteinyl metformin, a new synthesized agent, in alloxan and streptozocin induced diabetic rats. **Chemico-Biological Interactions**. 173: 68-75.
- Livage, J. (1991). Vanadium pentoxide gels. **Chemistry of Materials**. 3: 578-593.
- Lu, L.-P., Zhang, H.-M., Feng, S.-S., and Zhu, M.-L. (2004). Two *N,N*-dimethylbiguanidium salts displaying double hydrogen bonds to the counter-ions. **Acta Crystallographica Section C**. 60: o740-o743.

- Marre, H., Howlett, H., Lehertt, P., and Allavoine, T. (2002). Improved glycaemic control with metformin-glibenclamide combined tablet therapy (Glucovance[®]) in type 2 diabetes patients inadequately controlled on metformin. **Diabetes Medicine**. 19: 673-680.
- Mentreddy, S. R. (2007). Medicinal plant species with potential antidiabetic properties. **Journal of the Science of Food and Agriculture**. 87: 743-750.
- Mertz, W. and Schwarz, K. (1959). Chromium(III) and the glucose tolerance factor. **Archives of Biochemistry and Biophysics**. 85: 292-295.
- Messmore, J. M. and Raines, R. T. (2000). Decavanadate inhibits catalysis by ribonuclease A. **Archives of Biochemistry and Biophysics**. 381: 25-30.
- Meyerovitch, J., Farfel, Z., Sack, J., and Shechter, Y. (1987). Oral administration of vanadate normalizes blood glucose levels in streptozotocin treated rats. **The Journal of Biological Chemistry**. 262: 6658-6662.
- Morris, B. W., Kemp, G. J., and Hardisty, C. A. (1985). Plasma chromium and chromium excretion in diabetes. **Clinical Chemistry**. 31: 334-335.
- Mylari, B. L. and Vaman Rao, M. E. (2007). Metformin R-(+)-lipoate as an antidiabetic agent for control of diabetic hyperglycemia and diabetic complications. **World International Property Organization**. 2007/149313 A1.
- Nielsen, L. L. (2005). Incretin mimetics and DPP-IV inhibitors for the treatment of type 2 diabetes. **Drug Discovery Today**. 10: 703-710.
- Nomiya, K., Torii, H., Hasegawa, T., Nemoto, Y., Nomura, K., Hashino, K., Uchida, M., Kato, Y., Shimizu, K., and Oda, M. (2001). Insulin mimetic effect of a tungstate cluster: Effect of oral administration of homo-polyoxotungstates and vanadium substituted polyoxotungstates on blood glucose level of STZ mice. **Journal of Inorganic Biochemistry**. 86: 657-667.

- Okochi, V. I. and Okpuzor, J. (2005). Micronutrients as therapeutic tool in the management of sickle cell disease, malaria and diabetes. **African Journal of Biotechnology**. 4: 1568-1579.
- Pechova, A. and Pavlata, L. (2007). Chromium as an essential nutrient: A review. **Veterinarni Medicina**. 52: 1-18.
- Pereira, M. J., Carvalho, E., Eriksson, J. W., Crans, D. C., and Aureliano, M. (2009). Effect of decavanadate and insulin enhancing vanadium compounds on glucose uptake in isolated rat adipocytes. **Journal of Inorganic Biochemistry**. 103: 1687-1692.
- Piatti, P., Monnti, L. D., Valsecchi, G., Magni, F., Setola, E., Marchesi, F., Galli-Kienle, M., Pozza, G., and Alberti, K. G. M. M. (2001). Long-term oral L-arginine administration improves peripheral and hepatic insulin sensitivity in type 2 diabetes patients. **Diabetes Care**. 24: 875-880.
- Pinkerton, A. A. and Schwarzenbach, D. (1978). Structural studies on biguanide and related species. Correlation of protonation energy with molecular structure. **Journal of the Chemical Society, Dalton Transactions**. 8: 989-8996.
- Press, R. I., Geller, J., Diego, S., and Evans, G. W. (1990). The effect of chromium picolinate on cholesterol and apolipoprotein fractions in human subjects. **The Western Journal of Medicine**. 152: 41-45.
- Preuss, H. G., Bagchi, D., Bagchi, M., Rao, C.V. S., Satyanarayana, S., and Dey, D. K. (2004). Efficacy of a novel, natural extract of (-)-hydroxycitric acid (HCA-SX) and a combination of HCA-SX, niacin bound chromium and gymnema sylvestre extract in weight management in human volunteers: A pilot study. **Nutrition Research**. 24: 45-58.
- Ramos, S., Manuel, M., Tiago, T., Duarte, R., Martins, J., Gutiérrez-Merino, C., Moura, J. J. G., and Aureliano, M. (2006). Decavanadate interaction with actin:

- Inhibition of G-actin polymerization and stabilization of decameric vanadate. **Journal of Inorganic Biochemistry**. 100: 1734-1743.
- Rang, H. P., Dale, M. M., Ritter, J. M., and Flower, R. J. (2007). **Rang and Dale's Pharmacology**. 6th ed. Elsevier: London. pp. 397-409.
- Rapin, J.-R. and Halbitte, D. (2007). Medicinal association of a biguanide and carrier, for example metformin and arginine. **U.S. Patent**. 7,265,156 B2.
- Ray, P. (1960). Complex compounds of biguanide and guanylureas with metallic elements. **Chemical Reviews**. 61:313-359.
- Rehder, D. (2003). Biological and medicinal aspects of vanadium. **Inorganic Chemistry Communications**. 6: 604-617.
- Rosenstock, J., Brown, A., Fischer, J., Jain, A., Littlejohn, T., Nadeua, D., Sussman, A., Taylor, T., Krol, A., and Magner, A. (1998). Efficacy and safety of acarbose in metformin-treated patients with type 2 diabetes. **Diabetes Care**. 21: 2050-2055.
- Schwartz, K. and Mertz, W. (1957). A glucose tolerance factor and its differentiation from factor 3. **Archives of Biochemistry and Biophysics**. 72: 515-518.
- Shaw, J. E., Sicree, R. A., and Zimmet, P. Z. (2010). Global estimates of the prevalence of diabetes for 2010 and 2030. **Diabetes Research and Clinical Practice**. 87: 4-14.
- Shubhashish, S., Maddali, P., and Marita, R. A. (1996). Demonstration of the hypoglycemic action of *momordica charantia* in a valid animal model of diabetes. **Pharmacological Research**. 33: 1-4.
- Striffler, J. S., Law, J. S., Polansky, M. M., Bhatena, S. J., and Anderson, R. A. (1995). Chromium improves insulin response to glucose in rat. **Metabolism**. 44: 1314-1320.
- Tongia, A., Tongia, S. K., and Dave, M. (2004). Phytochemical determination and extraction of *momordica charantia* fruit and its hypoglycemic potentiation of oral

- hypoglycemic drugs in diabetes mellitus (NIDDM). **Indian Journal of Physiology and Pharmacology**. 48: 241-244.
- Verma, S., Cam, M. C., and McNeill, J. H. (1998). Nutritional factors that can favorably influence the glucose/insulin system: Vanadium. **Journal of the American College of Nutrition**. 17: 11-18.
- Vincent, J. B. (2000). The biochemistry of chromium. **The Journal of Nutrition**. 130: 715-718.
- Vincent, J. B. (2001). The bioinorganic chemistry of Chromium(III). **Polyhedron**. 20: 1-26.
- Vincent, J. B. (2007). **The Nutritional Biochemistry of Chromium(III)**. 1st ed.: Elsevier: Oxford.
- Waisundara, V. Y., Hsu, A., Tan, B. K.-H., and Huang, D. (2009). Baicalin improves antioxidant status of streptozotocin-induced diabetic wistar rats. **Journal of Agricultural and Food Chemistry**. 57: 4096-4102.
- Wikipedia, the Free Encyclopedia Homepage. http://en.wikipedia.org/wiki/List_of_bestselling_drugs. (accessed October 24,2012)
- Woo, L. C.Y., Yuen, V. G., Thompson, K. H., McNeill, J. H., and Orvig, C. (1999). Vanadyl-biguanide complexes as potential synergistic insulin mimics. **Journal of Inorganic Biochemistry**. 76: 251-257.
- Yraola, F., Garcia-Vicente, S., Marti, L., Albericio, F., Zorzano, A., and Royo, M. (2007). Understanding the mechanism of action of the novel SSAO substrate $(C_7H_{10}N)_6V_{10}O_{28} \cdot 2H_2O$, a prodrug of peroxovanadate insulin mimetics. **Chemical Biology & Drug Design**. 69: 423-428.
- Zorzano, A., Palacin, M., Marti, L., and Garcia-Vicente, S. (2009). Arylalkylamine vanadium salts as new antidiabetic compounds. **Journal of Inorganic Biochemistry**. 103: 559-566.

CHAPTER II

REVERSE MICELLES

2.1 Introduction

Microemulsions are systems in which droplets of water or oil are dispersed into small size domains that form thermodynamically stable, clear mixtures. Depending on the composition, they are dispersions of either oil in water (micelles) or water in oil (reverse micelles). The surfactant adsorbs on the oil-water interface and lowers the interfacial tension between oil and water. Numerous studies have been performed on microemulsions to better understand their phase behavior (De and Maitra, 1995).

Spherical reverse micelles are isolated, surfactant-coated water droplets, which have emerged as useful for biotechnological applications; confined water in biological systems, cell models, and biocatalysis reactors (Bachmann, Luisi, and Lang, 1992; Chang and Shiao, 1994; Holtz, Stec, and Kantrowitz, 1999), including acting as nanotemplates for materials synthesis in chemistry (Pileni, 2006; Dung, Buu, Quang, Ha, Bang, Chau, Ly, and Trung, 2009). An emphasis in the models and properties of reverse micelles is thus important. Determination of the actual structure of reverse micelles is a challenging problem due to very complex internal interactions and special assembly of components. Advanced physical techniques such as small angle neutron scattering (SANS) (Aswal, 2003; Tamura, Takeuchi, Mao, Csencsits, Fan, Otomo, and Saboungi, 2003), small angle X-ray scattering (SAXS) (Aswal, 2003), dynamic light scattering (DLS) (Bohidar and Behboudnia, 2001; Xu, Zhang, Yuan, Huang, and Li, 2001), transmission electron microscopy (TEM) (Fang and Yang, 1999), nuclear magnetic resonance (NMR) (Fang and Yang, 1999; Lindblom, Lindman and Mandell, 1970),

infrared spectroscopy, including FTIR (Xu, Zhang, Yuan, Huang, and Li, 2001; Zhong, Steinhurst, Carpenter, and Owrutsky, 2002), ultrafast IR pump-probe spectroscopy (Moilanen, Levinger, Spry, and Fayer, 2007; Fayer and Levinger, 2010; Tielrooij, Peterson, Rezus, and Bakker, 2009), and near IR spectroscopy, ultraviolet-visible spectroscopy (Hasegawa, 2001), viscosity, dielectric spectroscopy (Cole, Mashimo, and Winson, 1980), thermal conductivity and calorimetry are useful to unravel these complicated structures.

2.2 Molecular Aggregation of Surfactants

The process leading to the formation of molecular aggregates is described by the laws of chemical thermodynamics, and the shape and size are governed by the number of surfactant molecules, the relative volumes occupied of hydrophilic and hydrophobic parts of surfactant, and the solution conditions, including temperature and nature of the solvents.

Thermodynamics of Self-Assembly. The formation of a reverse micelle (RM) is interesting in that water, which is hydrophilic is being added to a system containing hydrophobic solvent. The literature suggests that the formation of reverse micelles is an entropy-driven process (Shen, Gao, and Wang, 1999; D'Aprano, Lizzio, and Liveri, 1987) that provides information as to why these stable microemulsions would form.

For the formation of an aggregate, B_n , consisting of n molecules of B_1 , one can write the reaction:



This reaction can be expressed in the equilibrium constant, k_{eq} , according to the familiar law of mass action:

$$k_{eq} = k_l / k_n = \frac{[B_n]}{[B_l]^n} = \frac{X_n}{nX_l^n}, \quad (2.2)$$

where X_n is the mole fraction of surfactant in aggregates on n molecules and X_l is a mole fraction of isolated molecules. The reaction constant k_{eq} is related to the difference in standard Gibbs free energy of formation between product and reactants:

$$k_{eq} = \exp\left(\frac{-\Delta G^0}{RT}\right) = \exp\left(\frac{-\Delta\mu^0}{k_B T}\right) \quad (2.3)$$

where $k_B = R/N_A$, and $\Delta\mu^0$ is the difference in the standard chemical potential between the products and reactants. For an aggregation number of n this difference is

$$\Delta\mu^0 = n \mu_n^0 - n \mu_l^0, \quad (2.4)$$

and μ_i^0 is the standard chemical potential in Joules/particle for a molecule in an aggregate of size i . The mole fraction of surfactant in aggregates of n molecules X_n as a function of molar fraction of isolated molecules X_l is given by:

$$X_n = n [X_l \exp(\mu_l^0 - \mu_n^0 / k_B T)]^n, \quad (2.5)$$

which together with the concentration relation for the total solute concentration C ,

$$C = \sum_{n=1}^{\infty} X_n \mu_n^0 \quad (2.6)$$

Aggregates will form when there is a difference in the free energies between the molecules in the aggregated and dispersed monomer states. When all are equal Equation 2.5 simplifies to

$$X_n = n X_1^n. \quad (2.7)$$

Considering Equation 2.7, found that $X_n \ll X_1$ thus molecules will be in the monomer state. Only when the Gibbs free energy in aggregated state is lower than in the monomer state ($\mu_n^0 < \mu_1^0$), the aggregates become more probable. For all X_n to be smaller than 1, that is a necessary condition for X_1 that

$$X_1 < \exp [- (\mu_1^0 - \mu_n^0) / k_B T] \approx \text{CMC}. \quad (2.8)$$

As mentioned above, since the mole fraction of surfactant above CMC (critical micelle concentration) so the added molecules will preferably take part in the formation of aggregates of n molecules. Typical CMC are on the order of 0.01-10 nM, when CMC is defined as the minimal concentration of surfactant molecules above which micelles are formed.

Geometrical Surfactant Parameter. As mentioned in the previous section, reverse micelles start to self-assemble as the total concentration oversteps the critical micelle concentration with a minimizing of their free energy. Another parameter that has to be considered regarding micelle formation is the geometrical surfactant factor, which helps to predict the shape and size of micellar structures.

When the effective area of the head group, a , the length of hydrocarbon chain in surfactant, l , and the volume the hydrocarbon chain occupies, V , (Figure 2.1), are

associated in the term of surfactant packing parameter, N_s , by the ratio of hydrocarbon volume to head group area in the term;

$$N_s = V / al. \quad (2.9)$$

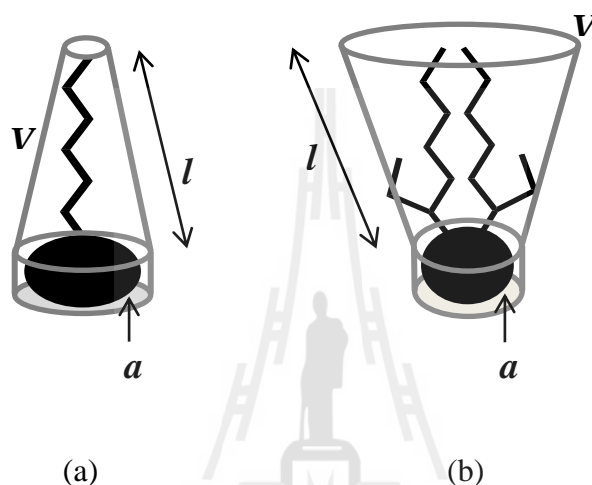


Figure 2.1 Geometrical model of surfactant molecules with different characteristics. (a) sodium dodecyl sulfate molecule, and (b) Sodium bis(2-ethylhexyl)sulfosuccinate molecule.

The surfactant packing parameter is concentration dependent, reflecting changes primarily in varying the amount of solvent. We can use the following relationship for extended length alkyl chains containing n_c carbon atoms with equation 2.10 (Hamley, 2000):

$$l \text{ (nm)} = 0.154 + 0.127n_c, \quad (2.10)$$

where 0.154 nm is a C–C bond length and 0.127 nm is the projection of this distance on the chain axis in the case of an all-trans conformation. If the length of hydrocarbon chains of solvent is longer than of hydrocarbon chains of surfactant molecules as it is in

the case of isooctane and AOT, the condition of nonpenetration applies (Auffret, 2008).

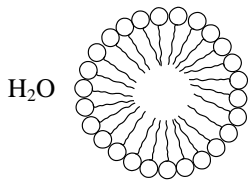
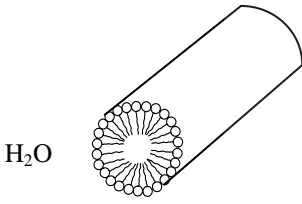
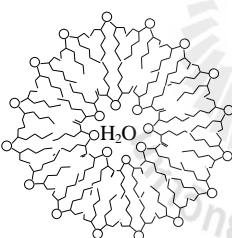
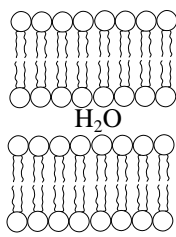
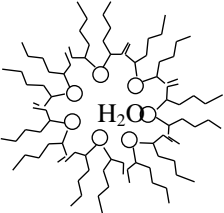
For volume, V , of hydrocarbon chain of surfactant has been found that

$$V (\text{nm}^3) = 0.027(n_c + n_{Me}), \quad (2.11)$$

where n_{Me} term accounts for the fact that methyl groups occupy twice the volume of a CH_2 group, for single chain surfactant $n_{Me} = 1$ but for double tail surfactant $n_{Me} = 2$.

Table 2.1 shows the range of surfactant packing parameter, N_s , for different aggregate shapes. The microemulsion can be considered to be built from the packing of cones, truncated cones, or cylinders resulting in the different aggregate shapes. As a spherical micelle can be built from the packing of cones and evaluates to reverse micelles as a function of N_s .

Table 2.1 Surfactant packing parameter range for various surfactant aggregates.

Expected aggregate structure	Packing parameter	Surfactant type
Spherical micelles 	$N_s < 1/3$	
Cylindrical micelles 	$1/3 < N_s < 1/2$	
Vesicles, flexible bilayers 	$1/2 < N_s < 1$	
Lamellae, planar bilayers 	$N_s \approx 1$	
Revers micelles 	$N_s > 1$	

From the phase diagram of a ternary water-oil-surfactant mixture, the size of reverse micelles is possible to control by the parameter w_0 , defined as the molar ratio of the concentrations of water and surfactant:

$$w_0 = \frac{[\text{H}_2\text{O}]}{[\text{Surf}]} \quad (2.12)$$

The surfactant aggregation number n_{avg} is given by

$$n_{avg} = 4\pi r^2 / a = [36\pi v_0^2 / a^3] \cdot w_0^2, \quad (2.13)$$

where a is head group area of surfactant, v_0 the effective volume of a water molecule (29.2 \AA^3), and r the average micelle radius.

Although the geometrical shape of the surfactant is useful to determine the shape of microemulsion entities, there is also a strong influence of temperature and counterion and of the polar solvent that are not accounted in the system.

2.3 Reverse Micelles

In reverse micelles, water molecules added to the surfactant/solvent system begin to form clusters. This is followed by monomer surfactant molecules surrounding the clustered water molecules and creating a dispersion of nanoparticles. It has been proposed that the clustering process is endothermic and involves the solvent molecules around the water molecule being disrupted, followed by an exothermic process, in which water molecules associate with the surfactant. Furthermore, there is a continuous equilibrium within this system, which involves water molecules within the water pool that are relatively free, close to the interface, and bound to the head group of the surfactant.

In an ionic RM, charged surfactant head groups are constrained to the outer radius of the water pool of the micelle. Each molecule has an associated counter ion that is free to dissociate from the surfactant. Thus, various studies suggest that it has an ionic charge distribution region or Stern layer containing a fraction of the counter ions, the ionic head groups of surfactant, and water (Bunton, Nome, Quina, and Romsted, 1991), which has about the width of the size of the surfactant head group (Berr, 1987; Boyd, 1992).

AOT/isooctane/water RMs. Sodium bis(2-ethylhexyl)sulfosuccinate or Aerosol OT (AOT) is an anionic surfactant in which the molecule is composed of a polar head (SO_3^- group) bonded to two hydrocarbon chains (as shown in Figure 2.2). The length of the apolar part is about 7.5 Å, the polar head group about 3 Å, and the molecular volume $\approx 50 \text{ \AA}^3$ (Dijk, Joosten, and Levine, 1989).

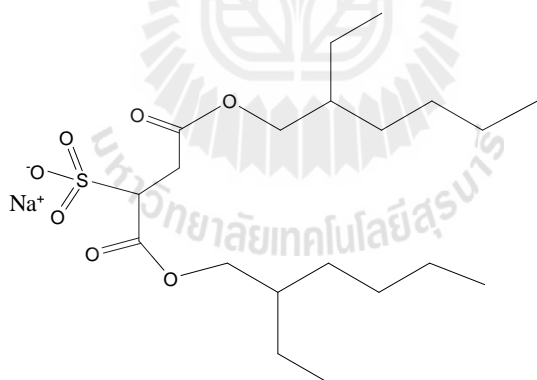


Figure 2.2 Structure of an AOT molecule.

The first discovery of AOT use in the context of microemulsion by Matton and coworkers found that adding AOT to a mixture of oil and water without cosurfactant produced reverse micelles (Mattoon and Mathews, 1949). Around room temperature the critical micelle concentration of AOT in nonpolar solvents like decane, heptane, or isooctane was found to be in the order of $\text{CMC} \approx 1 \text{ mM}$ (De and Maitra, 1995). Furthermore, AOT can dissolve large amounts of water to form discrete droplets. It is

clear that AOT reverse micelles have advantages over traditional microemulsion systems.

The AOT/isooctane/water ternary phase diagram has been studied extensively by different experimental techniques used to characterize the different structures as a function of their composition. The ternary phase diagram illustrated in Figure 2.3, was characterized by means of cross polarized light microscopy and X-ray scattering (Tamamushi and Watanabe, 1980).

In the phase diagram, L_1 and L_2 stand for direct (oil in water microemulsion) and reversed micellar (water in oil microemulsion) solutions, respectively. The L_2 region extends widely on the phase diagram over 40 to 60% water content. Following a line in isooctane, that is the water to AOT concentration ratio, w_0 , kept constant while isooctane content varies, a transition from the isotropic reversed micellar phase L_2 to lyotropic liquid crystal phases, LC, when the AOT and water concentrations increase, covers a wide area along AOT axis. $L + LC$ are a liquid crystalline structure in equilibrium with solution (chiefly L_2) and $2L$ is the unstable phases in which two separated phases are formed. Beside reverse micelle structures, hexagonal (F) and bilayer (lamellar; D) conformations can be formed by varying the composition in the ternary phase diagram.

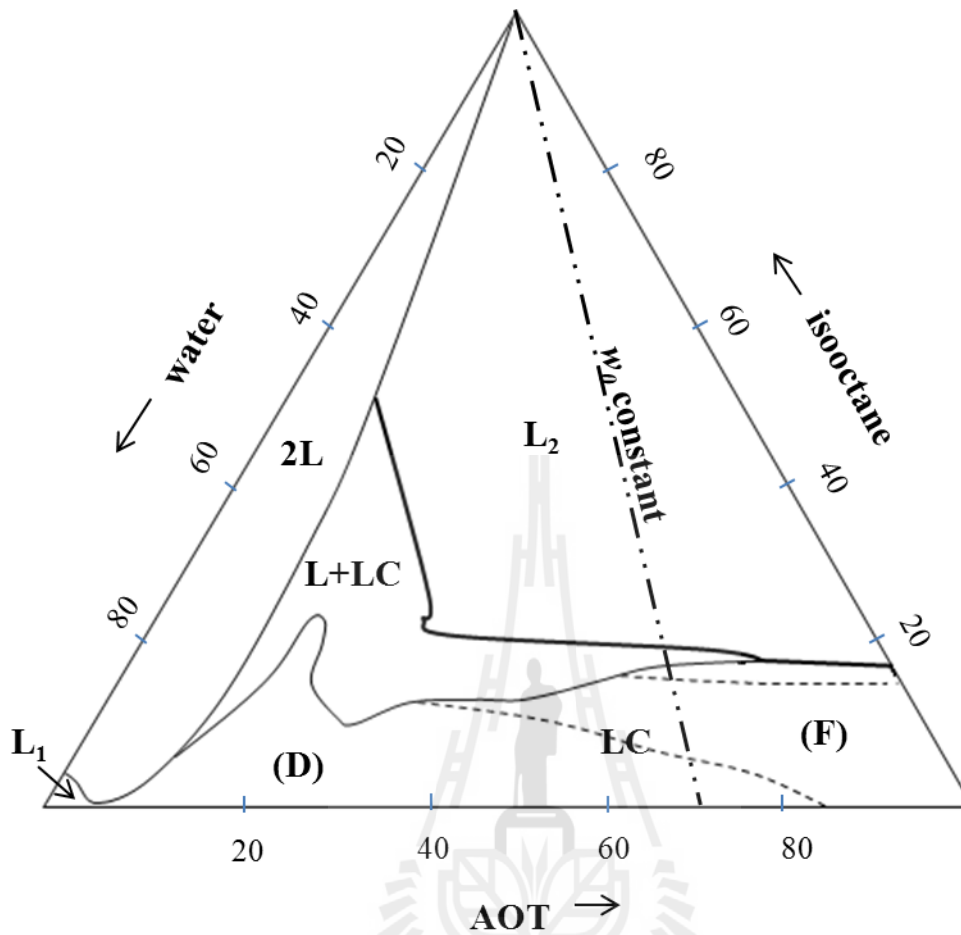


Figure 2.3 Phase diagram for AOT/isooctane/water ternary mixtures at ambient pressure and room temperature. Note the large part of the phase diagram covered by L_2 reverse micelles phase. (redrawn after Tamamushi and Watanabe, 1980; Auffret, 2008).

Under the assumption of a spherical water core covered by a mono-molecular shell of AOT (as shown in Figure 2.4) the polar radius r_w composed of water and AOT head groups can be calculated by combining the volume and area of droplet surrounded by n molecules of AOT, with equation 2.16.

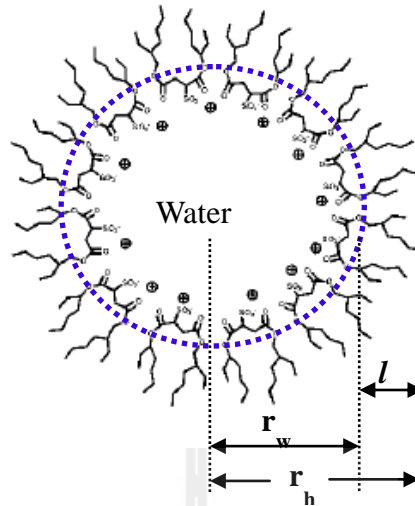


Figure 2.4 The schematic diagram of AOT reverse micelle, where r_w is the radius of water pool, r_h is the radius of micelle and l is length of apolar part.

$$\text{Droplet volume: } (4/3)\pi r_w^3 = n(v_0 \cdot w_0 + v_s). \quad (2.14)$$

$$\text{Droplet surface: } 4\pi r_w^2 = n \cdot a. \quad (2.15)$$

$$r_w = (3/a)(v_0 \cdot w_0 + v_s) \approx (1.4 w_0 + 2.3) \text{ \AA}, \quad (2.16)$$

where v_s is the AOT head group volume, and head group area $a \approx 65 \text{ \AA}^2$. The bulk water molecule $v_0 = 29.2 \text{ \AA}^3$, and r_w is a good estimate for the droplet size at room temperature.

The calculated values of the packing factor of surfactant for various sizes of AOT/isooctane/water reverse micelles have been reported in Maitra's work, it agreed with the chemical shifts of water proton resonance data (Maitra, 1984).

Polydispersity, PD. A sample of objects that have an inconsistent size, shape, and mass distribution is called polydisperse such as particles in a colloid, droplets in a cloud, or polymer molecules in a solvent (Hamley, 2000).

The degree of PD, is one important parameter of reverse micelle solutions. When combining water, surfactant, and nonpolar solvent, the size of the spherical particles

formed are not all the same. The PD of the reverse micelles depends on such factors as size (w_0), temperature, and pressure (Zulauf and Eicke, 1979). However, under ambient conditions the amount of PD is generally low. From a number of experimental and theoretical studies the PD was shown to be dependent on their size in which an increase in w_0 results in an increase in the degree of PD (Eicke, 1980; Zulauf and Eicke, 1979).

2.4 References

- Aswal, V. K. (2003). Small-angle scattering from micellar solutions. **Bhabha Atomic Research Centre Newsletter**. 237: 37-42.
- Auffret, Y. (2008). **Microscopic and Macroscopic Properties of AOT/Iso-octane/Water Sheared Lyotropic Lamellar Phases**. PhD. Thesis. University of Melbourne (Australia) and University Joseph Fourier (France).
- Bachmann, P. A., Luisi, P. L., and Lang J. (1992). Autocatalytic self-replicating micelles as models for prebiotic structures. **Nature**. 357: 57-59.
- Berr, S. S. (1987). Solvent isotope effects on alkyltrimethylammonium bromide micelles as a function of alkyl chain length. **Journal of Physical Chemistry**. 91: 4760-4765.
- Bohidar, H. B. and Behboudnia, M. (2001). Characterization of reverse micelles by dynamic light scattering. **Colloids and Surface A: Physicochemical and Engineering Aspects**. 178: 313-323.
- Boyd, R. W. (1992). **Nonlinear Optics**. Academic Press, San Diego. p. 122.
- Bunton, C. A., Nome, F., Quina, F. H., and Romsted, L. S. (1991). Ion binding and reactivity at charged aqueous interfaces. **Accounts of Chemical Research**. 24: 357-364.

- Chang, G. G. and Shiao, S. L. (1994). Possible kinetic mechanism of human placental alkaline phosphatase *in vivo* as implemented in reverse micelles. **European Journal of Biochemistry**. 220: 861-870.
- Cole, R. H., Mashimo, S., and Winson, P. (1980). Evaluation of dielectric behavior by time domain spectroscopy. 3. Precision difference methods. **Journal of Chemical Physics**. 84: 786-793.
- D'Aprano, A., Lizzio, A., and Liveri, V. T. (1987). Enthalpies of solution and volumes of water in reversed AOT micelles. **Journal of Physical Chemistry**. 91: 4749-4751.
- De, T. K. and Maitra, A. (1995). Solution behaviour of Aerosol OT in nonpolar solvents. **Advances in Colloid and Interface Science**. 59: 95-193.
- De, T. K., and Maitra, A. Solution behavior of aerosol OT in nonpolar solvents. **Advances in Colloid and Interface Science**. 59: 95-193.
- Dijk, M. A. V., Joosten, J. G. H., and Levine, Y. K. (1989), Dielectric study of temperature-dependent aerosol OT/water/isooctane microemulsion structure. **Journal of Physical Chemistry**. 93: 2506-2512.
- Dung, T. T. N., Buu, N. Q., Quang, D. V., Ha, H. T., Bang, L. A., Chau, N. H., Ly, N. T., and Trung, N. V. (2009). **Journal of Physics: Conference Series**. 187: 012054.
- Eicke, H.-F. (1980). Aggregation in surfactant solutions: Formation and properties of micelles and microemulsions. **Pure and Applied Chemistry**. 52: 1349-1357.
- Fang, X. and Yang, C. (1999). An experimental study on the relationship between the physical properties of CTAB/hexanol/water reverse micelles and ZrO₂-Y₂O₃ nanoparticles prepared. **Journal Colloid and Interface Science**. 212: 242-251.
- Fayer, M. D. and Levinger, N. E. (2010). Analysis of water in confined geometries and at interfaces. **Annual Review of Analytical Chemistry**. 3: 89-107.

- Hamley, L. W. (2000). **Introduction to Soft Matter**. John Wiley & Son: West Sussex. pp. 239-243.
- Hasegawa, M. (2001). Buffer-like action in water pool of Aerosol OT reverse micelles. **Langmuir**. 17: 1426-1431.
- Holtz, K. M., Stec, B., and Kantrowitz, E. R. (1999). A model of the transition state in the alkaline phosphatase reaction. **Journal of Biological Chemistry**. 274: 8351-8354.
- Lindblom, G., Lindman, B., and Mandell, L. (1970). A study of counterion binding to reversed micelles by nuclear magnetic quadrupole relaxation of ^{81}Br . **Journal of Colloid and Interface Science**. 34: 262-271.
- Mattoon, R. W. and Mathews, M. B. (1949). Micelles in nonaqueous media. **Journal of Chemical Physics**. 17: 496-497.
- Moilanen, D. E., Levinger, N. E., Spry, D. B., and Fayer, M. D. (2007). Confinement or the nature of the interface? Dynamics of nanoscopic water. **Journal of the American Chemical Society**. 129: 14311-14318.
- Pileni, M. P. (2006). Reverse micelles used as templates: A new understanding in nanocrystal growth. **Journal of Experimental Nanoscience**. 1: 13-27.
- Shen, X., Gao, H., and Wang, X. (1999). What makes the solubilization of water in reversed micelles exothermic or endothermic? A titration calorimetry investigation. **Physical Chemistry Chemical Physics**. 1: 463-469.
- Tamamushi, N. W. and Watanabe, N. (1980). The formation of molecular aggregation structure in ternary system: Aerosol OT/water/isooctane. **Colloid and Polymer Science**. 258: 174-178.
- Tamura, K., Takeuchi, K., Mao, G., Csencsits, R., Fan, L., Otomo, T., and Saboungi, M. L. (2003). Colloidal silver iodide: synthesis by a reverse micelle method and

investigation by a small-angle neutron scattering study. **Journal of Electroanalytical Chemistry**. 559: 103-109.

Tielrooij, K. J., Peterson, C., Rezus, Y. A. L., and Bakker, H. J. (2009). Reorientation of HOD in liquid H₂O at different temperatures: comparison of first and second order correlation functions. **Chemical Physics Letters**. 471: 71-74.

Xu, Y., Zhang, L., Yuan, S. L., Huang, X. R., and Li, G. Z. (2001). Effect of polyvinylpyrrolidone on the states of water in water-in-oil microemulsions with betaine surfactant. **Journal of Dispersion Science and Technology**. 22: 563-567.

Zhong, Q., Steinhurst, D. A., Carpenter, E. E., and Owrutsky, J. C. (2002). Fourier transform infrared spectroscopy of azide ion in reverse micelles. **Langmuir**. 18: 7401-7408.

Zulauf, M. and Eicke, H. F. (1979). Inverted micelles and microemulsions in the ternary system H₂O/Aerosol-OT/Isooctane as studied by photon correlation spectroscopy. **Journal of Physical Chemistry**. 83: 480-486.

CHAPTER III

EXPERIMENTAL

3.1 Materials, Methods, and Synthesis

Materials. Vanadium pentoxide, V_2O_5 , (Fluka, $\geq 98.0\%$), sodium metavanadate, $NaVO_3$, (Aldrich, 90.0%), metformin hydrochloride, $C_4H_{11}N_5 \cdot HCl$, (Sigma-Aldrich 97%, or isolated directly from tablets of Merck's diabetes drug Glucophage), activated charcoal, Carbon 6-12 mesh, (Fisher Scientific). Sodium bis(2-ethylhexyl)-sulfosuccinate, AOT, (Sigma-Aldrich, 98.0%) was purified as described previously (Baruah, Swafford, Crans, and Levinger, 2008; Chowdhury, Ashby, Datta, and Petrich, 2000). Deuterated dimethyl sulfoxide, d_6 -DMSO, tetrametylsilane, TMS, (Cambridge Isotope Laboratories), methanol (Sigma-Aldrich, 98.0%), and isooctane (Sigma-Aldrich, 99.0%) were used as received. Doubly distilled water was used for all reverse micelle systems.

Isolation of metformin hydrochloride. Two glucophage tablets containing 850 mg metformin hydrochloride per 896 mg tablet were ground in a mortar, mixed with 7.0 mL of deionized water, stirred, and heated at $60^\circ C$ for 15 min. The mixture was filtered and the filtrate evaporated at 45 - $50^\circ C$ about 1.5 hr to reduce volume until $1/3$ is left. The resulting solution was left at ambient temperature for crystallization. The crystals were characterized by FT-IR, XRD, and melting point techniques, and the results compared to standard metformin hydrochloride from Sigma-Aldrich.

Preparation of metformin hydrochloride with decavanadate solutions. Suspensions of V_2O_5 and MetHCl were acidified or neutralized using HCl and NaOH to pH values

ranging from 2 to 7. The ratio of V_2O_5 is in slight excess of the $HMet^+$ ions with 5 to 3 and the experimental ratio being 12 to 5. The solutions became the deep yellow/orange diagnostic color of V_{10} anion as the V_2O_5 dissolved.

Synthesis of Metformium Decavanadate; $[C_4H_{12}N_5]_3[H_3O]_3[H_2V_{10}O_{28}] \cdot 6H_2O$, $MetV_{10}$. The pH of a stirred aqueous suspension of V_2O_5 (0.220 g, 1.20 mmol), and $MetHCl$ (0.240 g, 1.45 mmol) in 8 mL of deionized water was adjusted to ~5 with 1.0 M HCl . The orange solution was heated at $60^\circ C$ for 15 hrs, filtered, and kept at ambient temperature to give 0.438 g of yellow-orange plate-like crystals, 0.300 mmol, about 25% based on vanadium.

Purify AOT. AOT was purified by dissolving AOT (20.0 g) in 100 mL of methanol, stirring overnight in the presence of 6-12 mesh activated charcoal (5.00 g), filtering the suspension, and removing the methanol by evaporation under vacuum at least 12 hrs (Baruah, Swafford, Crans, and Levinger, 2008; Chowdhury, Ashby, Datta, and Petrich, 2000). Purified AOT was dissolved in d_6 -DMSO for 1H NMR (Figure 3.1) and peak positions for the AOT protons were compared with those previously reported (Stahla, Baruah, James, Johnson, Levinger, and Crans, 2008), and the residual water content was found to be 0.5 water molecules per AOT molecule by integration of the H1 (one hydrogen atom) or H3/H3' (two hydrogen atoms) signal. When preparing reverse micelles in this work, all w_0 ratios are calculated including the 0.5 water from AOT.

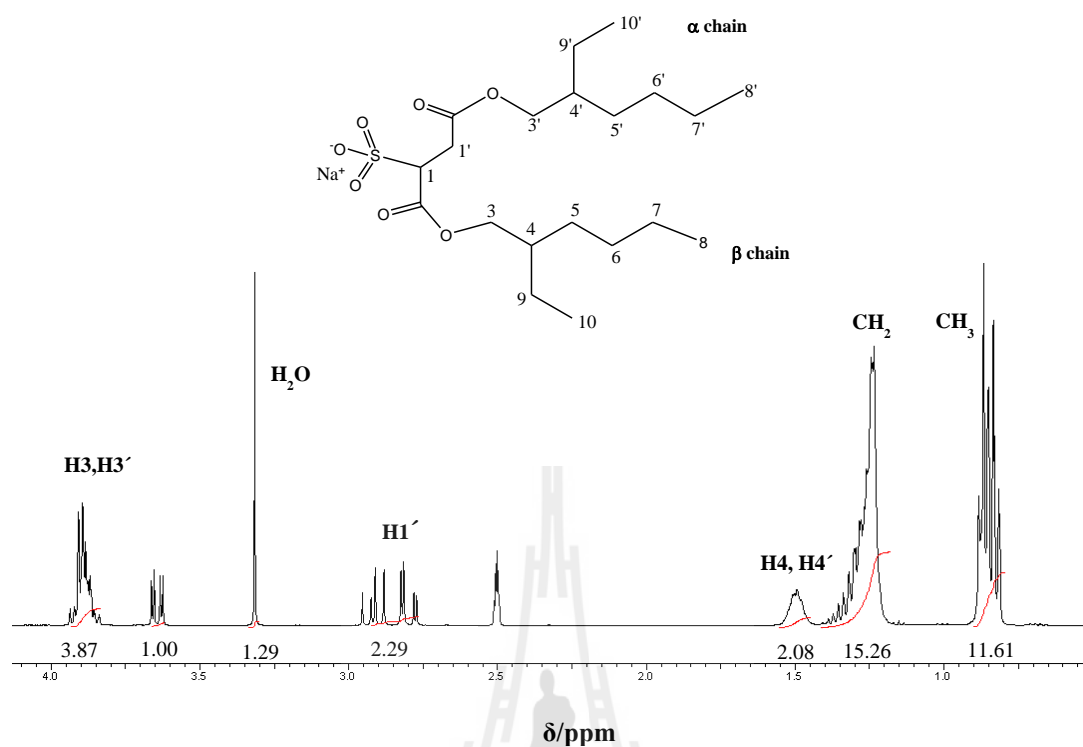


Figure 3.1 ¹H NMR of NaAOT in *d*₆-DMSO. (2.5 ppm is DMSO, and peak integration values are given below the spectrum)

Preparation of AOT/isooctane. AOT/isooctane stock solutions of 0.2 M and 0.75 M were prepared. The high concentration was used for preparing solutions of MetV₁₀, and the 0.2 M was used to prepare solutions for analysis by DLS and FTIR.

The 0.75 M AOT/isooctane stock solution was prepared by dissolving 8.335 g of AOT in 25 mL isooctane and vortically mixing until the solution cleared. The 0.2 M AOT/isooctane stock solution was prepared similarly, but using 2.223 g AOT in 25 mL isooctane.

Preparation of AOT/isooctane RMs with NaV₁₀. The total concentration of V₁₀ at 2.0 mM was used to make AOT RM of *w*₀ = 5.5, 6, 8, 10, and 16 by pipetting a specific volume (details in Table 3.1) of stock solution to aliquots of 0.75 M AOT/isooctane, and vortically mixing until the solution was clear and suitable for ¹H NMR analysis. Stock solution of decavanadate (V₁₀), from NaVO₃ at total concentration of V₁₀ 2.0 mM, pH ≈

4 was prepared by dissolving NaVO_3 in doubly distilled deionized water in 90% of the desired volume in a volumetric flask. The pH was adjusted to 4 by using 6 M HCl and 1 M NaOH, and finally making up the required volume.

Preparation of AOT/isooctane RMs with MetV₁₀. MetV₁₀ (0.0030 g, 2.0 mM) was added to 1 mL of 0.75 M AOT/isooctane and D₂O added to make up the desired w_0 . The samples were vortically mixed 45 min resulting in transparent, yellow solutions. ¹H NMR and ⁵¹V NMR spectra were recorded and in agreement with literature reports (Gadape and Parikh, 2011; Crans, 1994; Howarth, 1990; Baruah, Roden, Sedgwick, Correa, Crans, and Levinger, 2006).

Preparation of AOT/isooctane RMs with MetHCl. Specific volumes of MetHCl solution in D₂O were pipetted into aliquots of 0.75 M AOT in isooctane, the suspension vortically mixed for 15 min, and left until the solution was clear and suitable for ¹H NMR analysis.

Table 3.1 Component volumes in 1 mL samples of 0.2 M and 0.75 M AOT RMs at various w_0 . ($w_0 = [\text{H}_2\text{O}]/[\text{AOT}]$)

w_0	0.2 M AOT/isooctane		0.75 M AOT/isooctane	
	Aqueous stock, μL	AOT/isooctane, μL	Aqueous stock, μL	AOT/isooctane, μL
2	7	993	26	974
4	14	986	51	949
5.5	19	981	69	931
6	21	979	75	925
8	28	972	98	902
10	35	965	119	881
16	55	945	178	822

Sample preparation for DLS and IR experiments. Reverse micelles of V_{10} were formed using overall concentration of V_{10} from NaVO_3 and MetV_{10} 0.7 mM in 0.2 M AOT/isooctane at $w_0 = 6$ and 10. For DLS, the sample was filtered directly into the cuvette through a 0.2 μm filter before analysis. IR spectroscopy experiments, aqueous solutions were prepared using 5% HOD in H_2O , and with pure DI-water to allow us to explore the OD and OH stretching regions. Spectra that arise only from the OD stretching signal were obtained by subtracting the spectra with DI-water as the polar solvent from the spectra of reverse micelles containing 5% HOD in H_2O , which reported the highest peak positions.

3.2 Instrumentation

Fourier transform infrared spectroscopy, FTIR. Infrared spectra were recorded in the mid-IR range 4000-400 cm^{-1} . Solid state spectra were recorded on a Spectrum GX (Perkin Elmer, USA) spectrophotometer at 4 cm^{-1} resolution, 15 scans using KBr pellets. Solution spectra were recorded with a Magna 760 (Nicolet, USA) FTIR spectrophotometer at 1 cm^{-1} resolution using 128 scans and an IR microvolume cuvette with BaF_2 windows (2 mm thick) separated by a 50 μm Teflon spacer. Solution spectra were used to explore the OD and OH stretching region in the microemulsion systems. All sample were recorded at 25°C.

Thermogravimetric analysis, TGA. Spectra were recorded in the range 25-600°C with heating rate 10°C/min under helium gas on a TGA 2950 Thermogravimetric Analyzer, (TA Instruments, USA). The weight of a sample is monitored as a function of temperature or time in an inert atmosphere. It is useful for investigating composition of multicomponent compounds, moisture, and volatiles content of material.

Elemental analysis, CHN. Elemental analyses were performed on a LECO TruSpec Carbon, Hydrogen, Nitrogen, Sulfur (CHNS) Analyzer by Columbia Analytical

Service (Tucson, USA). This is useful for determining the chemical compositions of sample by combusting a sample and quantitatively analyzing the combustion products.

Melting point apparatus. Melting points were determined with a Griffin model MPA 350 BM2.5 (Gallenkamp, UK). Observed sample decomposes with temperature. Use for determined melting point of compounds.

Powder X-ray diffraction, XRD. Powder XRD spectra were recorded on a D5005 diffractometer (Bruker AXS, Germany) using Cu $K\alpha$ X-ray radiation ($\lambda = 1.54 \text{ \AA}$) and a 0.5 mm divergence slit with data collected over a 5.0-45.0° 2θ range using tube power level 40 kV and 40 mA. The JCPDS library (International Center for Diffraction Data, 2004) was utilized for phase identification

Single crystal X-ray diffraction. Intensity data measurements were carried out at 120(2) K on a Bruker SMART APEX II CCD diffractometer with a graphite monochromatized Mo $K\alpha$ ($\lambda = 0.71073 \text{ \AA}$) X-ray radiation source. Data were integrated and corrected for Lorentz and polarization effects using SAINT and semiempirical absorption corrections were applied using SADABS. The structure was solved by direct methods and was refined with the aid of successive Fourier difference maps against all data using the SHELX software package.

Dynamic Light Scattering, DLS. DLS experiments were performed at 25°C to measure the average particle size of the reverse micelles in solution using a DynaPro Titan with DynaPro DYNAMICS software V. 6.7.3 (Wyatt, USA).

Nuclear Magnetic Resonance, NMR. ^1H NMR solution spectra were recorded on a INOVA-300 or 400 MHz spectrometers (Varian, USA). Tetramethylsilane (TMS) was used as an internal reference (0.00 ppm) for HMet^+ in organic solvent.

^{51}V NMR spectra were recorded using parameters reported previously at 78.9 and 105.2 MHz (Crans, Baruah, and Levinger, 2006; Sedgwick, Crans, and Levinger, 2009; Crans, Rithner, and Theisen, 1990). Data analysis was conducted using MestReC

V. 4.5.9.1 NMR data processing software and ACD/NMR processor academic edition for Windows. The ^{51}V NMR spectral peaks were fitted to find the chemical shifts and line widths (OriginPro 7) using Gaussian or Lorentzian line shape functions. $\Delta_{1/2}$ is the full width at half height in Hertz assuming the system is described within the extreme motional narrowing limit (Stover, Rithner, Inafuku, Crans, and Levinger, 2005).

3.3 Research Procedure

This research aims to separate MetHCl from drug, and synthesize crystalline compounds containing metformin and decavanadate. Sample products are characterized by physical techniques to support property and structure of compound using melting point, FTIR, elemental analysis (CHN), thermal analysis (TGA), powder XRD, and single crystal X-ray diffractometry.

Moreover, solutions of sample products were studied in AOT reverse micelle (synthetic cell model) to investigate how these ions interact with the interface in RMs, how counterions affect water in the water pool, and the water organization near the interface, including the effect on size of reverse micelles, using ^1H and ^{51}V NMR, dynamic light scattering, and FTIR techniques.

3.4 References

- Baruah, B., Roden, J. M., Sedgwick, M. A., Correa, N. M., Crans, D. C., and Levinger, N. E. (2006). When is water not water? Exploring water confined in large reverse micelles using a highly charged inorganic molecular probe. **Journal of the American Chemical Society**. 128: 12758-12765.
- Baruah, B., Swafford, L. A., Crans, D. C., and Levinger, N. E. (2008). Do probe molecules influence water in confinement? **Journal of Physical Chemistry B**. 112: 10158-10164.

- Chowdhury, P. K., Ashby, K. D., Datta, A., and Petrich, J. W. (2000). Effect of pH on the fluorescence and absorption spectra of hypericin in reverse micelles. **Photochemistry and Photobiology**. 72: 612-618.
- Crans, D. C. (1994). Aqueous chemistry of labile oxovanadates: Relevance to biological studies. **Comments on Inorganic Chemistry**. 16: 1-33.
- Crans, D. C., Baruah, B., and Levinger, N. E. (2006). Oxovanadates: a novel probe for studying lipid-water interfaces. **Biomedicine & Pharmacotherapy**. 60: 174-181.
- Crans, D. C., Rithner, C. D., and Theisen, L. A. (1990). Application of time-resolved ^{51}V 2D NMR for quantitation of kinetic exchange pathways between vanadate monomer, dimer, tetramer, and pentamer. **Journal of the American Chemical Society**. 112: 2901-2908.
- Gadape, H. H. and Parikh, K. S. (2011). Quantitative determination and validation of metformin hydrochloride in pharmaceutical using quantitative nuclear magnetic resonance spectroscopy. **E-Journal of Chemistry**. 8: 767-781.
- Howarth, O. W. (1990). Vanadium-51 NMR. **Progress in Nuclear Magnetic Resonance Spectroscopy**. 22: 453-483.
- Sedgwick, M. A., Crans, D. C., and Levinger, N. E. (2009). What is inside a nonionic reverse micelle? Probing the interior of Igepal reverse micelles using decavanadate. **Langmuir**. 25: 5496-5503.
- Stahla, M. L., Baruah, B., James, D. M., Johnson, M. D., Levinger, N. E., and Crans, D. C. (2008). ^1H NMR studies of Aerosol-OT reverse micelles with alkaline and magnesium counterions: Preparation and analysis of MAOTs. **Langmuir**. 24: 6027-6035.
- Stover, J., Rithner, C. D., Inafuku, R. A., Crans, D. C., and Levinger, N. E. (2005). Interaction of dipicolinatodioxovanadium(V) with polyatomic cations and surfaces in reverse micelles. **Langmuir**. 21: 6250-6258.

CHAPTER IV

STRUCTURE AND ^1H NMR OF PHARMACEUTICAL DRUG METFORMIN HYDROCHLORIDE

4.1 Introduction

Metformin Hydrochloride (*N,N*-dimethylbiguanide hydrochloride, MetHCl) is called metformin and known as an agent that is used for treatment of type 2 diabetes. It also acts as an anticancer drug (Jung, Park, Lee, Seo, Trosko, and Kang, 2011; Blandino, Valerio, Cioce, Mori, Casadei, Pulito, Sacconi, Biagioni, Cortese, Galanti, Manetti, Citro, Muti, and Strano, 2012), antimicrobial agent (Olar, Badea, Lazar, Balotescu, Cristurean, and Marinescu, 2007), and antimalarial drug (Danquah, Bedu-Addo, and Mockenhaupt, 2010; Sweeney, Raymer, and Lockwood, 2003).

The drug metformin is usually the first-line agent for management of type 2 DM. It is anticipated to reduce insulin resistance, contribute to weight loss, and improve cardiovascular outcomes (Nathan, Buse, Davidson, Ferrannini, Holman, Sherwin, and Zinma, 2009). Metformin appears to have several and many studied but still incompletely understood mechanisms. The most important effect is it reduces blood glucose levels by decreasing glucose production in the liver, which helps in reducing gluconeogenesis and enhances insulin sensitivity in muscle and fats cells (Goodman, Hardman, Limbird, and Gilman, 2001; Rang, Dale, Ritter, and Fower, 2007). The efficacy of glycemic control achieved with MetHCl is similar to sulfonylurea but their mode is different when MetHCl facilitates glucose transport in cultured skeletal muscle in the absence of insulin. The bioavailability of MetHCl is approximately 50%, thus after

intravenous administration about 50% does not metabolize and is excreted in urine, and feces.

Several analytical methods have been used to determine or evaluate properties and mechanisms of MetHCl individually, or in combination with other drugs (Hundal, Krssak, Dufour, Laurent, Lebon, Chandramouli, Inzucchi, Schumann, Petersen, Landau, and Shulman, 2000; Zou, Kirkpatrick, Davis, John, Nelson, Walter, Wiles IV, Schlattner, Neumann, Brownlee, Freeman, and Goldman, 2004; Qu, Zhang, Liao, Chen, Zhao, and Pan, 2012; Sirtori and Christophe, 1994; Viollet, Guigas, Garcia, Leclerc, Foretz, and Andreelli, 2012). These mainly include vibrational analysis FTIR (Gunasekaran, Natarajan, Renganayaki, and Natarajan, 2006; Spectral database for organic compound SDBS website), NMR spectroscopy (Gadape and Parikh, 2011; Brittain, 1998; Hansen and McCormack, 2002), chromatographic techniques in association with HPLC (Onal, 2009; Jain, Jain, Jain, and Amin, 2008), and X-ray diffractometry (Hariharan, Rajan, and Srinivasan, 1989; Child, Chyall, Dunlap, Coates, Stahly, and Stahly, 2004).

This chapter reviews the physical properties, structure of MetHCl from data of Cambridge Structure Database, and primary results of Met:HCl in AOT reverse micelle systems using nuclear magnetic resonance technique. The AOT reverse micelle system is a simple model with controllable parameters that allow manipulation of the environment in a setting similar to cell interfaces to investigate how a given drug interacts with the interface and/or cell.

4.2 Experimental

4.2.1 Materials

Metformin hydrochloride was obtained from Sigma-Aldrich (97%) or isolated from Glucophage tablets (Merck). Vanadium pentoxide, V_2O_5 , (Fluka, $\geq 98.0\%$). Sodium bis(2-ethylhexyl)sulfosuccinate, AOT, (Sigma-Aldrich, 98%) was purified as described

previously (Baruah, Swafford, Crans, and Levinger, 2008; Chowdhury, Ashby, Datta, and Petrich, 2000). Deuterated dimethyl sulfoxide (d_6 -DMSO), deuterated methanol (d_4 -MeOH), and tetrametylsilane (TMS) (Cambridge Isotope Laboratories), and isooctane (Sigma-Aldrich, 99%) were used as received. Doubly distilled water was used for all reverse micelle systems.

4.2.2 Sample Preparation

Isolation of metformin hydrochloride. Two glucophage tablets (Merck and Co., containing 850 mg metformin hydrochloride in an 896 mg tablet) were ground in a mortar, mixed with 7.0 mL of deionized water, stirred, and heated at 60°C for 15 min. The mixture was filtered and the filtrate evaporated at 45-50°C about 1.5 hr to reduce volume until 1/3 is left. The resulting solution was left at ambient temperature for crystallization. The crystals were characterized by FT-IR, XRD, and melting point techniques, and compared to standard metformin hydrochloride (97%) from Sigma-Aldrich.

Preparation of AOT/isooctane RMs with MetHCl. Each sample was prepared by pipetting a specific volume of metformin in D₂O stock solution to the 0.2 M AOT in isooctane stock solution to prepare systems with various w_0 , pH, and concentration of metformium, HMet⁺, (see Table 3.1 in Chapter III). All samples were vortically mixed until the solution was clear.

4.2.3 Characterization

The crystals were characterized by comparing with standard MetHCl from Sigma-Aldrich. Reverse micelle samples with pH range 1-14, various concentrations of metformin, and various w_0 ratios were characterized using ¹H NMR.

4.2.4 Instrumentation

Fourier transform infrared spectroscopy, FTIR. Infrared spectra were recorded in the mid-IR range $4000\text{-}400\text{ cm}^{-1}$. Solid state spectra were recorded on a Spectrum GX (Perkin Elmer, USA) spectrophotometer at 4 cm^{-1} resolution, 15 scans using KBr pellets.

Powder X-ray diffraction, XRD. Powder XRD spectra were recorded on a D5005 diffractometer (Bruker AXS, Germany) using Cu $K\alpha$ X-ray radiation ($\lambda = 1.54\text{ \AA}$) and a 0.5 mm divergence slit with data collected over a $5.0\text{-}45.0^\circ$ 2θ range using tube power level 40 kV and 40 mA, with the JCPDS library (International Center for Diffraction Data, 2004).

Melting point apparatus. Melting points were determined with a Griffin model MPA 350 BM2.5 (Gallenkamp, UK). Observed sample decomposes with temperature. Use for determined melting point of compounds.

Nuclear Magnetic Resonance, NMR. ^1H NMR solution spectra were recorded on a INOVA-300 or 400 MHz spectrometers (Varian, USA). Tetrametylsilane (TMS) was used as an internal reference (0.00 ppm) for HMet^+ in organic solvent.

4.3 Results and Discussion

The IR and XRD spectra of MetHCl extracted from the drug were compared with the spectra of standard metformin hydrochloride or from Sigma, as shown in Figures 4.1 and 4.2, and IR band assignments in Table 4.1, respectively. The data demonstrate that the two samples are the same compound. The melting point of extracted drug is 223°C which compares favorably to the Sigma standard, 224°C , and the value in the Merck Index, which lists crystals of MetHCl from water with a melting point about 232°C (O'Neil, Smith, Heckelman, Obenchain, Gallipeau, D'Arecca, and Budavari, 2001).

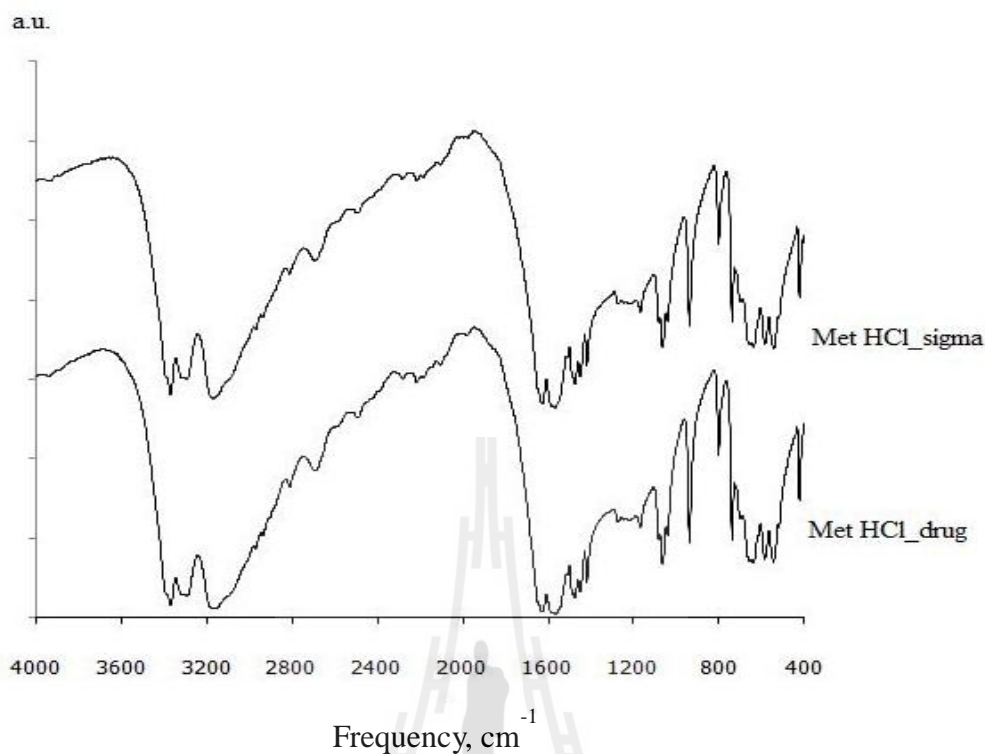


Figure 4.1 The IR spectrum of metformin hydrochloride.

Table 4.1 IR band assignments for metformin hydrochloride.

Assignment	Frequency (cm ⁻¹)	Structure
$\nu_a(\text{NH}_2)$	3371, 3296	
$\nu_s(\text{NH}_2)$	3173	
$\nu(\text{C}=\text{N})$	1626	
$\nu_a(\text{NCN})$	1584, 1586	
$\nu(\text{CN})$	1475, 1449	
$\nu(\text{CH}_3)$	1418	
$\rho(\text{NH}_2)$	1081, 1064	
$\nu_s(\text{NCN})$	938	
$\delta(\text{NCN})$	737, 658, 585	

(ρ is rocking, and δ is scissoring in plane bending)

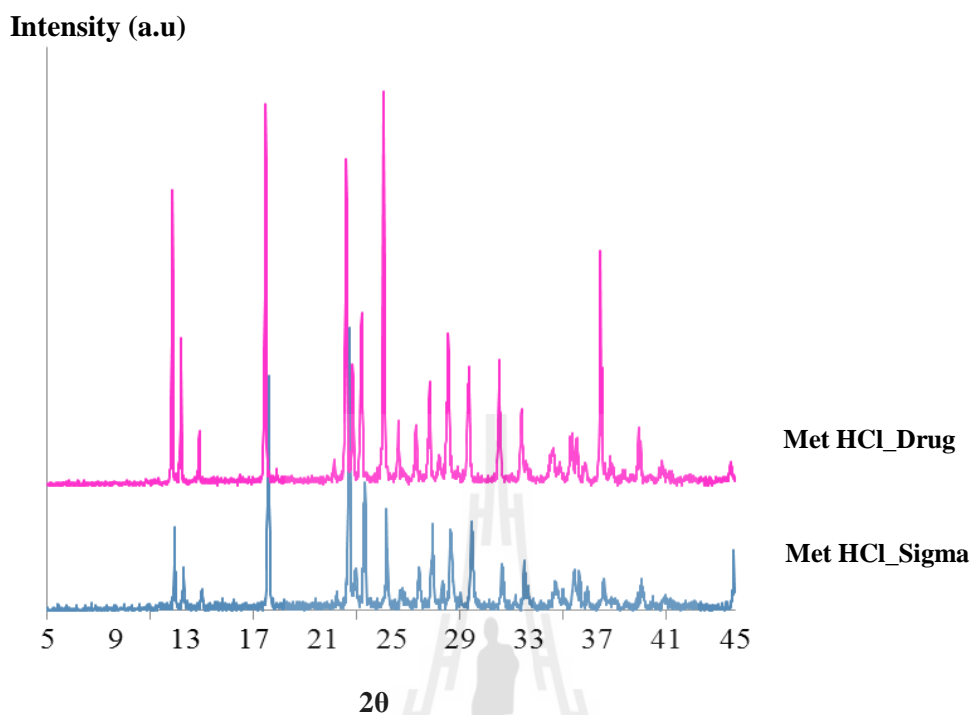


Figure 4.2 XRD spectra of metformin hydrochloride.

Structure of MetHCl. A review of the structural analysis literature of metformin hydrochloride was undertaken to establish the relationship of the C1=N2 and C2=N4 distances in biguanide (Figure 4.3 diagram of MetHCl). The crystal structures of MetHCl have been studied (Hariharan, Rajan, and Srinivasan, 1989; Childs, Chyall, Dunlap, Coates, Stahly, and Stahly, 2004). Shown that the C–N bond distance ranges from 1.330–1.358 Å in biguanide group (Table 4.2), intermediate between normal single and double bond distances (average C–N 1.461 and C=N 1.279 Å) (Burgi and Dunitz, 1994). The C3–N5 and C4–N5 bond distance ranges are consistent with single bonds. Protonation occurs at N4 (near the $-\text{N}(\text{CH}_3)_2$ group). The two guanidine groups (N1–C1–N2–N3, and N3–C2–N4–N5) are twisted with respect to one another (dihedral angle, φ) in the range 53–68°, thus HMet^+ is not planar and the π -electron delocalization is interrupted at the center nitrogen atom (N3).

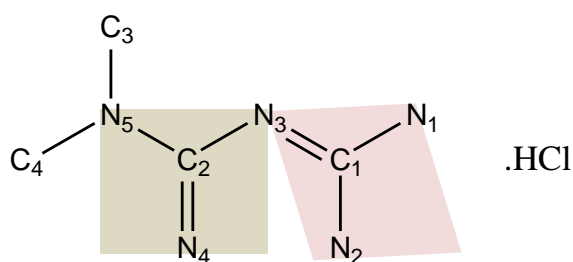


Figure 4.3 Diagram of metformin hydrochloride.

Table 4.2 Bond lengths of metformin hydrochloride.

Bond length, Å	C1–N1	C1–N2	C1–N3	C2–N3	C2–N4	C2–N5	C3–N5	C4–N5	φ , °
HMet ⁺ Cl ^a	1.331(5)	1.335(4)	1.332(4)	1.348(3)	1.330(4)	1.334(3)	1.461(4)	1.461(4)	67.9
HMet ⁺ Cl ^b	1.334(2)	1.339(2)	1.333(1)	1.358(1)	1.336(2)	1.336(2)	1.462(2)	1.467(1)	53.7

a. Hariharan, Rajan, and Srinivasan, 1989, b. Childs, Chyall, Dunlap, Coates, Stahly, and Stahly, 2004.

The HMet⁺ cations are interconnected into one dimensional chains along the *c* axis by intermolecular N2–H···N3' hydrogen bonds, as shown in Figure 4.4. Chains of cations are linked together through charge assisted N–H···Cl and C–H···Cl hydrogen bonds (Figure 4.5 and Table 4.3). The packing of molecules in the unit cell, the chloride anion has four N–H···Cl bond and one C–H···Cl bond with adjacent HMet⁺ cations. The C–H···Cl bond distances are longer than the average value 3.66(1) Å from neutron diffraction data (Steiner, 1998), but still within the range of C–H···Cl hydrogen bond (Davidson, Lambert, Lopez-Solera, Raithby, and Snaith, 1995), thus charge-assisted N–H···Cl, and C–H···Cl hydrogen bonds are identified to extend the structure into 3D network.

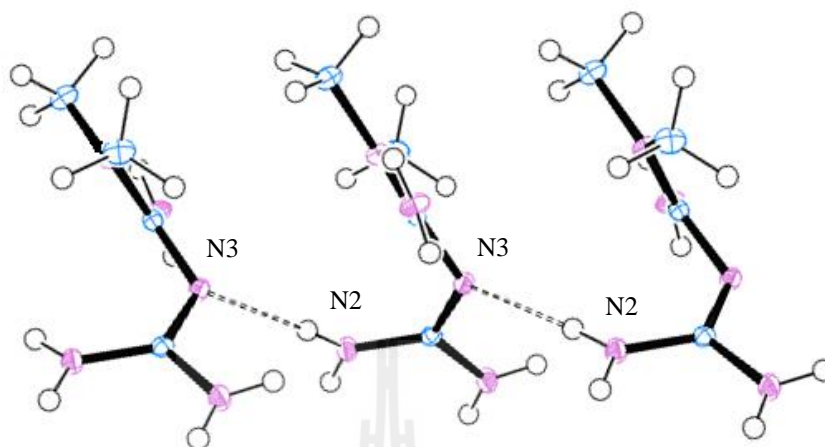


Figure 4.4 Aggregation of HMet^+ cations in one chain, projected parallel to $[010]$.

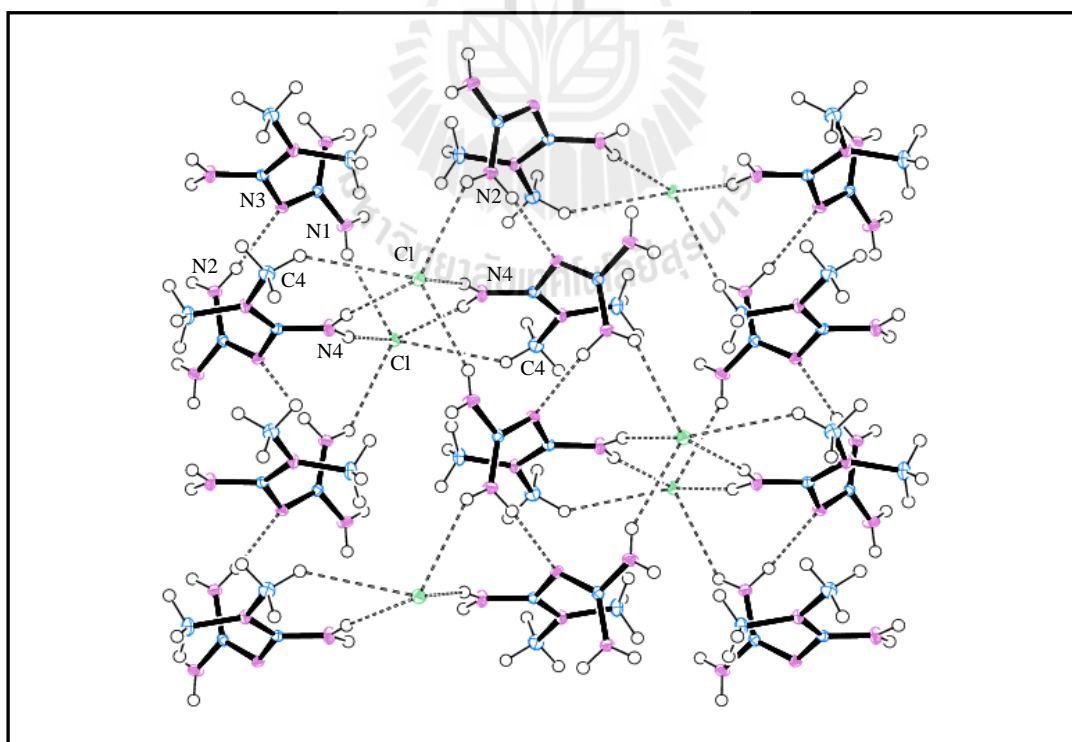


Figure 4.5 Packing diagram of metformin hydrochloride. Through $\text{N-H}\cdots\text{Cl}$ and $-\text{H}\cdots\text{Cl}$ hydrogen bond, view along $[100]$.

Table 4.3 Hydrogen bonding in metformin hydrochloride.

$D-H\cdots A$	$d[D-H], \text{\AA}$	$d(H\cdots A), \text{\AA}$	$\angle DHA, ^\circ$	$d[D\cdots A], \text{\AA}$
N1-H4 \cdots Cl	0.82	2.60	147.1	3.312(1)
N2-H2 \cdots Cl	0.86	2.71	128.6	3.312(1)
N4-H5 \cdots Cl	0.86	2.42	164.7	3.272(1)
N4-H6 \cdots Cl	0.85	2.46	165.7	3.284(1)
C4-H9 \cdots Cl	0.97	3.03	132.5	3.749(1)
N2-H1 \cdots N3	0.88	2.08	174.0	2.956(2)

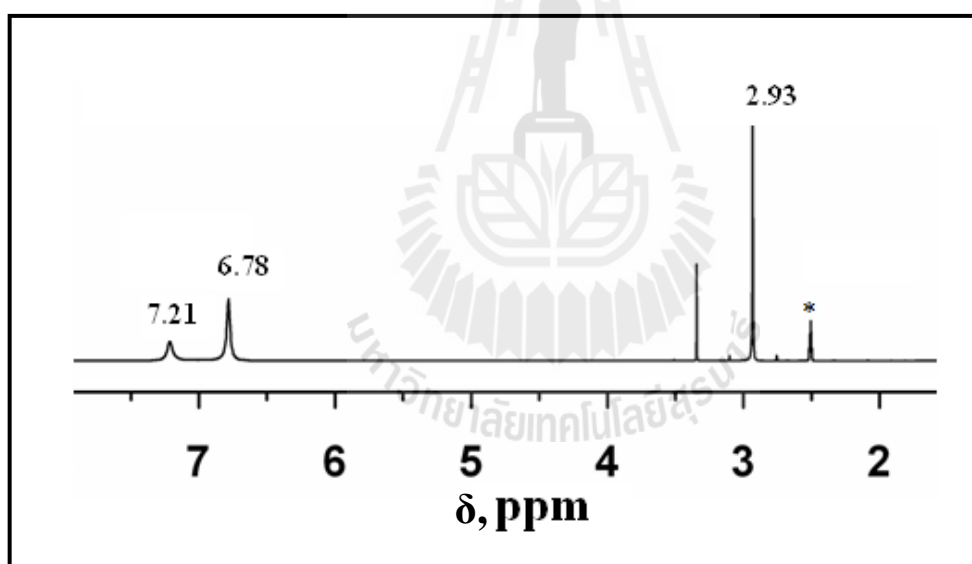
Solubility of MetHCl. MetHCl is readily water soluble, confirming the formation of strong hydrogen bonding of metformin with water similar to the behavior of urea (Rezus and Bakker, 2006; Vanzi, Madan, and Sharp, 1998). It is highly dissolved in DMSO and has limited solubility in AOT/isooctane RMs, 150 mM (0.0248 g) MetHCl at w_0 10 in 0.75 M AOT RMs is a highest value of dissolved. It is insoluble in isooctane, cyclohexane, and acetone organic solutions.

$^1\text{H NMR}$ of MetHCl. $^1\text{H NMR}$ spectra of MetHCl solution showed chemical shifts at 3.05 ppm at pH 1, 2.92 ppm at pH 7, and 2.77 ppm at pH 14 (Table 4.4). This is consistent with deprotonation of metformin at alkaline pH (Szakacs, Kraszni, and Noszal, 2004). In D_2O and d_4 -MeOH, the NH protons exchange and only one peak at 2.91 (D_2O) or 3.03 (MeOH) ppm of the CH_3 is observed. The CH_3 and NH protons in HMet^+ could be observed in d_6 -DMSO at 2.93, 6.78, and 7.21 ppm (Figure 4.6). Integration of CH_3 , NH_2 , and NH_2^+ signals give the ratio 3:2:1, respectively, and are consistent with the previous report (Gadape and Parikh, 2011).

Table 4.4 ^1H NMR chemical shifts of metformin hydrochloride as a function of pH.

pH	Chemical shift, (ppm)	pH	Chemical shift, (ppm)
1	3.05	8	2.91
2	3.04	9	2.90
3	3.03	10	2.90
4	2.93	11	2.90
5	2.91	12	2.89
6	2.91	13	2.88
7	2.91	14	2.77

(most samples were measured in duplicate)

**Figure 4.6** ^1H NMR spectrum of HMet^+ cation in d_6 -DMSO. (* solvent)

^1H NMR spectra of MetHCl in AOT RMs at various concentrations of 1.0, 0.75, 0.50, 0.25, and 0.15 M and different w_0 of 2, 4, 6, 10, and 16 (Table 4.5) show insignificant differences of the methyl proton shifts at ~ 3.06 ppm, downfield shift as compared with 2.91 ppm in aqueous solution, consistent with the existence of HMet^+ in the AOT/isooctane system.

Table 4.5 ^1H NMR chemical shifts of MetHCl in 0.2 M AOT/isooctane RMs.

w_0	Chemical shift of metformin, (ppm)					Mean δ , (ppm)
	1 M	0.75 M	0.50 M	0.25 M	0.15 M	
Stock	3.00	3.01	3.02	3.03	3.03	3.02 ± 0.01
2	3.05	3.05	3.05	3.04	3.03	3.04 ± 0.01
4	3.06	3.06	3.06	3.05	3.04	3.05 ± 0.01
6	3.07	3.06	3.06	3.07	3.05	3.06 ± 0.01
10	3.07	3.07	3.07	3.07	3.06	3.07 ± 0.01
16	3.07	3.07	3.07	3.07	3.06	3.07 ± 0.01

(most samples were measured in duplicate)

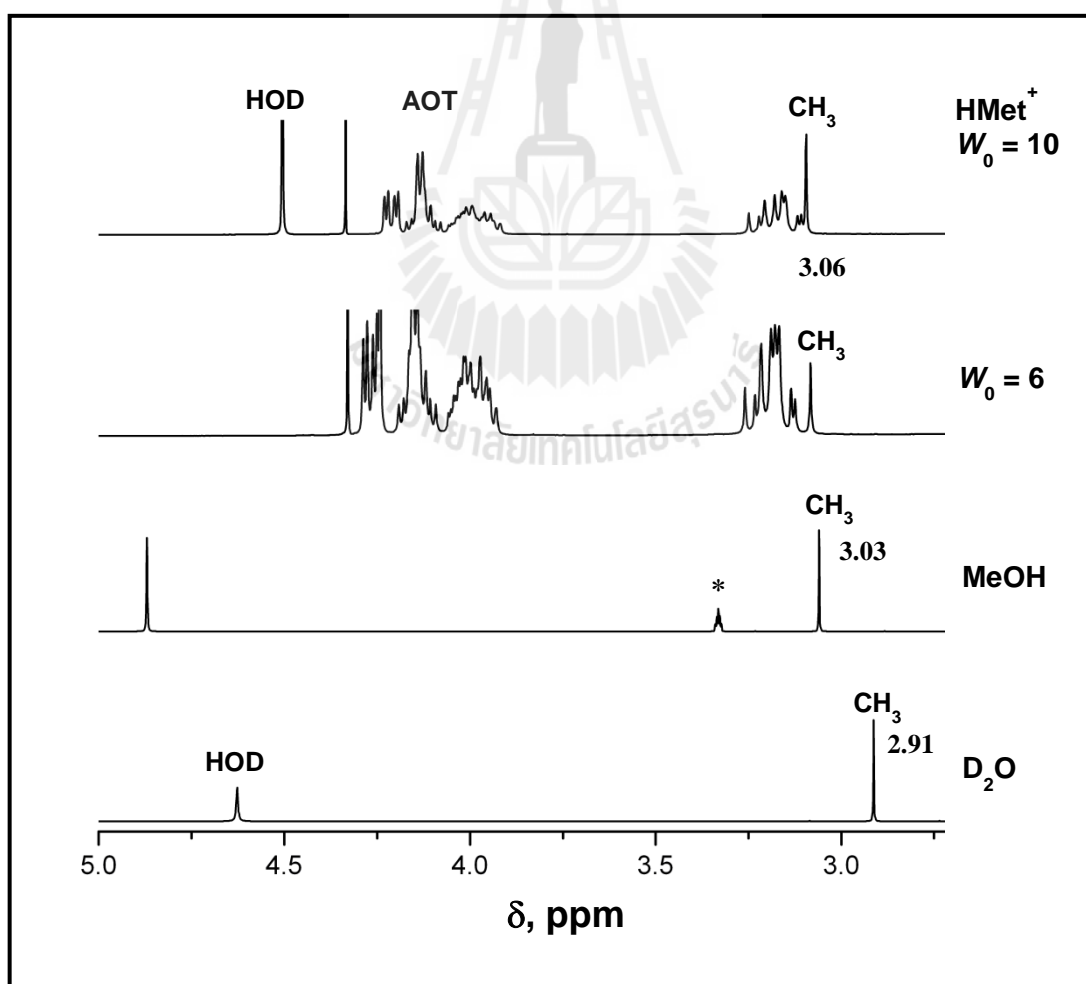


Figure 4.7 ^1H NMR spectra of HMet^+ in D_2O , MeOH, and 0.2 M AOT RMs at $w_0 = 6$ and 10. (* solvent, MetHCl 0.25 M in AOT RMs)

Representative spectra at $w_0 = 6$ and 10 are compared with the spectra of HMet^+ in D_2O and $d_4\text{-MeOH}$ in Figure 4.7. A recent study of competitive counterion binding to micelles and mixed micelles found essentially constant counterion binding with the ratio quantitatively modeled using a simple equilibrium model (Maneedaeng, Haller, Grady, and Flood, 2011). A similar effect will occur here with HMet^+ cations replacing sodium counter ions, an interpretation consistent with previous reports (Vermathen, Louie, Chodosh, Ried, and Simonis, 2000; Pal, Vishal, Gandhi, and Ayappa, 2005; Crans, Rithner, Baruah, Gourley, and Levinger, 2006).

The ^1H NMR chemical shift of HMet^+ moved to lower resonance when added to AOT RMs. The shift suggests that HMet^+ penetrates into the RM interface, rather than being located in the middle of the RM water pool. Previous ^1H and ^{51}V NMR studies, $[\text{VO}_2\text{dipic}]^-$ in CTAB RMs system have suggested that a shift toward lower field indicates the complex is associated with the interface, while a shift toward higher field indicates that the complex penetrates the nonpolar interface (Crans, Baruah, Gourley, and Levinger, 2006; Vermathen, Stiles, Bachofer, and Simonis, 2002). When the probe molecule is located at the highly charged interface layer of the polar headgroups, the increased proton-headgroup interaction reduces the electron density at the H atoms in HMet^+ ion, deshielding then giving the downfield chemical shift. If probe penetration into the nonpolar carbon chain results in additional shielding by the nonpolar environment an upfield shift as compared to aqueous solution will be observed. Magnitudes of chemical shifts were analyzed to determine the depths of naphthoate anion at the interface of a cationic micellar system (Bechofer, Simonis, and Nowicki, 1991). Thus HMet^+ , with a relatively small chemical shift relative to the stock solution (D_2O) of HMet^+ , does not appear to deeply penetrate the RM interface. How HMet^+ affects the reverse micelle system is investigated in the next chapter.

4.4 Conclusions

The solid state of MetHCl shows π -electron delocalization across the biguanide group but large dihedral angle between two planar guanidine groups are interrupted π -electron delocalized at bridging N atom. Furthermore, the results obtained by ^1H NMR of MetHCl at different pH values are consistent with deprotonation at alkaline pH. While proton chemical shift of $-\text{CH}_3$ in the inhomogeneous environment of AOT reverse micelles moves to lower resonance (compared with D_2O solution) indicating interface interaction of HMet^+ cation with reverse micelles.

4.5 References

- Baruah, B., Swafford, L. A., Crans, D. C., and Levinger, N. E. (2008). Do probe molecules influence water in confinement? **Journal of Physical Chemistry B.** 112: 10158-10164.
- Bechofer, S. J., Simonis, U., and Nowicki, T. A. (1991). Orientational binding of substituted naphthoate counterions to the tetradecyltrimethylammonium bromide micellar interface. **Journal of Physical Chemistry.** 95: 480-488.
- Blandino, G., Valerio, M., Cioce, M., Mori, F., Casadei, L., Pulito, C., Sacconi, A., Biagioni, F., Cortese, G., Galanti, S., Manetti, C., Citro, G., Muti, P., and Strano. S. (2012). Metformin elicits anticancer effects through the sequential modulation of DICER and C-MYC. **Nature Communications.** 3: 865.
- Brittain, H. G. (1998). **Analytical Profiles of Drug Substances and Excipients.**: Academic Press Inc.: California. Vol. 25. p. 291.
- Burgi, H.-B. and Dunitz, J. D. (1994). **Structure Correlation.** VCH: Weinheim. Vol. 2. pp. 767-848.
- Child, S. L., Chyall, L. J., Dunlap, J. T., Coates, D. A., Stahly, B. C., and Stahly, G. P. (2004). A metastable polymorph of metformin hydrochloride: Isolation and

- characterization using capillary crystallization and thermal microscopy techniques. **Crystal Growth & Design**. 4: 441-449.
- Chowdhury, P. K., Ashby, K. D., Datta, A., and Petrich, J. W. (2000). Effect of pH on the fluorescence and absorption spectra of hypericin in reverse micelles. **Photochemistry and Photobiology**. 72: 612-618.
- Crans, D. C., Rithner, C. D., Baruah, B., Gourley, B. L., and Levinger, N. E. (2006). Molecular probe location in reverse micelles determined by NMR dipolar interactions. **Journal of the American Chemical Society**. 128: 4437-4445.
- Danquah, I., Bedu-Addo, G., and Mockenhaupt, F. P. (2010). Type 2 diabetes mellitus and increased risk for malaria infection. **Emerging Infectious Diseases**. 16: 1601-1604.
- Davidson, M. G., Lambert, C., Lopez-Solera, I., Raithby, P. R., and Snaith, R. (1995). Aggregation of metaleed organics by hydrogen bonding: Synthesis and crystal structures of 2-aminophenoxy-aluminum and salen-aluminum ligand-separated ion pairs. **Inorganic Chemistry**. 34: 3765-3779.
- Fridrichová, M., Císařová, I., and Němec, I. (2012). 1,1-Dimethylbiguanidium(2+) dinitrate. **Acta Crystallographica Section E**. 68: o18-o19.
- Gadape, H. H. and Parikh, K. S. (2011). Quantitative determination and validation of metformin hydrochloride in pharmaceutical using quantitative nuclear magnetic resonance spectroscopy. **E-Journal of Chemistry**. 8: 767-781.
- Goodman, L. S., Hardman, J. G., Limbird, L. E., and Gilman, A. G. (2001). **Goodman & Gilman's the Pharmacological Basic of Therapeutics**. 10th ed. McGraw-Hill: New York. pp. 1679-1710.
- Gunasekaran, S., Natarajan, R. K., Renganayaki, V., and Natarajan, S. (2006). Vibrational spectra and thermodynamic analysis of metformin. **Indian Journal of Pure & Applied Physics**. 44: 495-500.

- Hansen, S. H. and McCormack, J. G. (2002). Application of ^{13}C -filtered ^1H NMR to evaluate drug action on gluconeogenesis and glycogenolysis simultaneously in isolated rat hepatocytes. **NMR in Biomedicine**. 15: 313-319.
- Hariharan, M., Rajan, S. S., and Srinivasan, R. (1989). Structure of metformin hydrochloride. **Acta Crystallographica Section C**. 45: 911-913.
- Huang, L., Xi, P.-X., Xu, M., Lui, T.-H., and Zeng, Z.-Z. (2008). Crystal structure of metformin ethyl-N-(3-tosylfonyl)carbamate. **Analytical Sciences**. 24: x289-x290.
- Hundal, R. S., Krssak, M., Dufour, S., Laurent, D., Lebon, V., Chandramouli, V., Inzucchi, S. E., Schumann, W. C., Petersen, K. F., Landau, B. R., and Shulman, G. I. (2000). Mechanism by which metformin reduces glucose production in Type 2 diabetes. **Diabetes**. 49: 2063-2069.
- Jain, D., Jain, S., Jain, D., and Amin, M. (2008). Simultaneous estimation of metformin hydrochloride, pioglitazone hydrochloride, and glimepiride by RP-HPLC in tablet formulation. **Journal of Chromatography Science**. 46: 501-504.
- Jung, J.-W., Park, S.-B., Lee, S.-J., Seo, M.-S., Trosko, J. E., and Kang, K.-S. (2011). Metformin represses self-renewal of the human breast carcinoma stem cells via inhibition of estrogen receptor-mediated OCT4 expression. **Plos One**. 6: e28068.
- Lu, L., Zhang, H., Feng, S., and Zhu, M. (2004). *N-N*-dimethylbiguanidium bromide. **Acta Crystallographica Section E**. 60: o640-o641.
- Lu, L.-P., Zhang, H.-M., Feng, S.-S., and Zhu, M.-L. (2004). Two *N-N*-dimethylbiguanidium salts displaying double hydrogen bonds to the counter-ions. **Acta Crystallographica Section C**. 60: o740-o743.
- Maneedaeng, A., Haller, K. J., Grady, B. P., and Flood, A. E. (2011). Thermodynamic parameters and counterion binding to the micelle in binary anionic surfactant systems. **Journal of Colloid Interface Science**. 356: 598-604.

- Nathan, D. M., Buse, J. B., Davidson, M. B., Ferrannini, E., Holman, R. R., Sherwin, R., and Zinman, B. (2009). Medical management of hyperglycaemia in type 2 diabetes mellitus: A consensus algorithm for the initiation and adjustment of therapy: A consensus statement from the American Diabetes Association and the European Association for the Study of Diabetes. **Diabetologia**. 52: 17-30
- O'Neil, M. J., Smith, A., Heckelman, P. E., Obenchain, J. R., Gallipeau, J. A. R., D'Arecca, M. A., and Budavari, S. (2001). **The Merck Index: An Encyclopedia of Chemicals, Drugs, and Biologicals**. 13th ed. Merck & Co., Inc.: New Jersey. p. 1061.
- Olar, R., Badea, M., Lazar, V., Balotescu, C., Cristurean, E., and Marinescu, D. (2007). Thermal behavior of some *N,N*-Dimethylbiguanide derivatives displaying antimicrobial activity. **Journal of Thermal Analysis and Calorimetry**. 2: 323-327.
- Onal, A. (2009). Spectrophotometric and HPLC determinations of anti-diabetic drugs, rosiglitazone maleate and metformin hydrochloride, in pure form and in pharmaceutical preparations. **European Journal of Medical Chemistry**. 44: 4998-5005.
- Pal, S., Vishal, G., Gandhi, K. S., and Ayappa, K. G. (2005). Ion exchange in reverse micelles. **Langmuir**. 21: 767-778.
- Qu, Z., Zhang, Y., Liao, M., Chen, Y., Zhao, J., and Pan, Y. (2012). *In vitro* and *in vivo* antitumoral action of metformin on hepatocellular carcinoma. **Hepatology Research**. 12: 922-933.
- Rang, H. P., Dale, M. M., Ritter, J. M., and Fower, R. J. (2007). **Pharmacology**. 6th Ed. Elsevier. pp. 397-409.
- Rezus, Y. L. A. and Bakker, H. J. (2006). Orientational dynamics of isotopically diluted H₂O and D₂O. **Journal of Chemical Physics**. 125: 144512-144520.

- Sirtori, C. R. and Christophe, P. (1994). Re-evaluation of a biguanide, metformin: mechanism of action and tolerability. **Pharmacological Research**. 30: 187-228.
- Spectral database for organic compounds SDBS website: http://riodb01.ibase.aist.go.jp/sdbs/cgi-bin/direct_frame_top.cgi. (on 20 September 2012)
- Steiner, T. (1998). Hydrogen-bond distances to halide ions in organic and organometallic crystal structures: Up-to-date database study. **Acta Crystallographica Section B**. 54: 456-463.
- Sweeney, D., Raymer, M. L., and Lockwood, T. D. (2003). Antidiabetic and antimalarial biguanide drugs are metal-interactive antiproteolytic agents. **Biochemical Pharmacology**. 66: 663-77.
- Szakacs, Z., Kraszni, M., and Noszal, B. (2004). Determination of microscopic acid-base parameters from NMR-pH titrations. **Analytical and Bioanalytical Chemistry**. 378: 1428-1448.
- Vanzi, F., Madan, B., and Sharp, K. (1998). Effect of the protein denaturants urea and guanidinium on water structure: A structural and thermodynamic study. **Journal of the American Chemical Society**. 120: 10748-10753.
- Vermathen, M., Louie, E. A., Chodosh, A. B., Ried, S., and Simonis, U. (2000). Interactions of water-insoluble tetraphenylporphyrins with micelles probed by UV-visible and NMR spectroscopy. **Langmuir**. 16: 210-221.
- Vermathen, M., Stiles, P., Bachofer, S. J., and Simonis, U. (2002). Investigations of monofluoro-substituted benzoates at the tetradecyltrimethylammonium micellar interface. **Langmuir**. 18: 1030-1042.
- Viollet, B., Guigas, B., Garcia N. S., Leclerc, J., Foretz, M., and Andreelli, F. (2012). Cellular and molecular mechanisms of metformin: An overview. **Clinical Science (London)**. 122: 253-270.

Zhu, M., Lu, L., and Yang, P. (2003). *N-N*-dimethylbiguanidium nitrate. **Acta Crystallographica Section E**. 59: o586-o588.

Zou, M.-H., Kirkpatrick, S. S., Davis, B. J., John, S., Nelson, J. S., Walter, G., Wiles IV, W. G., Schlattner, U., Neumann, D., Brownlee, M., Freeman, M. B., and Goldman, M. H. (2004). Activation of the AMP-activated protein kinase by the anti-diabetic drug metformin *in vivo*. **The Journal of Biological Chemistry**. 279: 43940-4395.



CHAPTER V

DECAVANADATE COUNTERION AFFECTS

INTERACTION WITH INTERFACES: COMPLEXATION

WITH THE ANTIDIABETIC DRUG METFORMIN

5.1 Introduction

Vanadium in oxidation state +5 readily forms oxometalates in aqueous solution of which decavanadate (variously protonated $V_{10}O_{28}$ species), V_{10} , is particularly stable at acidic pH. Since V_{10} was found to be insulin enhancing with two different counter ions (Yraola, Garcia-Vicente, Marti, Albericio, Zorzano, and Royo, 2007; Aureliano and Crans, 2009; Pereira, Carvalho, Eriksson, Crans, and Aureliano, 2009) we were interested in investigating the complex formed between V_{10} and a counterion such as metformium ($HMet^+$). Large anions such as V_{10} and Keggin ions such as $(PMo_{12}O_{40})^{-3}$, $(SiW_{12}O_{40})^{-4}$, and $(PW_{12}O_{40})^{-3}$ are presumed to less readily traverse membranes because of their large charges and size; thus fundamental information on their association with interfaces was desired. Recently, studies of how vanadium compounds interact with and traverse membranes (Zhang, Ruan, Chen, Lu, and Wang, 1997; Kotchevar, Ghosh, and Uckun, 1998; Goldwasser, Li, Gershonov, Armoni, Karnieli, Fridkin, and Shechter, 1999; Kotchevar, Ghosh, DuMez, and Uckun, 2001; Bakas, Verza, and Cortizo, 2001; Yang, Wang, Lu, and Crans, 2003; Yang, Yang, Yuan, Wang, and Crans, 2004; Crans, Baruah, and Levinger, 2006; Crans, Rithner, Baruah, Gourley, and Levinger, 2006; Hiromura, Nakayama, Adachi, Doi, and Sakurai, 2007; Roess, Smith, Winter, Zhou, Dou, Baruah, Trujillo, Levinger, Yang, Barisas, and Crans, 2008; Winter, Al-Qatati, Wolf-Ringwall, Schoeberl, Chatterjee, Barisas, Roess, and Crans, 2012), have shown that large

oxometalates such as decavanadate reside away from a negatively charged interface, and close to a positively charged interface as expected (Baruah, Roden, Sedgwick, Correa, Crans, and Levinger, 2006; Sedgwick, Crans, and Levinger, 2009; Stover, Rithner, Inafuku, Crans, and Levinger, 2005; Crans, Baruah, Ross, and Levinger, 2009). However, the smaller oxovanadates will associate with even negatively charged interfaces (Crans, Rithner, Baruah, Gourley, and Levinger, 2006; Crans, Baruah, Ross, and Levinger, 2009; Roess, Smith, Winter, Zhou, Dou, Baruah, Trujillo, Levinger, Yang, Barisas, and Crans, 2008). To obtain more information on the role of counterions the current study compared the properties of a V_{10} system in reverse micelles in the presence of Na^+ or $HMet^+$ counterions.

V_{10} contains three types of vanadium atoms with different environments as shown in Figure 5.1(a): two V atoms in the center (V_A), each binding to six bridging O atoms, including both of the μ_6 -O atoms of the cluster; four V atoms (V_B) completing a V_6O_{12} equatorial plane each binding one μ_6 -O atom, four μ_2 -O atoms, and a terminal O atom; and four V atoms (V_C), each with five bridging O atoms and one terminal O atom, capping the equatorial plane of the oxometalate (Crans, Smee, Gaidamauskas, and Yang, 2004; Rehder, 1982). Although vanadium forms a number of oxovanadates, the dominant species in aqueous solution at pH about 2-6 is V_{10} (Howarth, 1990), which can exist in various protonation states forming $V_{10}O_{28}^{6-}$, $HV_{10}O_{28}^{5-}$, $H_2V_{10}O_{28}^{4-}$, and $H_3V_{10}O_{28}^{3-}$ as the pH decreases from neutral to about 2. The reactions and pK_a values for these species are shown in Equation (4.1)-(4.3). V_{10} has three distinct signals by ^{51}V NMR spectroscopy and as pH increases and the V_{10} deprotonates a downfield chemical shift of the V_B and V_C signals can be observed, while that of the V_A atom, effectively buried in the center of the anion, does not shift as pH changes (Baruah, Roden, Sedgwick, Correa, Crans, and Levinger, 2006).



Metformin ($\text{C}_4\text{H}_{11}\text{N}_5$), Met, (Figure 5.1(b)) belongs to the biguanide family of compounds containing the guanidine structural unit. The reactions and two $\text{p}K_a$ values of Met in aqueous solution are 2.8 and 11.5 (Ray, 1961). During most of the studies described in this work Met will be monoprotonated, HMet^+ , as it is in metformin hydrochloride, the smallest of the antidiabetic drugs, $\text{C}_4\text{H}_{12}\text{N}_5\text{Cl}$, and on dissolution of metformium decavanadate (MetV_{10}) which results in formation of V_{10} and HMet^+ . Structural studies show that the electron delocalization enjoyed by the neutral form is disrupted at the central N atom of the biguanide unit in the monocation (Hariharan, Rajan, and Srinivasan, 1989; Childs, Chyall, Dunlap, Coates, Stahly, and Stahly, 2004; Hung, Xi, Xu, Liu, and Zeng, 2008). Met has only two types of protons as observed by ^1H NMR spectroscopy in organic solvents, but only the methyl protons are observable in D_2O . Part of the guanide functionality is similar with urea, and metformin does indeed have some similar properties with urea such as its high solubility and strong H-bonding interaction with water (Vanzi, Madan, and Sharp, 1998; Rezus and Bakker, 2006).

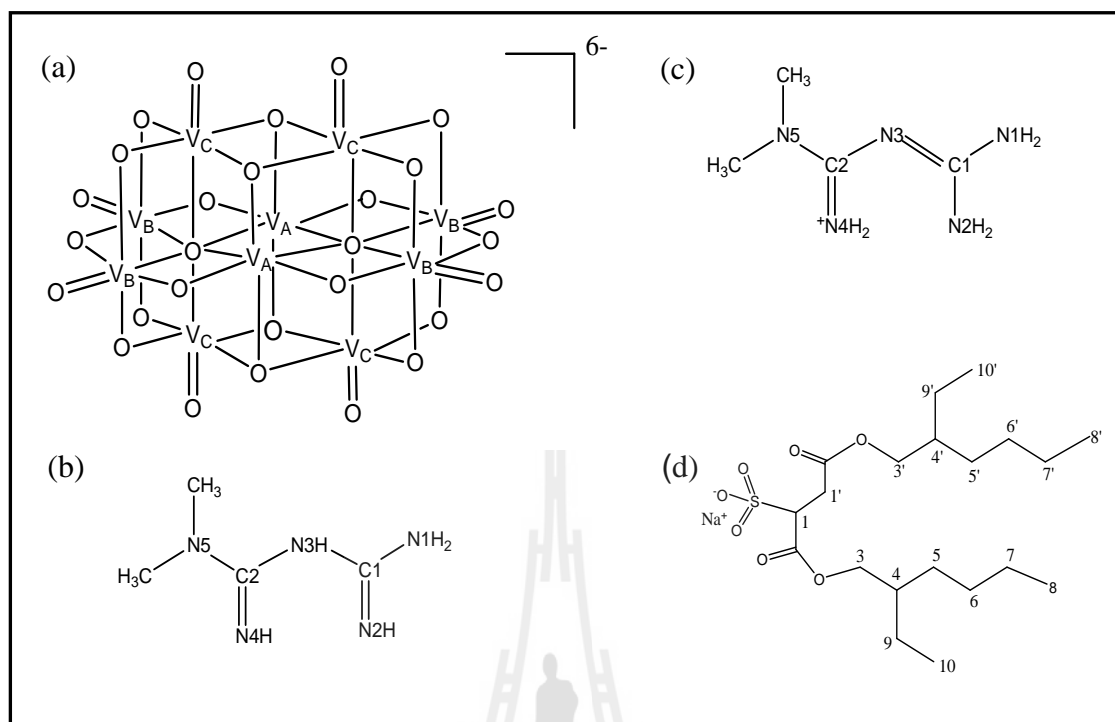


Figure 5.1 Structures of (a) decavanadate; $[V_{10}O_{28}]^{6-}$ (V_{10}), (b) neutral metformin, (c) the protonated form of metformin, and (d) AOT.

How vanadium compounds are transported in biological systems is a complex topic that has been investigated focusing both on transport by proteins in the blood as well as transport across membranes (Hiromura, Nakayama, Adachi, Doi, and Sakurai, 2007; Roess, Smith, Winter, Zhou, Dou, Baruah, Trujillo, Levinger, Yang, Barisas, and Crans, 2008; Zhang, Ruan, Chen, Lu, and Wang, 1997; Kotchevar, Ghosh, and Uckun, 1998; Goldwasser, Li, Gershonov, Armoni, Karnieli, Fridkin, and Shechter, 1999; Crans, Baruah, Ross, and Levinger, 2009; Peter, Winter, Al-Qatati, Wolf-Ringwall, Schoeberl, Chatterjee, Barisas, Roess, and Crans, 2012). The complexity of this topic is increased by the aqueous oxovanadate chemistry because multiple species, nuclearities, and protonation states exist under physiological conditions. The interaction of V_{10} with interfaces has been investigated in cells as well as in simple model systems such as reverse micelles (RMs) prepared from an organic solvent, water, and a surfactant (Baruah, Roden, Sedgwick, Correa, Crans, and Levinger, 2006; Sedgwick, Crans, and

Levinger, 2009; Crans, Baruah, Ross. and Levinger, 2009; Baruah, Swafford, Crans. and Levinger, 2008). While RMs can be prepared from a range of different surfactants, bis(2-ethylhexyl)sulfosuccinate (AOT) (Figure 5.1(d)) is the surfactant most frequently used. The RMs form a dynamic system, generally assumed to be spherical with radius proportional to the $w_o = [\text{H}_2\text{O}] / [\text{AOT}]$ ratio. Studies have shown that sodium- V_{10} (NaV_{10}) resides in the interior water pool in nanosized NaAOT reverse micelle (Baruah, Roden, Sedgwick, Correa, Crans, and Levinger, 2006). Depending on the specific location, the properties of V_{10} are likely to vary because interactions between solutes in the water pool and the interfaces can modify behavior of the system. The diversity of Met with regard to charge and the ability to associate with amphiphilic materials is likely to yield a very different system compared to for example sodium.

In this work the author report investigation of the interaction of metformin near neutral pH, that is the HMet^+ cation, with the AOT RM interface in the presence and absence of the V_{10} anionic cluster, allowing us to compare the properties of the MetV_{10} system with those of the NaV_{10} system. Although MetV_{10} is an ionic system and the ions dissociate in solution, it is our hypothesis that HMet^+ changes the interaction of V_{10} with the RM interface. The spectroscopic changes between MetV_{10} and NaV_{10} in chemical shifts (δ) and line widths ($\Delta_{1/2}$) with ^1H NMR and ^{51}V NMR studies report on both the environments of V_{10} and HMet^+ , demonstrating the differences induced by the association of HMet^+ with the micellar interface, while dynamic light scattering studies report on the accompanying changes in RM size. Considering the high negative charge of the V_{10} ion, these studies show in a simple model system how the positive counter ion can modify the properties of even a large charged complex and result in different effects at the interface (Morris, 1994; Zhang, Yang, Wang, and Crans, 2006). This system documents the importance of counterion association to charged species in the interactions with interfaces and thus could be important for drug uptake.

5.2 Experimental

5.2.1 Materials

Vanadium pentoxide, V_2O_5 , (Fluka, $\geq 98.0\%$), sodium metavanadate, $NaVO_3$, (Aldrich, 90.0%), metformin hydrochloride, $C_4H_{12}N_5Cl$, (Sigma-Aldrich, or isolated directly from tablets of Merck's diabetes drug Glucophage), DMSO (Sigma-Aldrich, 99%), and isooctane (Sigma-Aldrich, 99.0%) were used as obtained. Sodium bis(2-ethylhexyl)sulfosuccinate, AOT, (Sigma-Aldrich, 98.0%) was purified as described previously (Chowdhury, Ashby, Datta, and Petrich, 2000; Baruah, Swafford, Crans, and Levinger, 2008). Doubly distilled water was used for all reverse micelle systems.

5.2.2 Sample preparation

Preparation of $[C_4H_{12}N_5]_3[H_3O]_3[V_{10}O_{28}] \cdot 3H_2O$ (MetV₁₀). V_2O_5 (0.220 g, 1.20 mmol), and metformin hydrochloride (0.240 g, 1.45 mmol) was added to 8 mL of deionized water and the pH of the suspension was adjusted to ~ 5 by 1.0 M HCl. The orange solution was heated at $60^\circ C$ for 15 hr. The mixture was filtered and the filtrate kept at ambient temperature to give yellow-orange plate-like crystals 0.438 g, 0.300 mmol, about 25% based on vanadium. Anal. Calcd. for $[C_4H_{12}N_5]_3[H_3O]_3[V_{10}O_{28}] \cdot 3H_2O$, MW 1459.02: C, 9.88; H, 3.53; N, 14.40%. Found: C, 9.48; H, 3.72; N, 14.70%. IR (KBr, cm^{-1}): 3360 (br), 3314 (w), 3046 (w), 1645 (m), 1584 (w), 1568 (w), 1553 (w), 1498 (w), 1463 (w), 1421 (w), 1067 (w), 987 (w), 961 (s), 844 (m), 819 (w), 743 (m), 589 (m), 558 (w). ^{51}V NMR (78.9 MHz, d_6 -DMSO): δ -422.78 (2V), -503.07 (4V), -518.93 (4V). 1H NMR (d_6 -DMSO): δ 2.93 (s, 6H), 6.55 (s, 4H), 7.21 (s, 2H).

Preparation of AOT. AOT was purified by dissolution in methanol and stirring overnight in the presence of activated charcoal (6-12 mesh). The suspension was filtered and methanol removed by evaporation under vacuum for at least 12 hr (Chowdhury, Ashby, Datta, and Petrich, 2000; Baruah, Swafford, Crans, and Levinger, 2008). The water content in the purified AOT, measured from the elemental analysis or by

integration of the H1 (one hydrogen) or H3/H3' (two hydrogens) signal in dry d_6 -DMSO, was 0.5 water molecule per AOT molecule. Clear stock solutions of 0.2 M AOT and 0.75 M AOT were prepared by dissolving 2.223 g and 8.335 g of AOT, respectively, in 25 mL isooctane and vortically mixing about 45 min until the solutions cleared.

AOT RMs with NaV₁₀. Total V₁₀ concentration of 2.0 mM was used to make AOT RMs with $w_0 = 5.5, 6, 8, 10,$ and 16 by pipetting specific volumes of stock solution to aliquots of 0.75 M AOT/isooctane and vortically mixing until the solution was clear and suitable for ¹H NMR analysis. Stock solution of V₁₀, from NaVO₃ at total concentration of V₁₀ 2.0 mM was prepared by dissolving NaVO₃ in doubly distilled DI water in 90% of the desired volume in a volumetric flask, adjusting pH to 4.3 using 6 M HCl and 1 M NaOH, and finally making up the required volume.

AOT RMs with MetHCl. Pipetting a specific volume of MetHCl solution in D₂O to aliquots of 0.75 M AOT in isooctane. This suspension was vortically mixed for 15 min and left until the solution was clear, suitable for ¹H NMR analysis.

AOT RMs with MetV₁₀. MetV₁₀ (0.0030 g, 2.0 mM) was added to 1 mL of 0.75 M AOT/isooctane and D₂O added to make up the desired w_0 . The samples were vortically mixed 45 min resulting in transparent, yellow solutions. ¹H NMR and ⁵¹V NMR spectra were recorded and in agreement with literature reports (Gadape and Parikh, 2011; Crans, 1994).

Sample preparation for NMR, DLS, and IR experiments. RMs of V₁₀ were formed using overall concentration of V₁₀ from NaVO₃ and MetV₁₀ 0.7 mM in 0.2 M AOT/isooctane at $w_0 = 6$ and 10. Solutions to be investigated by ¹H NMR contained D₂O and samples to be examined by ⁵¹V NMR contained H₂O. Standard MetHCl solutions at 1 M (stock solution) and 0.7 mM in 0.2 M AOT/isooctane were prepared for comparison. For IR spectroscopy experiments, aqueous solutions were prepared using 5% HOD in H₂O.

5.2.3 Characterization

Materials were submitted for elemental analyses (C, H, and N) from Columbia Analytical Service, Tucson US. Thermogravimetric analysis (TGA) spectra were recorded in the range 25-600°C with heating rate 10 °C/min under helium gas on a TGA 2950 thermogravimetric analyzer, TA universal analysis 2000. Infrared (FTIR) spectra were recorded in the mid-IR region (4000-400 cm⁻¹), resolution 4 cm⁻¹ using KBr pellets on a Perkin Elmer GX spectrophotometer. Powder X-ray diffraction were recorded with a D5005 X-ray diffractometer from Bruker Analytical X-ray Systems GMBH-Germany, EVA V. 3 evaluation program, tube power level 40 kV and 40 mA. The database of powder diffraction patterns maintained by the Joint Committee on Powder Diffraction Standards (JCPDS), library 2004 was used for phase identification.

Solution infrared vibrational spectra were collected at 25°C with an FTIR spectrophotometer Magna 760 (Nicolet, USA). Individual spectra used 128 scans, 1 cm⁻¹ resolution with IR microvolume cuvette with BaF₂ windows (2 mm thick) separated by a 50 μm Teflon spacer. Spectra obtained from samples with 5% HOD in H₂O, and with pure DI-water allow us to explore the OD and OH stretching regions. Spectra that arise only from the OD stretching signal were obtained by subtracting the spectra with DI-water as the polar solvent from the spectra of reverse micelles containing 5% HOD in H₂O. The highest peak positions are reported.

¹H NMR solution spectra were recorded on Varian INOVA-300 or 400 MHz spectrometers. ⁵¹V NMR spectra were recorded using parameters reported previously at 78.9 and 105.2 MHz (Crans, Rithner, and Theisen, 1990; Sedgwick, Crans, and Levinger, 2009). Data analysis was conducted using MestReC V. 4.5.9.1 NMR data processing software and ACD/NMR processor academic edition for Windows. The ⁵¹V NMR spectral peaks were fitted to find the chemical shifts and line widths (OriginPro 7) using Gaussian or Lorentzian line shape functions. Δ_{1/2} is the full width at half height in

Hertz assuming the system is described within the extreme motional narrowing limit (Stover, Rithner, Inafuku, Crans, and Levinger, 2005). TMS is used as an internal reference (0.00 ppm) for HMet⁺ in organic solvent.

DLS experiments were performed at 25°C to confirm the formation and size of RMs and to measure their average particle size in solution using a Wyatt DynaPro Titan with DynaPro DYNAMICS software V. 6.7.3 (Sedgwick, Trujillo, Hendricks, Levinger, and Crans, 2011). Each measurement consisted of 10 acquisitions of 15 scans each.

5.2.4 Instrumentation

Fourier transform infrared spectroscopy, FTIR. Spectra of solid compounds were recorded in the mid-IR range 4000-400 cm⁻¹, resolution 4 cm⁻¹ using KBr pellets on a Spectrum GX (Perkin Elmer, USA), and the solution infrared vibrational spectra were collected at 25°C with an FTIR spectrophotometer (Nicolet, Magna 760) using BaF₂ windows.

Single crystal X-ray diffraction. Intensity data measurements were carried out at 120 (2) K on a SMART APEX II CCD diffractometer (Bruker AXS, USA) with a graphite monochromatized Mo K α ($\lambda = 0.71073 \text{ \AA}$) radiation.

Powder X-ray Diffraction, PXRD. Powder XRD spectra were recorded on a D5005 diffractometer (Bruker AXS, Germany) using Cu K α X-ray radiation ($\lambda = 1.54 \text{ \AA}$) and a 0.5 mm divergence slit with data collected over a 5.0-45.0° 2 θ range, tube power level 40 kV and 40 mA, and JCPDS library 2004.

Nuclear magnetic resonance. ¹H NMR solution spectra were recorded on a Varian INOVA-300 or 400 MHz spectrometer. ⁵¹V NMR spectra were recorded at 78.9 and 105.2. Data analysis was conducted using MestReC V. 4.5.9.1 NMR data processing software and ACD/NMR processor academic edition for Windows.

Dynamic Light Scattering, DLS. DLS experiments were performed at 25° using DynaPro Titan with DynaPro DYNAMICS software V. 6.7.3 (Wyatt, USA).

Effective data requires intensities of 10^5 - 10^6 counts, GaAs laser power between 10-20 mW, scattered light was collected at 90° .

5.3 Results and Discussion

Characterization. MetV₁₀ obtained from solutions at pH ~5 were analyzed using FTIR, elemental analysis, TGA, crystal characterization, NMR, and DLS. The spectra also contain several bands of HMet⁺ cation and are in agreement with literature values (Woo, 1998; Gunasekaran, Natarajan, Renganayaki, and Natarajan, 2006). TGA analysis of MetV₁₀ is consistent with three molecules of Met, presumably in a cationic form, and 6 molecules of water (Appendix C). The water molecules are associated differently with the V₁₀ anion because they desorb at different temperatures. Three water molecules are distinctly different than the others coming off at much higher temperatures. The crystals of this material appear twinned and while the X-ray structure clearly shows two HMet⁺ per decavanadate anion, it does not allow unambiguous determination of the third Met region nor the placement of some hydrogen atoms. The black residue remaining after heating to 600°C for TGA analysis had an IR spectrum with only two weak bands below 1000 cm⁻¹ (746 cm⁻¹ and 538.7 cm⁻¹), neither corresponding to the characteristic bands of V₁₀ salts, and when measured by XRD, gave a spectrum different from the vanadium oxide compounds in the JCPDS library such as V₂O₅, NH₄VO₃, V₂O₃ and V₂O₄ (Appendix C) and consistent with a mixed valence 1:2 vanadium oxide (V₁₀O₂₀) as reported previously (Roman, Macias, Luque, and Guzmanmiralles, 1992).

Solubility of MetV₁₀. MetV₁₀ is not soluble in D₂O or H₂O even upon sonication for several hours. However, MetV₁₀ was slightly soluble in DMSO (0.0010 g/mL), but it readily dissolves in the heterogeneous environment of AOT RMs. Solid MetV₁₀ dissolves into both 0.2 M AOT/isooctane RMs and into 0.2 M AOT/cyclohexane RMs; after vortically mixing about 30 min the suspensions turn clear. When the solubility of

MetV₁₀ is compared with known NaV₁₀ compound in AOT/isooctane RMs, MetV₁₀ was found to have better solubility than NaV₁₀. For example, an overall 5 mM MetV₁₀, 0.75 M AOT/isooctane solution can be prepared at $w_0 = 10$ whereas a corresponding sample from NaV₁₀ could only be prepared up to about 2.5 mM V₁₀. The higher solubility of MetV₁₀ over NaV₁₀ into AOT/isooctane RMs was observed even though the solubility of NaV₁₀ in water is higher than that of MetV₁₀. Importantly, the concentration of NaV₁₀ in the stock solution (787.4mM) that corresponded to the overall 5 mM MetV₁₀ 0.75 M AOT/isooctane solution could not be prepared.

Characterization of MetV₁₀ in d₆-DMSO, d₄-MeOH, and AOT RMs by multinuclear NMR spectroscopy. ¹H NMR signals of MetV₁₀ in DMSO and AOT RMs are shown in Figure 5.2. In DMSO protons of HMet⁺ in the compound could be observed at 2.93, 6.55, and 7.20, only the NH₂ signal at 6.55 ppm is significantly shifted from that observed in DMSO of MetHCl (6.78 ppm). In AOT/isooctane reverse micelle at $w_0 = 6$, 10, and 16, there are insignificant shifts for the CH₃ proton (Figure 5.2). The downfield shift of the HMet⁺ signal (from MetV₁₀) reflects the penetration of HMet⁺ into the RM interface. Because of the possibility that the effect on chemical shift could be attributed to a change in water pool pH, ⁵¹V NMR studies were also carried out.

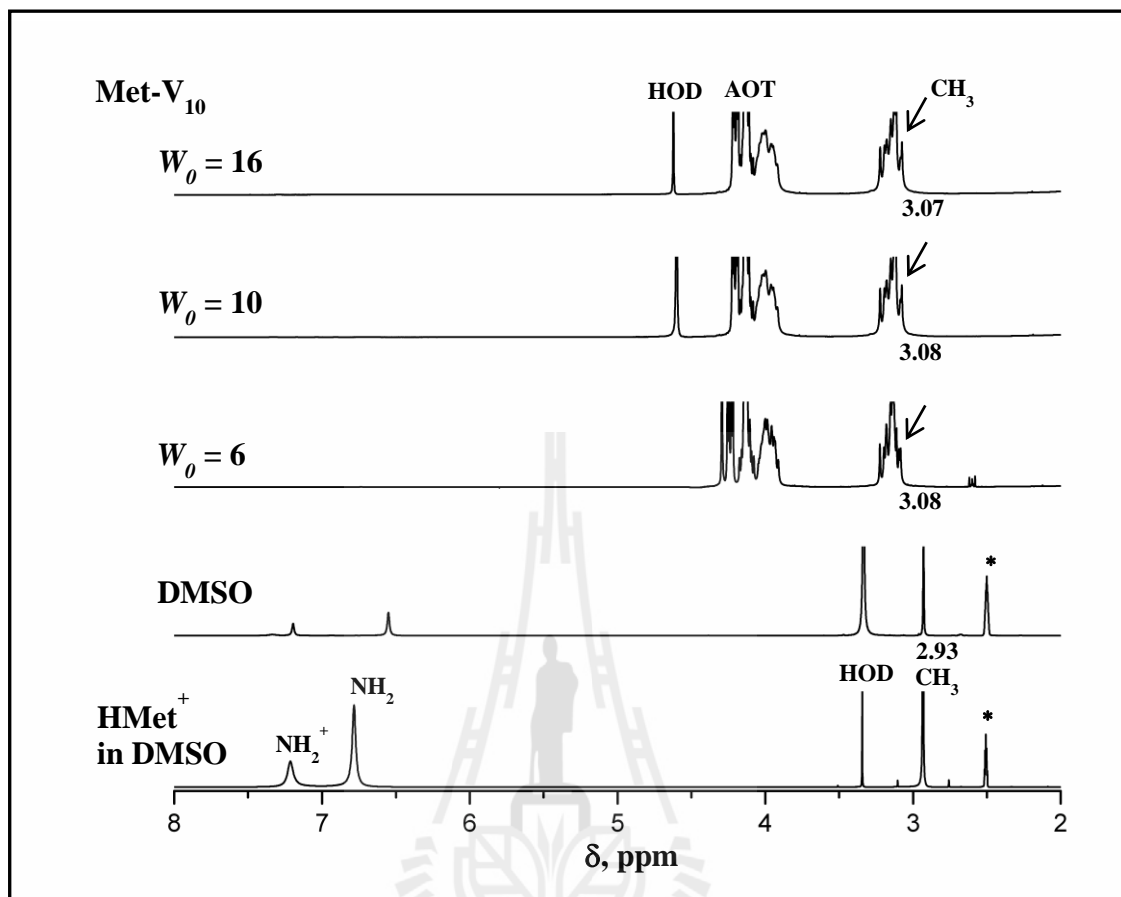


Figure 5.2 ^1H NMR spectra of MetHCl in DMSO and MetV₁₀ in DMSO and in 0.75 M AOT RMs (5.0 mM overall concentration) with $w_0 = 6, 10,$ and 16.

^{51}V NMR signals of V₁₀ in NaV₁₀ and MetV₁₀ in 0.75 M AOT RM with $w_0 = 5.5, 6, 8, 10,$ and 16 are shown in Figure 5.3 and the chemical shifts and line widths are summarized in Table 5.1. Since the compound is insoluble in water the pH of the water droplets in the AOT/isooctane suspension are not known. Previous studies with V₁₀ solutions at different pH values were found to yield similar environment for V₁₀ in the RMs, because V₁₀ was found to be located in the center of the water droplets (Baruah, Swafford, Crans, and Levinger, 2008; Sedgwick, Crans, and Levinger, 2009; Roess, Smith, Winter, Zhou, Dou, Baruah, Trujillo, Levinger, Yang, Barisas, and Crans, 2008; Baruah, Roden, Sedgwick, Correa, Crans, and Levinger, 2006; Crans, Baruah, and Levinger, 2006). The ^{51}V NMR of NaV₁₀ stock solution at pH 4 gave rise to three signals

at -519.3 , -503.4 , and -424.8 ppm in agreement with previous reports (Baruah, Swafford, Crans, and Levinger, 2008). Several spectra of NaV_{10} and MetV_{10} in AOT/isooctane RMs were recorded for comparison for a range of w_0 values.

From Figure 5.3, the line broadening of V_A and all three lines broaden as the RM size decreases are observed. At $w_0 = 6$, the line widths for V_B and V_C are five times greater than the line widths in stock solution. The line widths in ^{51}V NMR spectra reflect the mobility of the V_{10} anion in the RM with line width increases with decreasing RM size consistent with decreasing mobility of the anion. The large line widths for the small RMs indicate the restricted movement of V_{10} in the small RM size with the V_{10} approaching the interfacial layers of the RM (Hunt, Jaye, and Meech, 2005; Silber, Biasutti, Abuin, and Lissi, 1999).

As shown in Table 5.1, distinct, but not significantly different, chemical shifts are observed for V_B and V_C between the sodium and metformium systems, and no experimentally significant difference is observed in the line widths between the two systems. These results suggest that the V_{10} remains in the water phase, but the HMet^+ counter ion may change the manner in which V_{10} interacts with the interface. Because NaV_{10} stock solutions prepared corresponding to the concentration of MetV_{10} in 0.75 M AOT/isooctane solution resulted in precipitation. It is clear that the HMet^+ is affecting the interactions of V_{10} with the RM interface. These results demonstrate that the HMet^+ affects the RM system or the water in the water pool or both. Therefore, dynamic light scattering (DLS) measurements were carried out on a series of reverse micelles to determine if the HMet^+ changed the size of reverse micelles.

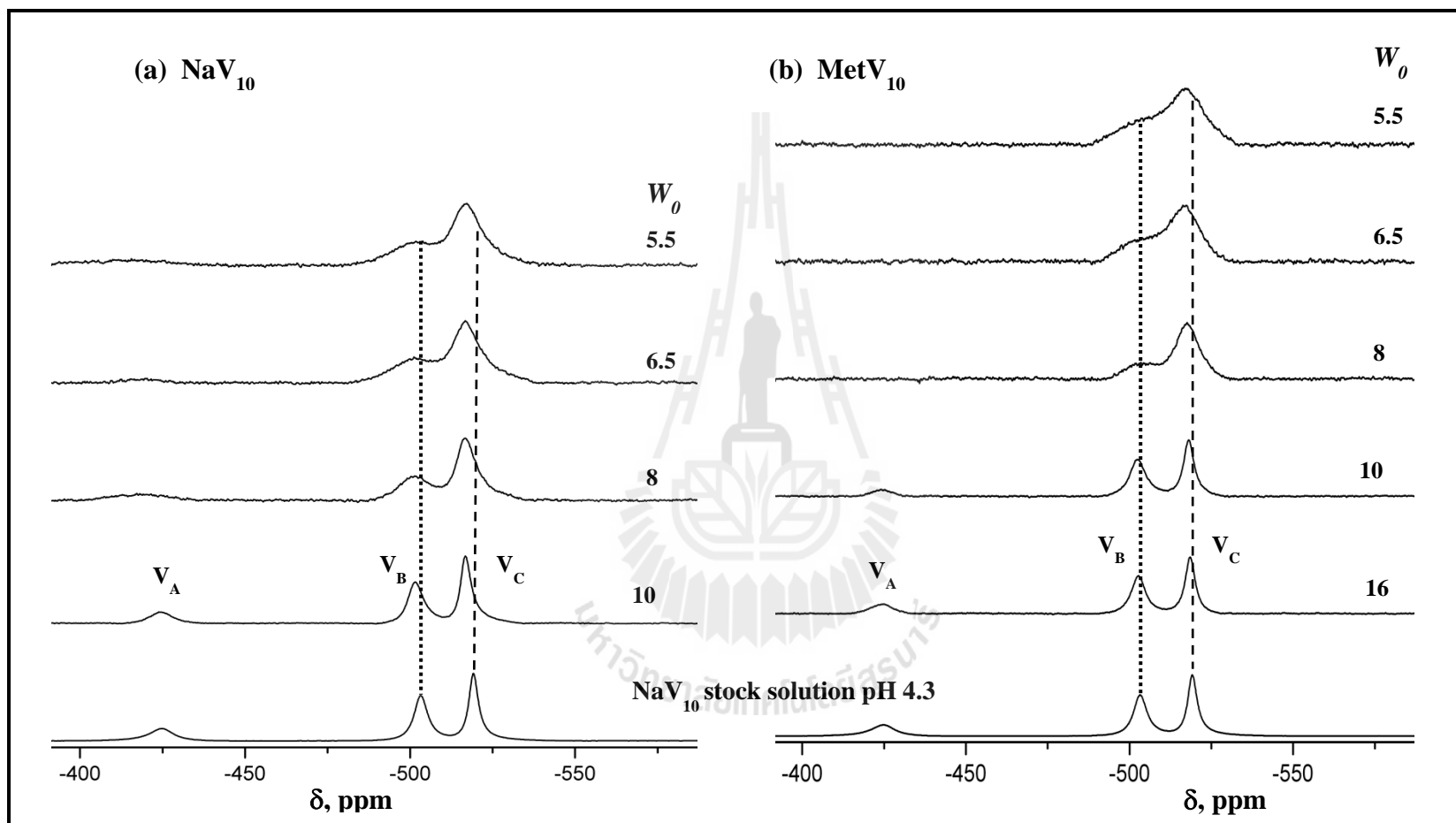


Figure 5.3. ^{51}V NMR spectra of 2.0 mM (overall V_{10} concentration) of (a) NaV_{10} and (b) MetV_{10} in 0.75 M AOT RMAs with $w_0 = 5, 6, 8, 10,$ and 16 . The spectrum for $w_0 = 16$ could not be obtained for NaV_{10} due to its limited solubility

Table 5.1 Chemical shifts and line widths for the three ^{51}V NMR signals of V_{10} in NaV_{10} and MetV_{10} (V_{10} 2.0 mM – overall concentration) in 0.75 M AOT RMs with various w_0 .

	w_0									
	Sodium decavanadate					Metformium decavanadate				
	5.5	6	8	10	16	5.5	6	8	10	16
	^{51}V NMR chemical shift, (ppm)									
V_A	-	-	-	-422 ± 3	-	-	-	-	-422 ± 3	-422 ± 3
V_B	-500 ± 2	-500 ± 2	-501 ± 1	-501 ± 2	-	-500 ± 4	-502 ± 3	-503 ± 0.5	-501 ± 2	-502 ± 2
V_C	-515 ± 3	-515 ± 3	-517 ± 1	-517 ± 1	-	-516 ± 2	-516 ± 2	-517 ± 0.5	-517 ± 2	-518 ± 2
	Line width, (Hz)									
V_A	-	-	-	640 ± 84	-	-	-	-	739 ± 99	620 ± 89
V_B	1142 ± 99	1110 ± 99	705 ± 84	402 ± 21	-	1168 ± 99	1084 ± 99	750 ± 99	461 ± 80	373 ± 21
V_C	814 ± 59	773 ± 90	492 ± 87	287 ± 19	-	998 ± 89	763 ± 57	620 ± 11	261 ± 40	264 ± 20
	Number of V_{10}/RM (MetV_{10})					Number of Met/RM				
	0.14	0.15	0.22	0.31	0.71	0.42	0.45	0.66	0.93	2.13

All RM solutions are made by using 0.75 M AOT/isooctane and 2 mM pH 4.35 ± 0.05 aqueous V_{10} stock solution. Chemical shifts of V_A , V_B , and V_C of aqueous stock solution occur at -423 ± 2 , -502 ± 1 , and -518 ± 1 ppm, respective

DLS of MetV₁₀ in RMs. The size of the reverse micelles containing NaV₁₀ in water and MetV₁₀ in water were measured for selected w_o , and the results are shown in Table 5.2. The size of the AOT RMs (Maitra, 1984; Chowdhury, Ashby, Datta, and Petrich, 2000; Bohidar and Behboudnia, 2001) and RMs containing NaV₁₀ systems are similar to those reported previously (Baruah, Roden, Sedgwick, Correa, Crans, and Levinger, 2006). For the RMs containing MetV₁₀, the sizes for medium sized RMs are slightly larger than anticipated based on the hydration level. Larger reverse micelles can result from interaction between the water pool and the interface ordering of the palisade layer or the interface of the micelles. How much of this effect is due to the complex was examined by testing the HMet⁺.

Table 5.2 The sizes of 0.2 M AOT/isooctane RMs containing water with MethCl, NaV₁₀, and MetV₁₀ as determined by dynamic light scattering.

system	Radii for reverse micelle, (nm)			
	$w_o = 6$	PD%	$w_o = 10$	PD%
AOT RMs	2.1 (0.17)	13	4.6 (0.19)	14
NaV ₁₀ 0.7 mM (overall)	3.6 (0.21)	11	4.4 (0.20)	12
MetV ₁₀ 0.7 mM (overall)	5.0 (0.25)	11	5.5 (0.22)	17
HMet ⁺ 0.7 mM	5.0 (0.13)	9	6.1 (0.18)	9
MethCl 1.0 M (stock)	3.3 (0.20)	9	4.2 (0.34)	8

The effect of HMet⁺ on the RMs was examined by checking samples containing different size RMs in the presence of MethCl. Samples were prepared containing both high and low concentration of HMet⁺. As shown in Table 5.2, the data demonstrate that HMet⁺ at both low and high concentration has little effect, but at medium concentrations

its presence results in larger RMs. In general increased salt concentration results in decreased RMs (Leodidis and Hatton, 1989) so these observations are not simply the result of salt effects and suggest at least two counteracting effects in this involved system. The DLS results provide size information and do not distinguish whether HMet^+ is located in the water pool or whether it is associated with the interface. Since it has been reported that metformin interacts strongly with water (Vanzi, Madan, and Shrrp, 1998), further information on how the H-bonding in the water pool is affected can be obtained from the OD stretch observed by differential IR spectroscopy.

FTIR studies of MetV_{10} in RMs. The FTIR studies were carried out hypothesizing that HMet^+ orders the water pool, and in addition that HMet^+ cations replace a few of the Na^+ cations near the RM interface, and as a result solubilize more V_{10} in the water pool. These hypotheses were examined by measuring the FTIR vibrational spectra of the OD stretching region of RMs prepared with 5% HOD in DI water. Absorption profiles for the OD stretching mode in HOD are simpler than those for the corresponding OH mode and thus provide qualitative information about the structure of water present inside the RMs. The extent of hydrogen bond formation or its perturbation can be inferred from these spectra. Figure 5.4 shows a significant blue shift of the OD peak maximum and spectral broadening for the $w_0 = 6$ RMs containing MetV_{10} compared to RMs measured in the absence of MetV_{10} . The blue shift in the position of the OD peak maximum is of similar magnitude as reported previously for RMs containing NaV_{10} (Crans, Baruah, Ross, and Levinger, 2009; Baruah, Swafford, Crans, and Levinger, 2008). These results suggest that the presence of MetV_{10} in the RMs results in a significant disruption of the H-bonding network present in the water pool. Interestingly, although a blue shift was observed for the absorption maximum for MetV_{10} this signal has a shoulder at low frequency, which traces with the signal observed for samples containing no probes. It is therefore very possible that these spectra are composed of at least two distinct types of

water molecules. Considering that these spectra are very broad and the noise levels in the spectra are significant, we refrain from extensive modeling of these results. These signals can be modeled by two species using Gaussian fits. However, the impact of this modeling is diminished when recognizing that the spectra recorded in the absence of probe can also be modeled by two species. We conclude that the data are consistent with the observation of at least two unique water environments, consistent with two RMs some that contain MetV₁₀ and some that do not.

Considering the possibility that HMet⁺ ion may impact the RM system if it interacts with the interface, samples containing only HMet⁺ cation were also investigated. The presence of high concentration of HMet⁺ ion results in a red shift in the OD stretch of the water pool in the RMs whereas similar results were not observed with low concentration of HMet⁺. These results suggest that the HMet⁺ interacts in a complex manner in this system and that the effects presumably involve interaction with both the water pool and the interface.

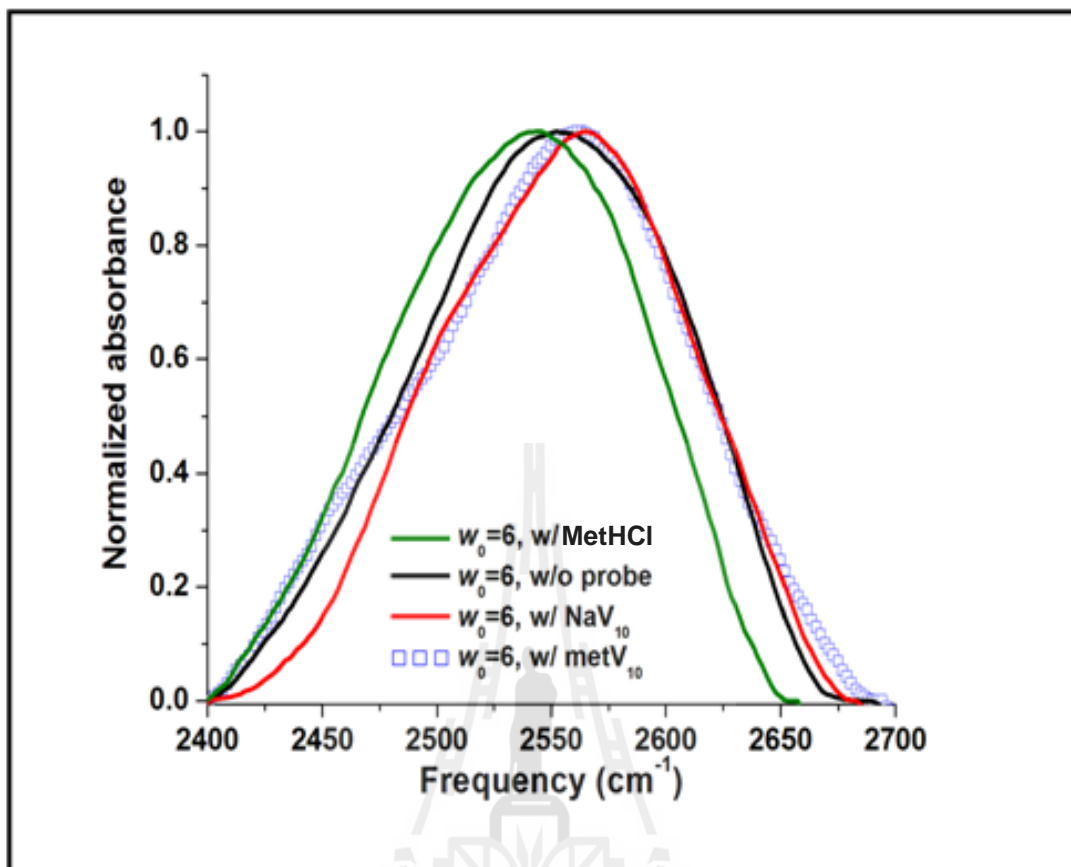


Figure 5.4 Absorbances for the O–D stretch in AOT RMs containing aqueous solutions of MetHCl, NaV₁₀, and MetV₁₀ measured using IR spectroscopy.

Table 5.3 FT-IR data for the OD stretch of 5% HOD in H₂O in 0.2 M AOT RMs prepared with and without MetV₁₀, NaV₁₀, and MetHCl.

Probes	w_0	$\nu_{(OD)}$, (cm ⁻¹)	No. of probes / RM
No probe, just with water	6	2552 ± 1	
	10	2543 ± 1	
MetV ₁₀	6	2563 ± 1	0.19
	10	2549 ± 1	0.36
NaV ₁₀	6	2564 ± 1	0.19
	10	2550 ± 1	0.36
MetHCl	6	2544 ± 1	8.06

(MetV₁₀ 0.7 mM, NaV₁₀ 0.7 mM, and MetHCl 31.65 mM at pH~7)

The calculated average occupancy number of V_{10} anions for each RM (see Table 5.3) for this series of studies is near 0.5, consistent with only half of the RMs containing V_{10} (considering a statistical distribution a small fraction of RMs may contain two V_{10} molecules). Recognizing that about 50% of the RMs would not contain V_{10} is consistent with the observations, that more than one unique water environment is present for the MetV_{10} samples. Modeling can be done under several imposed restrictions, however, even if no restrictions on peak maximum are made, one of the OD maximum signals in the MetV_{10} AOT RM sample is near the absorbance maximum observed in the absence of probe. However, considering that the MetV_{10} samples showed larger RMs than NaV_{10} , the RMs containing MetV_{10} also contain HMet^+ and presumably a similar number of water molecules as the NaV_{10} .

These results are consistent with the V_{10} anion of the MetV_{10} residing in the center of the water pool as observed previously for the NaV_{10} (Crans, Baruah, Ross, and Levinger, 2009; Baruah, Swafford, Crans, and Levinger, 2008). The fact that the size of the RMs containing MetV_{10} are larger than those containing NaV_{10} suggests that the HMet^+ ion is either causing the water pool to increase or the palisade layer to increase. An increase can take place through interaction with the interface expanding the interface, or by expanding the core ordering of the water in the water pool requiring a greater volume per molecule. Chemical intuition may suggest that the HMet^+ should be penetrating the AOT interface because of chemical compatibility, and Columbic attraction, and we have previously measured such effect for other systems such as dipic^{2-} (Crans, Trujillo, Bonetti, Rithner, Baruah, and Levinger, 2008) and metal complexes such as $[\text{VO}_2\text{dipic}]^-$ and BMOV (Winter, Al-Qatati, Wolf-Ringwall, Schoeberl, Chatterjee, Barisas, Roess, and Crans, 2012; Crans, Rithner, Baruah, Gourley, and Levinger, 2006). NMR spectroscopic results show that the chemical shift for the metformium methyl proton does not change significantly, which suggests that if this

cation penetrates the interface, it is not buried very deeply into the interface. The IR spectroscopic results show that HMet^+ ion significantly affects the H-bonding network present in the water pool. Presumably, in order to have the observed effect on the water pool the HMet^+ ion does not penetrate the interface significantly (Figure 5.5). These spectral results, in conjunction with the larger micelle radii observed by DLS when HMet^+ is present, suggest that the HMet^+ is located near the interface, presumably in or near the palisade layer of the reverse micelle.

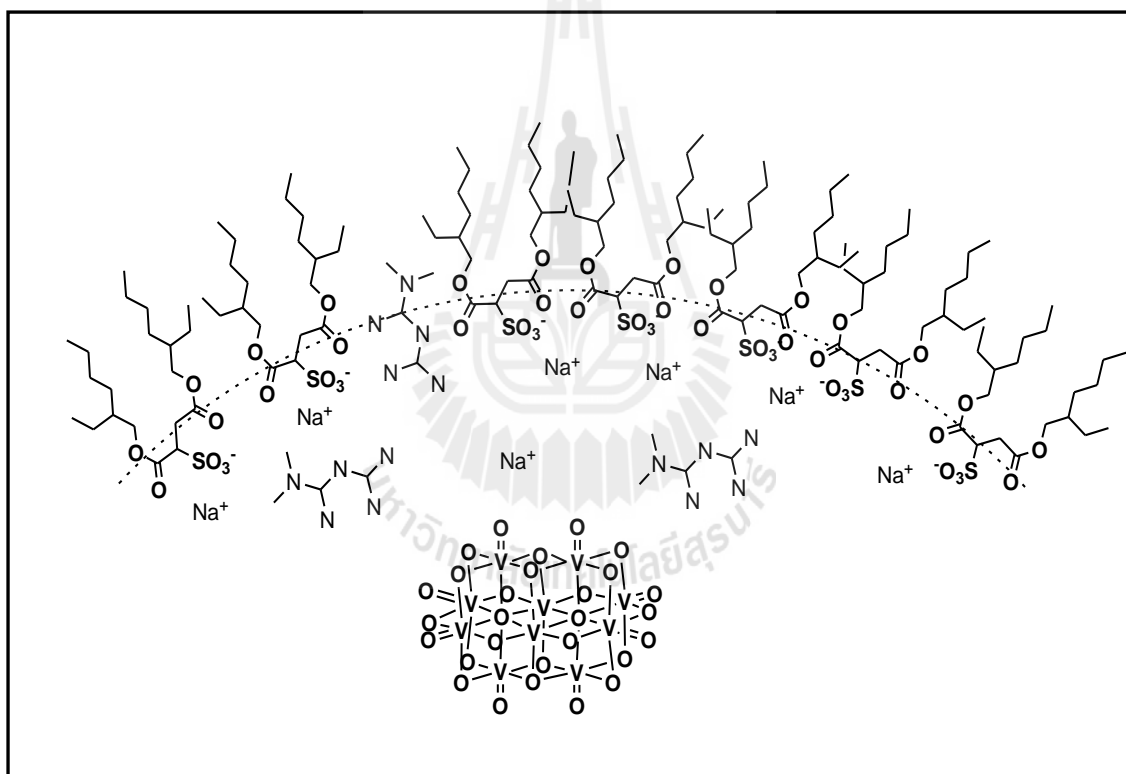


Figure 5.5 Schematic representation of MetV_{10} in RMs consistent with the spectroscopic observations by NMR and IR as well as DLS experiments.

Biological Implications. A wide range of coordination complexes and complex ions with vanadium (V) have been prepared and are known to exert insulin-enhancing effects (Yraola, Garcia-Vicente, Marti, Albericio, Zorzano, and Royo, 2007; Aureliano and Crans, 2009; Goldwasser, Li, Gershonov, Armoni, Karnieli, Fridkin, and Shechter, 1999; Hiromura, Nakayama, Adachi, Doi, and Sakurai, 2007; Willsky, Chi, Godzala,

Kostyniak, Smee, Trujill, Alfano, Ding, Hu, and Crans, 2011; Passadouro, Metelo, Melão, Pedro, Faneca, Carvalho, and Castro, 2010; Thompson, Lichter, LeBel, Scaife, McNeill, and Orvig, 2009; Li, Smee, Ding, and Crans, 2009; Faneca, Figueiredo, Tomaz, Gonçalves, AVECILLA, Pedroso de Lima, Geraldés, Pessoa, and Castro, 2009; Fu, Wang, Yang, Yang, and Wang, 2008; Thompson, McNeill, and Orvig, 1999; Thompson and Orvig, 2004; Buglyo, Crans, Nagy, Lindo, Yang, Smee, Jin, Chi, Godzala, and Willsky, 2005). These materials alleviate the symptoms of diabetes by reducing elevated glucose and lipid levels and normalizing liquid and food intake. Many studies have been carried out *in vivo* and *in vitro* to understand how these compounds act in order to develop new and superior compounds. (Yraola, Garcia-Vicente, Marti, Albericio, Zorzano, and Royo, 2007; Aureliano and Crans, 2009; Rehder, Pessoa, Geraldés, Castro, Kabanos, Kiss, Meier, Micera, Pettersson, Rangel, Salifoglou, Turel, and Wang, 2002; Goldfine, Patti, Zuberi, Goldstein, LeBlanc, Landaker, Jiang, Willsky, and Kahn, 2000; McNeill, Yuen, Hoveyda, and Orvig, 1992; Degani, Gochin, Karlsh, and Shechter, 1981; Sakurai, Shimomura, Fukuzawa, and Ishizu, 1980; Sanna, Dbuglyó, Bíró, Micera, and Garribba, 2012; Pessoa and Tomaz, 2010; Sanna, Buglyo, Micera, and Garribba, 2010; Posner, Faure, Burgess, Bevan, Lachance, Zhangsun, Fantus, Ng, Hall, Lum, and Shaver, 1994).

The modes of action of vanadium compounds are poorly understood, in part because the compounds undergo protonation and oligomerization reactions as well as redox chemistry. Therefore, the mode of action and active species is unlikely to be the compound actually administered in the studies. However, most vanadium compounds are generally invoked in the inhibition of regulatory protein tyrosine phosphatases, they are known to interact with transport proteins such as transferrin, and they have also been implicated in the redox state of the cell. MetHCl is an oral antidiabetic drug, often the preferred drug in early stages of diabetes treatment (Wiernsperger and Bailey, 1999; Krentz and Bailey, 2005; Carpello and Howlett, 2008; Graham, Punt, Arora, Day,

Doogue, Duong, Furlong, Greenfield, Greenup, Kirkpatrick, Ray, Timmins, and Williams, 2011), commonly used in combination therapy, and previously reported to form an insoluble, difficult to characterize complex with V (Woo, Yuen, Thompson, McNeill, and Orvig, 1999; Thompson, and Orvig, 2004; Woo, 1998). However, considering that metformin at neutral pH is cationic (HMet⁺), it can serve as a counter ion to an anionic oxovanadate. Vanadium forms a range of oxovanadates depending on pH and specific conditions (Crans, Smee, Gaidamauskas, and Yang, 2004), and in combination with metformium (Wiernsperger and Bailey, 1999; Krentz and Bailey, 2005; Carpello and Howlett, 2008; Graham, Punt, Arora, Day, Doogue, Duong, Furlong, Greenfield, Greenup, Kirkpatrick, Ray, Timmins, and Williams, 2011) has the potential to form a material that will have antidiabetic effects superior to that observed for each of the drugs independently. While this work was underway preliminary reports were presented characterizing HMet⁺V₁₀ complexes (Vergara, Lara, Benítez, and Mendoza, 2011; Chatkon, Haller, and Crans, 2011) as well as the effects of such a complex in STZ-induced diabetic rats (Vergara, Lara, Benítez, and Mendoza, 2011).

V₁₀, Keggin, and Dawson oxometalates are large anions that have been reported to result in lowering of elevated blood glucose levels in animal studies with STZ induced diabetic rats (Nomiya, Torii, Hasegawa, Nemoto, Nomura, Hashino, Uchida, Kato, Shimizu, and Oda, 2001; Pereira, Carvalho, Eriksson, Crans, and Aureliano, 2009; Aureliano and Crans, 2009) and other biological effects (Li, Zhu, Wu, Jiang, and Yan, 2010). Since V₁₀ is one of the largest vanadium compounds tested for its antidiabetic and anticancer properties, and this highly charged anion was found to be more potent than other oxovanadates (Pereira, Carvalho, Eriksson, Crans, and Aureliano, 2009; Aureliano and Crans, 2009; Li, Zhu, Wu, Jiang, and Yan, 2010), information on the fundamental properties of this compound is desirable. Considering that it is an anion with a -6 charge, undoubtedly the counterions in this salt are important to its properties and potential

processing that may take place in aqueous solution. Indeed, drug uptake has previously been found to be sensitive to counterions (Morris, 1994; Zhang, Yang, Wang, and Crans, 2006).

In the current manuscript investigation of the properties of V_{10} combined with the successful cationic antidiabetic drug, metformium ($[HMet]^+$) are reported. $MetHCl$ is often used to assist administration of other drugs (Goldstein, Feinglos, Lunceford, Johnson, Williams-Herman, and Group, 2007; Graefe-Mody, Padula, Ring, Withopf, and Dugi, 2009; Tajima, Hirata, Taniguchi, Kondo, Kato, Saito-Hori, Ishimoto, and Yamamoto, 2011), and is known to interact with water (Vanzi, Madan, and Shrrp, 1998). The formation of a salt from metformium and V_{10} does provide a new material, which although insoluble in aqueous solution, is more soluble than NaV_{10} in the inhomogenous environment existing in microemulsions. Therefore, these studies demonstrate that the most promising material to be used for administration of both V and metformin would be prepared from an oxovanadate such as decavanadate. The previously reported studies with the 1:2 vanadium:metformin complex documenting the insulin enhancing properties of this material found this system had no benefit over coadministration of V and metformin (Woo, Yuen, Thompson, McNeill, and Orvig, 1999; Vergara, Lara, Benítez, and Mendoza, 2011). As described in the study, it is possible that the $MetV_{10}$ system may show improved insulin enhancing properties.

5.4 Conclusions

A complex between $HMet^+$ cation and V_{10} was prepared and characterized using a range of spectroscopic studies. The complex was not soluble in water but was found to be very soluble in the inhomogenous environment of RMs. As the Na^+ salt of V_{10} has insulin enhancing activity in STZ induced diabetic rats, how this complex interacted with interfaces was investigated. Since metformin is known to affect the H-bonding in the

water pool of RMs and we show that the size of the RMs is changed, the water organization in the water pool or near the RM interface is changed. Differential FTIR spectroscopy was used to test the H-bonding properties in the water pool, and MetV₁₀ and HMet⁺ were both found to significantly affect the H-bonding pattern in the water pool. These studies therefore demonstrate that the counterion of V₁₀ significantly affects the solubility of the salt in aqueous solution and in a complex media used to study interface properties. These results highlight the importance of cation effects on the membrane interface in inhomogeneous environments. Perhaps surprisingly the presence of even 1% HMet⁺ cations that can replace the counter ion in NaAOT in AOT RMs affects the organization of the nanostructure and the H-bonding in the water pool.

5.5 References

- Aureliano, M. and Crans, D. C. (2009). Decavanadate and oxovanadates: Oxometalates with many biological activities. **Journal of Inorganic Biochemistry**. 103: 536-546.
- Bakas, L., Verza, G., and Cortizo, A. (2001). Effect of vanadium compounds on the lipid organization of liposomes and cell membranes. **Biological Trace Element Research**. 80: 269-279.
- Baruah, B., Roden, J. M., Sedgwick, M., Correa, N. M., Crans, D. C., and Levinger, N. E. (2006). When is water not water? Exploring water confined in large reverse micelles using a highly charged inorganic molecular probe. **Journal of the American Chemical Society**. 128: 12758-12765.
- Baruah, B., Swafford, L. A., Crans, D. C., and Levinger, N. E. (2008). Do probe molecules influence water in confinement?. **Journal of Physical Chemistry B**. 112: 10158-10164.

- Bohidar, H. B. and Behboudnia, M. (2001). Characterization of reverse micelles by dynamic light scattering. **Colloids and Surfaces: Physicochemical and Engineering Aspects**. 178: 313-323.
- Buglyo, P., Crans, D. C., Nagy, E. M., Lindo, R. L., Yang, L. Q., Smee, J. J., Jin, W. Z., Chi, L. H., Godzala, M. E., and Willsky, G. R. (2005). Aqueous chemistry of the vanadium(III) (V-III) and the V-III-dipicolinate systems and a comparison of the effect of three oxidation states of vanadium compounds on diabetic hyperglycemia in rats. **Inorganic Chemistry**. 44: 5416-5427.
- Chatkon, A., Haller, K. J., and Crans, D. C. (2011). Synthesis and characterization of a metformium decavanadate compound. In 242nd ACS National Meeting, Denver CO United States, pp. Tech-129.
- Childs, S. L., Chyall, L. J., Dunlap, J. T., Coates, D. A., Stahly, B. C., and Stahly, G. P. (2004). A metastable polymorph of metformin hydrochloride: Isolation and characterization using capillary crystallization and thermal microscopy techniques. **Crystal Growth & Design**. 4: 441-449.
- Chowdhury, P. K., Ashby, K. D., Datta, A., and Petrich, J. W. (2000). Effect of pH on the fluorescence and absorption spectra of hypericin in reverse micelles. **Photochemistry and Photobiology**. 72: 612-618.
- Crans, D. C. (1994). Aqueous chemistry of labile oxovanadates: Relevance to biological studies. **Comments on Inorganic Chemistry**. 16: 1-33.
- Crans, D. C., Baruah, B., and Levinger, N. E. (2006). Oxovanadates: a novel probe for studying lipid-water interfaces. **Biomedicine & Pharmacotherapy**. 60: 174-181.
- Crans, D. C., Baruah, B., Ross, A., and Levinger, N. E. (2009). Impact of confinement and interfaces on coordination chemistry: Using oxovanadate reactions and proton transfer reactions as probes in reverse micelles. **Coordination Chemistry Reviews**. 253: 2178-2185.

- Crans, D. C., Rithner, C. D., Baruah, B., Gourley, B. L., and Levinger, N. E. (2006). Molecular probe location in reverse micelles determined by NMR dipolar interactions. **Journal of the American Chemical Society**. 128: 4437-4445.
- Crans, D. C., Rithner, C. D., and Theisen, L. A. (1990). Application of time-resolved ^{51}V 2D NMR for quantitation of kinetic exchange pathways between vanadate monomer, dimer, tetramer, and pentamer. **Journal of the American Chemical Society**. 112: 2901-2908.
- Crans, D. C., Smee, J., Gaidamauskas, E., and Yang, L. (2004). Vanadium chemistry and biochemistry and biological activities exerted by vanadium compounds. **Chemical Reviews**. 104: 849-902.
- Crans, D. C., Trujillo, A. M., Bonetti, S., Rithner, C. D., Baruah, B., and Levinger, N. E. (2008). Penetration of negatively charged lipid interfaces by the doubly deprotonated dipicolinate. **Journal of Organic Chemistry**. 73: 9633-9640.
- Degani, H., Gochin, M., Karlsh, S. J. D., and Shechter, Y. (1981). Electron paramagnetic resonance studies and insulin-like effects of vanadium in rat adipocytes. **Biochemistry**. 20: 5795-5799.
- Faneca, H., Figueiredo, V. A., Tomaz, I., Gonçalves, G., Avecilla, F., Pedroso de Lima, M. C., Geraldés, C. F. G. C., Pessoa, J. C., and Castro, M. M. C. A. (2009). Vanadium compounds as therapeutic agents: Some chemical and biochemical studies. **Journal of Inorganic Biochemistry**. 103: 601-608.
- Fu, Y., Wang, Q., Yang, X. G., Yang, X. D., and Wang, K. (2008). Vanadyl bisacetylacetonate induced G1/S cell cycle arrest via high-intensity ERK phosphorylation in HepG2 cells. **Journal of Biological Inorganic Chemistry**. 13: 1001-1009.

- Gadape, H. H. and Parikh, K. S. (2011). Quantitative determination and validation of metformin hydrochloride in pharmaceutical using quantitative nuclear magnetic resonance spectroscopy. **E-Journal of Chemistry**. 8: 767-781.
- Goldfine, A. B., Patti, M. E., Zuberi, L., Goldstein, B. J., LeBlanc, R., Landaker, E. J., Jiang, Z. Y., Willsky, G. R., and Kahn, C. R. (2000). Metabolic effects of vanadyl sulfate in humans with non- insulin-dependent diabetes mellitus: In vivo and in vitro studies. **Metabolism-Clinical and Experimental**. 49: 400-410.
- Goldstein, B. J., Feinglos, M. N., Luncford, J. K., Johnson, J., Williams-Herman, D. E., and Group, S. S. (2007). Effect of initial combination therapy with Sitagliptin, a dipeptidyl peptidase-4 inhibitor, and metformin on glycemic control in patients with Type 2 Diabetes. **Diabetes Care**. 30: 1979-1987.
- Goldwasser, I., Li, J. P., Gershonov, E., Armoni, M., Karnieli, E., Fridkin, M., and Shechter, Y. (1999). L-glutamic acid gamma-monohydroxamate - A potentiator of vanadium-evoked glucose metabolism in vitro and in vivo. **Journal of Biological Chemistry**. 274: 26617-26624.
- Graefe-Mody, E. U., Padula, S., Ring, A., Withopf, B., and Dugi, K. A. (2009). Evaluation of the potential for steady-state pharmacokinetic and pharmacodynamic interactions between the DPP-4 inhibitor linagliptin and metformin in healthy subjects. **Current Medical Research and Opinion**. 25: 1963-1972.
- Graham, G. G., Punt, J., Arora, M., Day, R. O., Doogue, M. P., Duong, J. K., Furlong, T. J., Greenfield, J. R., Greenup, L. C., Kirkpatrick, C. M., Ray, J. E., Timmins, P., and Williams, K. M. (2011). Clinical Pharmacokinetics of Metformin. **Clinical Pharmacokinetics**. 50: 81-98.

- Gunasekaran, S., Natarajan, R. K., Renganayaki, V., and Natarajan, S. (2006). Vibrational spectra and thermodynamic analysis of metformin. **Indian Journal of Pure & Applied Physics**. 44: 495-500.
- Hariharan, M., Rajan, S. S., and Srinivasan, R. (1989). Structure of metformin hydrochloride. **Acta Crystallographica Section C**. 45: 911-913.
- Hirromura, M., Nakayama, A., Adachi, Y., Doi, M., and Sakurai, H. (2007). Action mechanism of bis(allixinato)oxovanadium(IV) as a novel potent insulin-mimetic complex: Regulation of GLUT4 translocation and FoxO1 transcription factor. **Journal of Biological Inorganic Chemistry**. 12: 1275-1287.
- Howarth, O. W. (1990). Vanadium-51 NMR. **Progress in Nuclear Magnetic Resonance Spectroscopy**. 22: 453-483.
- Hung, L., Xi, P.-X., Xu, M., Liu, T.-H., and Zeng, Z.-Z. (2008). Crystal structure of setformin-ethyl-N-(3-tossulfonyl)carbamate. **Analytical Sciences**. 24: x289-x290.
- Hunt, N. T., Jaye, A. A., and Meech, S. R. (2005). Reactive dynamics in confined water droplets: Auramine O in AOT/water/heptane microemulsions. **Chemical Physics Letters**. 416: 89-93.
- Kotchevar, A. T., Ghosh, P., DuMez, D. D., and Uckun, F. M. (2001). Induction of aerobic peroxidation of liposomal membranes by bis(cyclopentadienyl)-vanadium(IV) (acetylacetonate) complexes. **Journal of Inorganic Biochemistry**. 83: 151-160.
- Kotchevar, A. T., Ghosh, P., and Uckun, F. M. (1998). Interactions of vanadocene(IV)-chelated complexes with artificial membranes. **Journal of Physical Chemistry B**. 102: 10925-10930.
- Krentz, A. J. and Bailey, C. J. (2005). Oral antidiabetic agents - current role in type 2 diabetes mellitus. **Drugs**. 65: 385-411.

- Leodidis, E. B. and Hatton, T. A. (1989). Specific ion effects in electrical double layers: Selective solubilization of cations in Aerosol-OT reversed micelles. **Langmuir**. 5: 741-753.
- Li, M., Smee, J. J., Ding, W., and Crans, D. C. (2009). Anti-diabetic effects of sodium 4-amino-2,6-dipicolinatodioxovanadium(V) dihydrate in streptozotocin-induced diabetic rats. **Journal of Inorganic Biochemistry**. 103: 585-589.
- Li, Y. T., Zhu, C. Y., Wu, Z. Y., Jiang, M., and Yan, C. W. (2010). Synthesis, crystal structures and anticancer activities of two decavanadate compounds. **Transition Metal Chemistry**. 35: 597-603.
- Maitra, A. (1984). Determination of size parameters of water Aerosol OT oil reverse micelles from their NMR data. **Journal of Physical Chemistry**. 88: 5122-5125.
- Maneedaeng, A., Haller, K. J., Grady, B. P., and Flood, A. E. (2011). Thermodynamic parameters and counterion binding to the micelle in binary anionic surfactant systems. **Journal of Colloid Interface Science**. 356: 598-604.
- McNeill, J. H., Yuen, V. G., Hoveyda, H. R., and Orvig, C. (1992). Bis(maltolato)oxovanadium(IV) Is a potent insulin mimic. **Journal of Medicinal Chemistry**. 35: 1489-1491.
- Morris, J. B. (1994). *In vivo* measurements of uptake. **Inhalation Toxicology**. 6: 99-111.
- Nomiya, K., Torii, H., Hasegawa, T., Nemoto, Y., Nomura, K., Hashino, K., Uchida, M., Kato, Y., Shimizu, K., and Oda, M. (2001). Insulin mimetic effect of a tungstate cluster. effect of oral administration of homo-polyoxotungstates and vanadium-substituted polyoxotungstates on blood glucose level of STZ mice. **Journal of Inorganic Biochemistry**. 86: 657-667.
- Passadouro, M., Metelo, A. M., Melão, A. S., Pedro, J. R., Faneca, H., Carvalho, E., and Castro, M. M. C. A. (2010). Study of the antidiabetic capacity of the VO(dmpp)₂ complex. **Journal of Inorganic Biochemistry**. 104: 987-992.

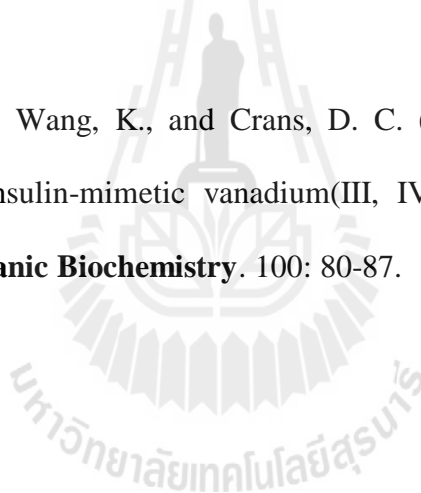
- Pereira, M. J., Carvalho, E., Eriksson, J. W., Crans, D. C., and Aureliano, M. (2009). Effects of decavanadate and insulin enhancing vanadium compounds on glucose uptake in isolated rat adipocytes. **Journal of Inorganic Biochemistry**. 103: 1687-1692.
- Pessoa, J. C. and Tomaz, I. (2010). Transport of therapeutic vanadium and ruthenium complexes by blood plasma components. **Current Medicinal Chemistry**. 17: 3701-3738.
- Peter W., Winter, P. W., Al-Qatati, A., Wolf-Ringwall, A. L., Schoeberl, S., Chatterjee, P. B., Barisas, B. G., Roess, D. A., and Crans, D. C. (2012). The anti-diabetic bis(maltolato)oxovanadium(IV) decreases lipid order while increasing insulin receptor localization in membrane microdomains. **Dalton Transactions**. 41: 6419-6430.
- Posner, B. I., Faure, R., Burgess, J. W., Bevan, A. P., Lachance, D., Zhangsun, G. Y., Fantus, I. G., Ng, J. B., Hall, D. A., Lum, B. S., and Shaver, A. (1994). Peroxovanadium compounds- A new class of potent phosphotyrosine phosphatase inhibitors which are insulin mimetics. **Journal of Biological Chemistry**. 269: 4596-4604.
- Ray, P. (1961). Complex compounds of biguanides and guanyleureas with metallic elements. **Chemical Reviews**. 61: 313-359.
- Rehder, D. (1982). A survey of ^{51}V NMR spectroscopy. **Bulletin of Magnetic Resonance**. 4: 33-83.
- Rehder, D., Pessoa, J. C., Geraldes, C., Castro, M., Kabanos, T., Kiss, T., Meier, B., Micera, G., Pettersson, L., Rangel, M., Salifoglou, A., Turel, I., and Wang, D. R. (2002). In vitro study of the insulin-mimetic behaviour of vanadium(IV, V) coordination compounds. **Journal of Biological Inorganic Chemistry**. 7: 384-396.

- Rezus, Y. L. A. and Bakker, H. J. (2006). Orientational dynamics of isotopically diluted H₂O and D₂O. **Journal of Chemical Physics**. 125: 144512.
- Roess, D. A., Smith, S. M. L., Winter, P., Zhou, J., Dou, P., Baruah, B., Trujillo, A. M., Levinger, N. E., Yang, X. D., Barisas, B. G., and Crans, D. C. (2008). Effects of vanadium-containing compounds on membrane lipids and on microdomains used in receptor-mediated signaling. **Chemistry & Biodiversity**. 5: 1558-1570.
- Roman, P., Macias, R., Luque, A., and Guzmanmiralles, C. (1992). Thermal features and behavior of protonated diethylenetriamine isopolyvanadates. **Thermochimica Acta**. 209: 189-194.
- Sakurai, H., Shimomura, S., Fukuzawa, K., and Ishizu, K. (1980). Detection of oxovanadium(IV) and characterization of its ligand environment in subcellular fractions of the liver of rat treated with pentavalent vanadium(V). **Biochemical and Biophysical Research Communications**. 96: 293-298.
- Sanna, D., Buglyó, P., Bíró, L., Micera, G., and Garribba, E. (2012). Coordinating properties of pyrone and pyridinone derivatives, tropolone and catechol toward the VO²⁺ ion: An experimental and computational approach. **European Journal of Inorganic Chemistry**. 2012: 1079-1092.
- Sanna, D., Buglyo, P., Micera, G., and Garribba, E. (2010). A quantitative study of the biotransformation of insulin-enhancing VO²⁺ compounds. **Journal of Biological Inorganic Chemistry**. 15: 825-839.
- Scarpello, J. H. B. and Howlett, H. C. S. (2008). Metformin therapy and clinical uses. **Diabetes & Vascular Disease Research**. 5: 157-167.
- Sedgwick, M. A., Crans, D. C., and Levinger, N. E. (2009). What is inside a nonionic reverse micelle? Probing the interior of igepal reverse micelles using decavanadate. **Langmuir**. 25: 5496-5503.

- Sedgwick, M. A., Trujillo, A. M., Hendricks, N., Levinger, N. E., and Crans, D. C. (2011). Coexisting aggregates in mixed Aerosol OT and cholesterol microemulsions. **Langmuir**. 27: 948-954.
- Silber, J. J., Biasutti, A., Abuin, E., and Lissi, E. (1999). Interactions of small molecules with reverse micelles. **Advances in Colloid and Interface Science**. 82: 189-252.
- Stover, J., Rithner, C. D., Inafuku, R. A., Crans, D. C., and Levinger, N. E. (2005). Interaction of dipicolinatodioxovanadium(V) with polyatomic cations and surfaces in reverse micelles. **Langmuir**. 21: 6250-6258.
- Szakacs, Z., Kraszni, M., and Noszal, B. (2004). Determination of microscopic acid-base parameters from NMR-pH titrations. **Analytical and Bioanalytical Chemistry**. 378:1428-1448.
- Tajima, A., Hirata, T., Taniguchi, K., Kondo, Y., Kato, S., Saito-Hori, M., Ishimoto, T., and Yamamoto, K. (2011). Combination of TS-021 with metformin improves hyperglycemia and synergistically increases pancreatic β -cell mass in a mouse model of type 2 diabetes. **Life Sciences**. 89: 662-670.
- Thompson, K. H., Lichter, J., LeBel, C., Scaife, M. C., McNeill, J. H., and Orvig, C. (2009). Vanadium treatment of type 2 diabetes: A view to the future. **Journal of Inorganic Biochemistry**. 103: 554-558.
- Thompson, K. H., McNeill, J. H., and Orvig, C. (1999). Vanadium compounds as insulin mimics. **Chemical Reviews**. 99: 2561-2571.
- Thompson, K. H. and Orvig, C. (2004). **Metal Ions and Their Complexes in Medication**. New York: Marcel Dekker. pp. 221-252.
- Vanzi, F., Madan, B., and Sharp, K. (1998). Effect of the protein denaturants urea and guanidinium on water structure: A structural and thermodynamic study. **Journal of the American Chemical Society**. 120: 10748-10753.

- Vergara, E. G., Lara, E. S., Benítez, A. P., and Mendoza, A. (2011). Decavanadate salts of 4-dimethylaminopyridine and metforminium dication as potential pro-drugs for the treatment of type II Diabetes. In 15th International Conference on Biological Inorganic Chemistry: Vancouver, Canada, 2011.
- Wiernsperger, N. F. and Bailey, C. J. (1999). The antihyperglycaemic effect of metformin - Therapeutic and cellular mechanisms. **Drugs**. 58: 31-39.
- Willsky, G. R., Chi, L.-H., Godzala, M., Kostyniak, P. J., Smee, J., Trujill, A. M., Alfano, J. A., Ding, D.; Hu, Z., and Crans, D. C. (2011). Anti-diabetic effects of a series of vanadium dipicolinate complexes in rats with streptozotocin-induced diabetes. **Coordination Chemistry Reviews**. 255: 2258- 2269.
- Winter, P. W., Al-Qatati, A., Wolf-Ringwall, A. L., Schoeberl, S., Chatterjee, P. B., Barisas, B. G., Roess, B. A., and Crans, D. C. (2012). The anti-diabetic bis(maltolato)oxovanadium(IV) decreases lipid order while increasing insulin receptor localization in membrane microdomains. **Dalton Transactions**. 41: 6419-6430.
- Woo, L. C. Y. (1998). The design and synthesis of vanadyl-biguanide complexes as potential synergistic insulin mimics. PhD. Thesis. University of British Columbia, Canada.
- Woo, L. C. Y., Yuen, V. G., Thompson, K. H., McNeill, J. H., and Orvig, C. (1999). Vanadyl-biguanide complexes as potential synergistic insulin mimics. **Journal of Inorganic Biochemistry**. 76: 251-257.
- Yang, X.-G., Wang, K., Lu, J., and Crans, D. C. (2003). Membrane transport of vanadium compounds and the interaction with the erythrocyte membrane. **Coordination Chemistry Reviews**. 237: 103-111.

- Yang, X.-G., Yang, X.-D., Yuan, L., Wang, K., and Crans, D. C. (2004). The permeability and cytotoxicity of insulin-mimetic vanadium compounds. **Pharmaceutical Research**. 21: 1026-1033.
- Yraola, F., Garcia-Vicente, S., Marti, L., Albericio, F., Zorzano, A., and Royo, M. (2007). Understanding the mechanism of action of the novel SSAO substrate $(C_7NH_{10})_6(V_{10}O_{28}) \cdot 2H_2O$, a prodrug of peroxovanadate insulin mimetics. **Chemical Biology & Drug Design**. 69: 423-428.
- Zhang, B. Y., Ruan, L., Chen, B. W., Lu, J. F., and Wang, K. (1997). Binding of vanadate to human erythrocyte ghosts and subsequent events. **Biometals**. 10: 291-298.
- Zhang, Y., Yang, X.-D., Wang, K., and Crans, D. C. (2006). The permeability and cytotoxicity of insulin-mimetic vanadium(III, IV, V)-dipicolinate complexes. **Journal of Inorganic Biochemistry**. 100: 80-87.



CHAPTER VI

CONCLUSIONS

Metformin hydrochloride is a biguanide derivative, widely used against type 2 diabetes and malaria. However, its mechanism of action is still unclear although many researchers have studied it *in vitro* and *in vivo* using various techniques for more than a decade to investigate the reactivity and interaction with target cells. Thus, it is important to clarify basic knowledge of its structural features and the chemical reactivity they induce to improve understanding of the compound.

The active pharmaceutical ingredient, metformin hydrochloride, was isolated from the diabetic drug, Glucophage, and its purity confirmed by comparing with a standard compound using FTIR, melting point, and powder X-ray diffraction methods. The crystallographic data of metformin and its salts were reviewed. MetHCl shows [C–N] bond distances in biguanide intermediate between single and double bonds but a large dihedral angle between the two planar guanidine groups suggests that π -electron delocalization is interrupted at the bridging N atom. Intermolecular N–H \cdots N' hydrogen bonding interaction between cation groups and N–H \cdots Cl and C–H \cdots Cl hydrogen bonding between HMet⁺ cation and Cl[–] anion form a 3D network structure.

Results obtained from ¹H NMR of MetHCl at different pH show chemical shifts at 3.05 ppm at pH 1 and 2.77 ppm at pH 14 for the –CH₃ group, consistent with protonation at acidic pH. The proton chemical shift in the inhomogeneous environment of AOT reverse micelles moves to a lower resonance value, δ 2.91 ppm, compared with the value

in D₂O solution, which is interpreted to indicate interface interaction of metformium cation with reverse micelles.

We were also interested in the synthesis of new crystalline materials containing metformin in combination with therapeutic agents of decavanadate. These would be potential candidates for new synergistic materials to decrease the required dosage of metformin or metal complexes used in treating diabetes, resulting in a decrease in their toxicity to humans. A complex between HMet⁺ cation and V₁₀ was prepared at varying pH values over the range from 2 to 6 with slight excess of the HMet⁺. Crystallographic data show the same unit cell for crystals containing metformium, decavanadate, and water when prepared over the pH range 2 to 5, while at higher pH a mixed salt crystal was formed. The product obtained from pH ~5 gave higher yield than the other pH values and was used for further characterization.

[C₄H₁₂N₅]₃[H₃O]₃[V₁₀O₂₈]·3H₂O or MetV₁₀ was characterized by FTIR, CHN, TGA, and XRD techniques to clarify its structure and physical properties. The single crystal X-ray structure clearly shows three regions per decavanadate anion, two fully resolved and one disordered, suitable to contain HMet⁺, a result consistent with the elemental analysis and TGA analysis. The residue remaining after heating to 600°C measured by XRD gave a spectrum different from vanadium oxide compounds of V₂O₅, NH₄VO₃, V₂O₃, and V₂O₄.

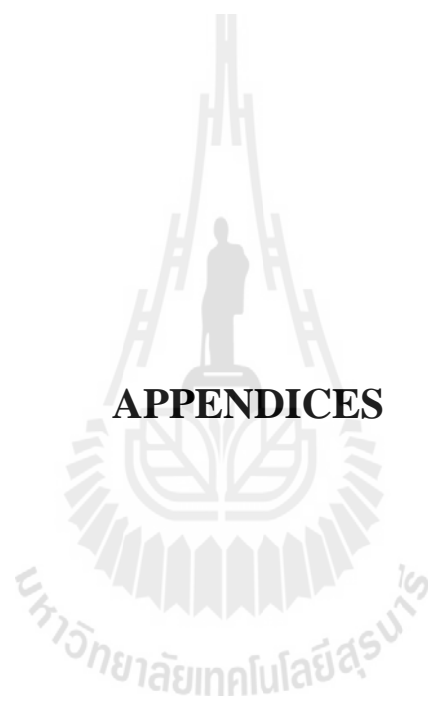
The complex is insoluble in water but was found to be very soluble in the inhomogenous environment of RMs. Since the Na⁺ salt of V₁₀ has insulin enhancing activity in STZ induced diabetic rats, how this complex interacted with interfaces was investigated. Since previous work, metformin is known to affect the H-bonding in the water pool of RMs, and the size of the RMs is changed, the water organization in the water pool or near the RM interface is changed. Differential FTIR spectroscopy was used to test the H-bonding properties in the water pool, and MetV₁₀ and MetHCl were both

found to significantly affect the H-bonding pattern in the water pool. These studies therefore demonstrate that the counterion of V_{10} significantly affects the solubility of the salt in aqueous solution and in a complex media used to study interface properties. These results highlight the importance of cation effects on the membrane interface in inhomogeneous environment. Since $MetV_{10}$ is more soluble than NaV_{10} in the inhomogeneous microemulsion, it is possible that $MetV_{10}$ system may show improved insulin enhancing properties. Perhaps surprisingly the presence of even 1% $HMet^+$ cations that can replace the counter ion in NaAOT in AOT RMs affects the organization of the nanostructure and the H-bonding in the water pool.

Suggestions for future work. This is the first time for studying metformium ion in an AOT reverse micelle system. This result shows $HMet^+$ affects the hydrogen bonding pattern in the water pool and size of the RM is changed. Therefore, it is interestingly to study the size of RMs by DLS with various $MetHCl$ concentrations, w_0 , and solvent (D_2O , H_2O) for more understanding of how $HMet^+$ affects the RM system. Moreover, study $HMet^+$ in another type of surfactant such as cationic, neutral, or mixed surfactants and figure out the precise location of $HMet^+$ in RMs by 2D NMR.

From X-ray crystallography, the third $HMet^+$ region in $MetV_{10}$ is ambiguous in the refinements. Changing parameters for a good result and clarify the crystal structure is important.

How drugs or complexes traverse cell membranes is interesting, but the complexity of living systems and limitations of current techniques keep us from obtaining insight into life phenomena. The Reverse micelles are interesting as mimics of cell membranes but monolayer AOT RMs are still quite different from the lipid bilayer of phospholipid biomembranes. For more understanding of $HMet^+$ and $MetV_{10}$ interaction with the interface of cell membranes they should be studied in bilayer micellar systems.



APPENDICES

APPENDIX A

GLOSSARY

Adipocyte – lipocytes or fat cells in body. These cells specialized in secreting hormones and other chemicals which may play a role in appetite regulation and other aspects of metabolism

Bioavailability – expressed as a percentage of drug that reaches the target organs tissues. Intravenous administration results in 100 percent bioavailability because the drug is injected directly into the bloodstream

Cerebrovascular disease – disease that affects in the circulation of the blood to the brain

Cocrystal – crystalline material with two or more distinct species in the same crystal lattice, each with essentially molecular properties, that can in principle be separated into pure components with similar chemical nature to those they possess in the crystal lattice. With small modification this definition can also apply to many solvates and pharmaceutical salts as well

Coronary heart disease – a narrowing of the small blood vessels limit the supply blood to the heart

Fasting blood glucose – blood glucose level after 8-12 hours overnight fast

Gastrointestinal tract – the part of the digestive system consisting of the mouth, esophagus, stomach, and intestines

Gestational diabetes – diabetes arising during pregnancy

Glucagon – hormone from pancreas that stimulates the breakdown of stored glycogen into glucose

Gluconeogenesis – process by which glucose is made, primarily in the liver, from noncarbohydrate sources

Glucose Tolerance Test – a laboratory blood test to make the diagnosis of type 2 diabetes mellitus

Diagnosis	Fasting plasma glucose (mg/dL)	2-hour plasma glucose (mg/dL)
Normal glucose tolerance (NGT)	< 110	< 140
Impaired fasting glucose (IFG)	110-125	< 140
Impaired glucose tolerance (IGT)	< 126	140-199
Diabetes mellitus (DM)	≥ 126	≥ 200
Gestational diabetes (22-24 weeks of pregnant)	> 95	> 155

Glycemia – existence of glucose in the bloodstream

GTF – putative cellular substance, originally proposed by Schwarz and Mertz (1957) involved in maintaining normal blood glucose levels. It was suggested to prevent and cure impairment of glucose removal from the blood. When it is deficient in the diet, cells have a lower tolerance to accept glucose from the bloodstream and thus glucose removal from the bloodstream is impaired

Heart failure – chronic condition that damage to the heart causes weakening of the cardiovascular system

Hemoglobin A_{1c} – the main fraction of glycosylated hemoglobin (glycohemoglobin) which is hemoglobin to which glucose is bound

High density lipoprotein cholesterol – one of a group of proteins that transport lipids in the blood. They can help protect against atherosclerosis, the so-called “good” cholesterol

Hyperglycemia – symptom of diabetes in which there are elevated levels of blood sugar, or glucose, in the bloodstream

Hyperlipidemia – high levels of fats (or lipids) in the blood. These fats include cholesterol and triglycerides

Hypertension – raised blood pressure. The WHO defines hypertension as a blood pressure over 140/90

Hypoglycemia – an abnormally low level of glucose in the blood when glucose levels fall below 50 milligrams per deciliter (mg/dL)

Hypoglycemic drugs – drugs used to lower blood glucose levels in the treatment of diabetes

Incretin – hormone produced by the gastrointestinal tract in response to food intake and necessary for glucose homeostasis

Incretin mimetics – a class of agents used for managing type 2 diabetes that mimics the enhancement of glucose dependent insulin secretion and other gluco-regulatory actions of naturally occurring incretins

Insulin dependent diabetes mellitus – Type 1 diabetes, due to lack of insulin production by the pancreatic beta cells

Impaired Fasting Glycemia – raised fasting blood glucose concentration that does not exceed the diagnostic limit for diabetes

Impaired glucose tolerance – raised blood glucose concentration two hours after intake of a standard glucose solution

Insulin – hormone formed by the beta cells in the pancreas. Insulin is necessary for the transport of glucose from the blood to the cells

Insulin resistance – state in which the body's cells do not react sufficiently to a given concentration of insulin in the organism

Lactic acidosis – acidosis (too much acid in the body) due to the buildup of lactic acid in the body

Low-density lipoprotein cholesterol – one of a group of proteins that are combined with lipids in the plasma. An excess of low-density lipoprotein cholesterol are associated with atherosclerosis, the so-called “bad” cholesterol

LMWCr – a naturally occurring oligopeptide (about 1500 Da) composed of glycine, cysteine, aspartate and glutamate with carboxylates. The oligopeptide molecule binds four equivalents of chromium ion as part of the autoamplification system for insulin signaling

Nephropathy – kidney disease

Neuropathy – disorders of the peripheral nerves

Noninsulin dependent diabetes mellitus – Type 2 diabetes, a disorder that is characterized by high blood glucose in the context of insulin resistance and relative insulin deficiency

Oral hypoglycemic agents – drugs are used to lower blood glucose levels

Peripheral vascular disease – diseases of blood vessels outside the heart and brain, it's often a narrowing of vessels that carry blood to the legs, arms, stomach or kidneys

Polydisperse – sample of objects that have an inconsistent size, shape and mass distribution

Postprandial plasma glucose – level of glucose in the blood plasma 2 hours after drinking the glucose solution (glucose 75 grams); used to diagnose diabetes

Prevalence – the proportion of a population that has a disease at a given point in time.

Compare with incidence

Retinopathy – changes/lesions in the periphery of the retina caused by disturbances of the blood supply to the retina

Reverse micelle – dissolving a surfactant in organic solvent with limited amount of water to produce a homogeneous transparent solution

APPENDIX B

OCCUPATION NUMBER

Occupation number or number of probe per reverse micelle (O_{cc}):

$$O_{cc} = \text{number of probe} / \text{number of RMs},$$

and number of surfactant per 1 RM is called aggregation number; n_{avg} (this value used from Mitra, 1984).

Ex. Calculated O_{cc} of probe V_{10} in 0.75 M AOT RMs at $w_0 = 6$, which 28.8 mM of V_{10} stock solution. Using 75.2 μL V_{10} stock solution and 925 μL AOT/isooctane for 1 mL RMs. When n_{avg} at $w_0 = 6 = 50$ molecule AOT.

Thus

$$\begin{aligned} \text{number of probe} &= (28.8 \text{ mmol/L})(1 \text{ L}/10^{-6} \mu\text{L})(10^{-3} \text{ mol/mmol}) \cdot (75 \mu\text{L}), \\ &= 2.1 \times 10^{-6} \text{ molecule probe.} \end{aligned}$$

$$\begin{aligned} \text{Number of RMs} &= (0.75 \text{ mol/L})(1 \text{ L}/10^{-6} \mu\text{L}) \cdot (925 \mu\text{L}) \cdot (1 \text{ mol}/50 \text{ molecule AOT}), \\ &= 13.9 \times 10^{-6} \text{ molecule AOT.} \end{aligned}$$

$$\begin{aligned} O_{cc} &= 2.1 \times 10^{-6} / 13.875 \times 10^{-6}, \\ &= 0.15 \text{ molecule } V_{10} \text{ in 1 RM.} \end{aligned}$$

Or calculate from;
$$O_{cc} = \frac{[\text{stock solution in Molar}] \cdot w_0 \cdot n_{avg}}{\text{molar of water}}$$

where molar of water = 55.5 mol/L.

In this work, concentration of V_{10} stock solution in various w_0 (each sample 2 mM V_{10}), in 0.75 M AOT RMs were shown in table below.

w_0	n_{avg}	[V_{10} stock solution], mM	O_{cc}
6	50	28.8	0.15
8	72	21.7	0.22
10	98	17.5	0.31
16	215	11.5	0.71



APPENDIX C

SUPPORTING INFORMATION CHAPTER V

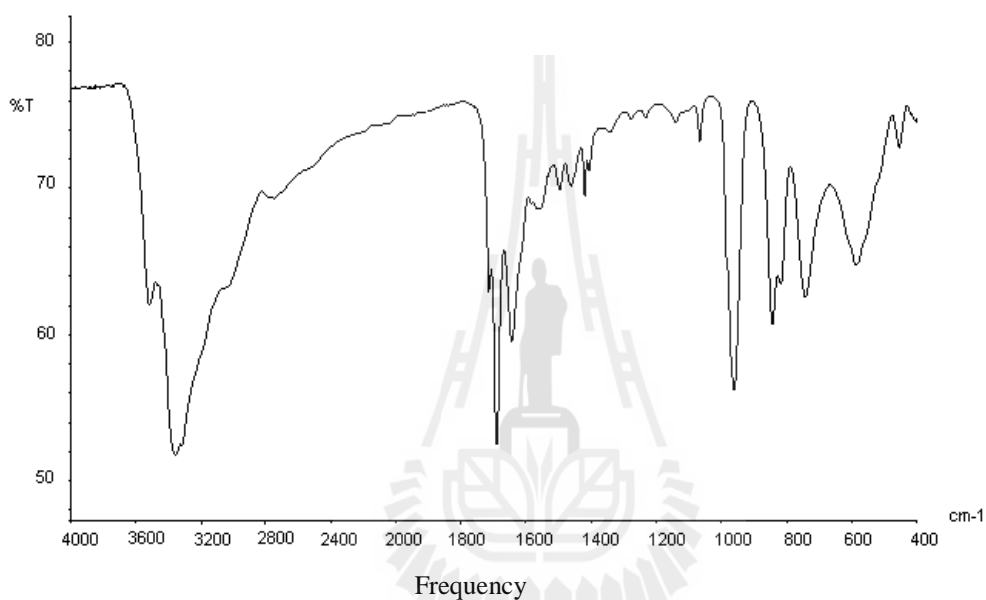


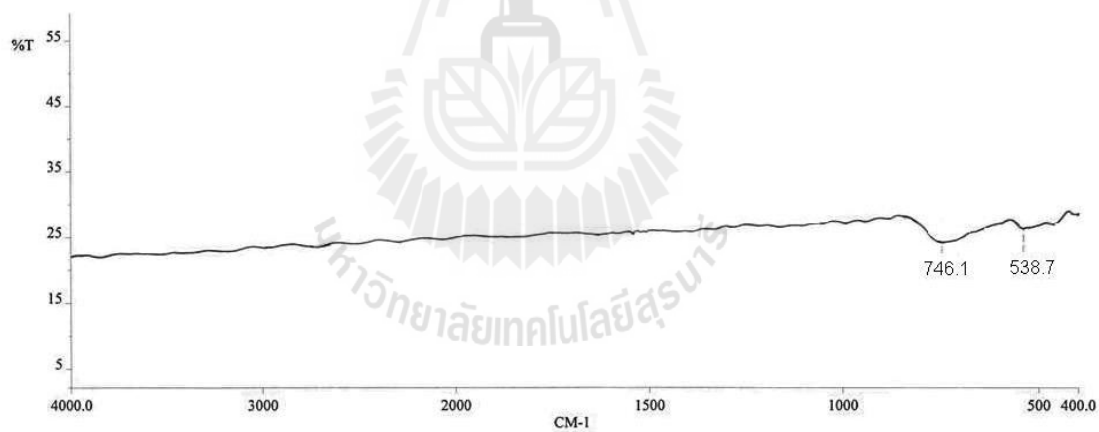
Figure C1 The IR spectrum of metformium decavanadate.

Table C1 IR band assignments for metformium decavanadate.

Assignment	Frequency (cm ⁻¹)
$\nu(\text{NH}_2)$	3360, 3346
$\nu(\text{C}=\text{N})$	1691
$\delta_{\text{as}}(\text{NCN})$	1645
$\nu(\text{CN})$	1498, 1469
$\nu(\text{CH}_3)$	1421
$\rho(\text{NH}_2)$	1067
$\nu(\text{V}=\text{O})$	961
$\nu(\text{V}-\text{O})$ and $\delta(\text{V}-\text{O}-\text{V})$	844, 743, and 589

Table C2 Data from TGA analysis of metformium decavanadate.

Step	T _i -T _f , (TGA, °C)	%Δ _{wt} (Theory)	%Δ _{wt} (Calc.)	Propose
1	75-105	-3.69	-3.75	3H ₂ O
2	105-168	-3.90	-3.87	3H ₂ O ⁺
3	168-460	-26.76	-26.92	3(HMet)
4	460-610	-8.77	-8.80	4O ₂
	%Δ _{wt}	-43.12	- 43.34	

**Figure C2** The IR spectrum of metformium decavanadate after heating to 600°C.

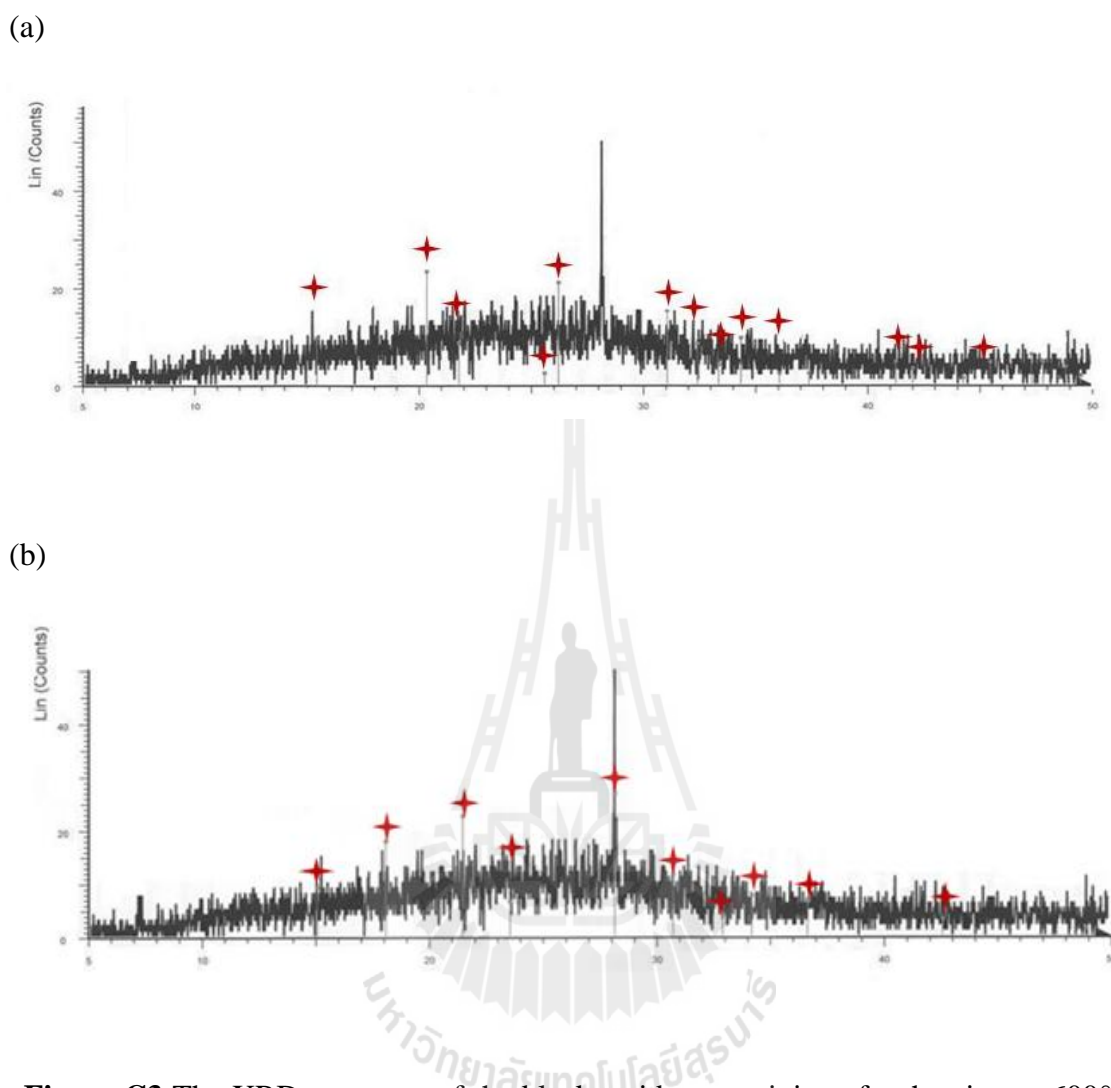


Figure C3 The XRD spectrum of the black residue remaining after heating to 600°C of metformium decavanadate compared with (a)vanadium pentoxide, and (b) ammonium metavanadate. (asterisk is vanadium pentoxide or ammonium metavanadate)

CURRICULUM VITAE

AUNGKANA CHATKON

Date of Birth: October 16, 1973

Place of Birth: Sa Kaeo, Thailand

Education

2007- 2012 Ph.D., Chemistry, Suranaree University of Technology, Thailand

1998-2000 M.Sc., Chemistry, Suranaree University of Technology, Thailand

1991-1994 B.Sc., Chemistry, Rajabhat Institute, Nakhon Ratchasima, Thailand

Publications

Aungkana Chatkon; Kenneth J. Haller; Ian D. Williams, Proceedings of 1th SUT Graduate Conference, 2007.

Aungkana Chatkon; Kenneth J. Haller, Debbie C. Crans, Acta Cryst. (2011). A67, C584.

Aungkana Chatkon; Alexa Barres, Kenneth J. Haller, Debbie C. Crans, Acta Cryst. (2012). A68, s154.

Awards

Registration Scholarship Grant for ACA 2007, Taipei, Taiwan.

Travel grant for ACA 2007, Taipei, Taiwan.

Registration Scholarship Grant for ACA 2010, Busan, Korea.

Scholarships and Honors:

M.Sc. Thai Government Scholarship, Ministry of Education

Ph.D. The Commission on Higher Education, Ministry of Education